



Faculté de génie

Génie électrique et informatique

Auditory System for a Mobile Robot

Thèse de doctorat

Specialité: génie électrique

Jean-Marc Valin

Abstract

The auditory system of living creatures provides useful information about the world, such as the location and interpretation of sound sources. For humans, it means to be able to focus one's attention on events, such as a phone ringing, a vehicle honking, a person talking, etc. For those who do not suffer from hearing impairments, it is hard to imagine a day without being able to hear, especially in a very dynamic and unpredictable world. Mobile robots would also benefit greatly from having auditory capabilities.

In this thesis, we propose an artificial auditory system that gives a robot the ability to locate and track sounds, as well as to separate simultaneous sound sources and recognising simultaneous speech. We demonstrate that it is possible to implement these capabilities using an array of microphones, without trying to imitate the human auditory system. The sound source localisation and tracking algorithm uses a steered beamformer to locate sources, which are then tracked using a multi-source particle filter. Separation of simultaneous sound sources is achieved using a variant of the Geometric Source Separation (GSS) algorithm, combined with a multi-source post-filter that further reduces noise, interference and reverberation. Speech recognition is performed on separated sources, either directly or by using Missing Feature Theory (MFT) to estimate the reliability of the speech features.

The results obtained show that it is possible to track up to four simultaneous sound sources, even in noisy and reverberant environments. Real-time control of the robot following a sound source is also demonstrated. The sound source separation approach we propose is able to achieve a 13.7 dB improvement in signal-to-noise ratio compared to a single microphone when three speakers are present. In these conditions, the system demonstrates more than 80% accuracy on digit recognition, higher than most human listeners could obtain in our small case study when recognising only one of these sources. All these new capabilities will allow humans to interact more naturally with a mobile robot in real life settings.

Sommaire

La plupart des êtres vivants possèdent un système auditif leur fournissant de l'information utile sur leur environnement, comme la direction et l'interprétation des source sonores. Cela permet de diriger notre attention sur des événements, comme une sonnerie de téléphone, le klaxon d'un véhicule, une personne qui parle, etc. Pour ceux qui ne souffrent pas d'un problème auditif, il est difficile d'imaginer passer une journée sans pouvoir entendre, particulièrement dans un environnement dynamique et imprévisible. Les robots mobiles pourraient eux aussi tirer un bénéfice important de capacités auditives.

Dans cette thèse, nous proposons un système d'audition artificielle dotant un robot de la capacité de localiser et suivre des sons, ainsi que de la capacité de séparer des sources sonores sonores simultanées et de reconnaître ce qui est dit. Nous démontrons qu'il est possible de réaliser ces capacités à l'aide d'un réseau de microphones, sans la nécessité d'imiter le système auditif humain. L'algorithme de localisation et suivi de sources sonores utilise un *beamformer* dirigé pour localiser les sources, qui sont ensuite suivies en utilisant un filtre particulière. La séparation de sources sonores simultanées est accomplie par une variante de l'algorithme de séparation géométrique des sources (*Geometric Source Separation*), combinée à un post-traitement multi-source permettant de réduire le bruit, les interférences et la réverbération. Les sources séparées sont ensuite utilisées pour effectuer la reconnaissance vocale, soit directement, soit en utilisant la théorie des données manquantes (*Missing Feature Theory*) qui tient compte de la fiabilité des paramètres de la parole séparée.

Les résultats obtenus montrent qu'il est possible de suivre jusqu'à quatre sources sonores simultanées, même dans des environnements bruités et réverbérants. Nous démontrons aussi le contrôle en temps réel d'un robot se déplaçant pour suivre une source en mouvement. De plus, lorsque trois personnes parlent en même temps, l'approche proposée pour la séparation des sources sonores permet d'améliorer de 13.7 dB le rapport signal-à-bruit si on compare à l'utilisation d'un seul microphone. Dans ces conditions, le système obtient un taux de reconnaissance supérieur à 80% sur des chiffres, ce qui est supérieur à ce que la plupart des auditeurs humains ont obtenu lors de tests simples de reconnaissance sur une seule de ces sources. Ces nouvelles capacités auditives permettront aux humains d'interagir de façon plus naturelle avec un robot mobile.

Acknowledgements

I would like to express my gratitude to my thesis supervisor François Michaud and my thesis co-supervisor Jean Rouat for their support and feedback during the course of this thesis. Their knowledge and insight have greatly contributed to the success of this project.

During this research, I was supported financially by the National Science and Engineering Research Council of Canada (NSERC), the Quebec *Fonds de recherche sur la nature et les technologies* (FQRNT) and the Université de Sherbrooke. François Michaud holds the Canada Research Chair (CRC) in Mobile Robotics and Autonomous Intelligent Systems. This research is supported financially by the CRC Program and the Canadian Foundation for Innovation (CFI).

I would like to thank Hiroshi G. Okuno for receiving me at the Kyoto University Speech Media Processing Group for an internship from August to November 2004, during which I was introduced to the missing feature theory. During this stay, I was supported financially by the Japan Society for the Promotion of Science (JSPS) short-term exchange student scholarship.

Special thanks to Brahim Hadjou for help formalising the particle filtering notation, to Dominic Létourneau and Pierre Lepage for implementing what was necessary to control the robot in real time using my algorithms and to Yannick Brosseau for performing speech recognition experiments. Thanks to Serge Caron and Jonathan Bisson for the design and fabrication of the microphones. Many thanks to everyone at the Mobile Robotics and Intelligent Systems Research Laboratory (LABORIUS) who took part in my numerous experiments. I would like to thank Nuance Corporation for providing us with a free license to use its Nuance Voice Platform.

I am grateful to my wife, Nathalie, for her love, encouragement and unconditional support throughout my PhD, and to my son, Alexandre, for giving me a reason to finish on schedule!

Contents

1	Overview of the Thesis	1
1.1	Audition in Mobile Robotics	4
1.2	Experimental Setup	6
1.3	Thesis Outline	8
2	Sound Source Localisation	11
2.1	Related Work	12
2.2	System Overview	13
2.3	Localisation Using a Steered Beamformer	14
2.3.1	Delay-And-Sum Beamformer	15
2.3.2	Spectral Weighting	17
2.3.3	Direction Search on a Spherical Grid	18
2.3.4	Direction Refining	21
2.4	Particle-Based Tracking	22
2.4.1	Prediction	24
2.4.2	Instantaneous Direction Probabilities from Beamformer Response . . .	25
2.4.3	Probabilities for Multiple Sources	27
2.4.4	Weight Update	30
2.4.5	Adding or Removing Sources	31
2.4.6	Parameter Estimation	32

2.4.7	Resampling	32
2.5	Results	33
2.5.1	Characterisation	33
2.5.1.1	Detection Reliability	34
2.5.1.2	Localisation Accuracy	34
2.5.2	Source Tracking	36
2.5.2.1	Moving Sources	36
2.5.2.2	Moving Robot	37
2.5.2.3	Sources with Intersecting Trajectories	38
2.5.2.4	Number of Microphones	38
2.5.2.5	Audio Bandwidth	39
2.5.3	Localisation and Tracking for Robot Control	40
2.6	Discussion	41
3	Sound Source Separation	43
3.1	Related Work	44
3.2	System Overview	46
3.3	Linear Source Separation	46
3.3.1	Geometric Source Separation	47
3.3.2	Proposed Improvements to the GSS algorithm	49
3.3.2.1	Stochastic Gradient Adaptation	49
3.3.2.2	Regularisation Term	50
3.3.3	Initialisation	50
3.4	Multi-Source Post-Filter	51
3.4.1	Noise Estimation	52
3.4.2	Suppression Rule in the Presence of Speech	53
3.4.3	Optimal Gain Modification Under Speech Presence Uncertainty	55
3.4.4	Post-filter Initialisation	56

3.5	Results	57
3.6	Discussion	60
4	Speech Recognition of Separated Sound Sources	65
4.1	Related Work in Robust Speech Recognition	66
4.1.1	Missing Feature Theory Overview	67
4.1.2	Applications of Missing Feature Theory	68
4.2	ASR on Separated Sources	69
4.3	Missing Feature Recognition	71
4.3.1	Computation of Missing Feature Masks	71
4.3.2	Speech Analysis for Missing Feature ASR	73
4.3.3	Automatic Speech Recognition Using Missing Feature Theory	74
4.4	Results	74
4.4.1	Direct Coupling	75
4.4.1.1	Human Capabilities	76
4.4.1.2	Moving Sources	78
4.4.2	Missing Feature Theory Coupling	79
4.4.2.1	Separated Signals	80
4.4.2.2	Speech Recognition Accuracy	81
4.5	Discussion	82
5	Conclusion	85
5.1	Future Work	87
5.2	Perspectives	88

List of Figures

1.1	Microphones used on the Spartacus robot.	7
1.2	Spartacus robot in configurations.	8
1.3	Overview of the proposed artificial auditory system.	9
2.1	Overview of the Localisation subsystem.	14
2.2	Recursive subdivision of a triangular element.	19
2.3	TDOA for the far field approximation.	20
2.4	Probabilistic tracking of multiple sources using a fixed grid.	22
2.5	Example of two sources being represented by a particle filter.	24
2.6	Beamformer output probabilities P_q for azimuth as a function of time.	26
2.7	Assignment example where two of the tracked sources are observed, with one new source and one false detection.	27
2.8	Tracking of four moving sources, showing azimuth as a function of time.	32
2.9	Source trajectories (robot represented as an X, sources represented with dots).	36
2.10	Four speakers moving around a stationary robot. False detection shown in black.	37
2.11	Two stationary speakers with the robot moving. False detection shown in black.	37
2.12	Two speakers intersecting in front of the robot.	38
2.13	Tracking of four sources using C2 in the E1 environment, using 4 to 7 micro- phones.	39

2.14	Tracking of four sources using C2 in the E1 environment for reduced audio bandwidth.	40
3.1	Overview of the separation system.	46
3.2	Overview of the complete separation system.	52
3.3	Signal-to-noise ratio (SNR) and log-spectral distortion (LSD) for each source of interest.	59
3.4	Attenuation of noise and interference in the direction of each source of interest.	60
3.5	Temporal signals for separation of first source.	61
3.6	Spectrograms for separation of first source comparing different processing.	62
4.1	Direct integration of speech recognition.	69
4.2	Speech recognition integration using missing feature theory	70
4.3	Speech recognition results for two simultaneous speakers.	76
4.4	Speech recognition results for three simultaneous speakers.	77
4.5	Human versus machine speech recognition accuracy.	78
4.6	Source trajectories (azimuth as a function of time): recognition on two moving speakers.	79
4.7	SIG 2 robot with eight microphones (two are occluded).	80
4.8	Missing feature masks for separation of three speakers.	81
4.9	Speech recognition accuracy results for 30° separation between speakers.	83
4.10	Speech recognition accuracy results for 60° separation between speakers.	84
4.11	Speech recognition accuracy results for 90° separation between speakers.	84

List of Tables

2.1	Detection reliability for C1 and C2 configurations.	35
2.2	Correct localisation rate as a function of sound type and distance for C2 configuration.	35
2.3	Localisation accuracy (root mean square error).	35

List of Algorithms

2.1	Steered beamformer direction search.	19
2.2	Localisation of multiple sources.	21
2.3	Particle-based tracking algorithm	24

Lexicon

ASR. Automatic Speech Recognition.

CMS. Cepstral Mean Subtraction (also cepstral mean normalisation).

DCT. Discrete Cosine Transform.

DSP. Digital Signal Processor.

FFT. Fast Fourier Transform.

GSS. Geometric Source Separation.

LSS. Linear Source Separation.

MCRA. Minima-Controlled Recursive Average.

MFCC. Mel-Frequency Cepstral Coefficient.

MFT. Missing Feature Theory.

MMSE. Minimum Mean Square Error.

pdf. Probability density function.

Reverberation Time (T_{60}). Time for reverberation to decrease by 60 dB.

SNR. Signal-to-Noise Ratio.

SRR. Signal-to-Reverberant Ratio.

TDOA. Time Delay of Arrival.

Chapter 1

Overview of the Thesis

The auditory system of living creatures provides significant information about the world, such as the location and the interpretation of sound sources. For humans, it means to be able to focus one's attention on events, such as a phone ringing, a vehicle honking, a person taking, etc. For those who do not suffer from hearing impairments, it is hard to imagine a day without being able to hear, especially in a very dynamic and unpredictable world.

Brooks *et al.* [1] postulate that the essence of intelligence lies in four main aspects: development, social interaction, embodiment, and integration. It turns out that hearing plays a role in three of these factors. Obviously, speech is by far the preferred means of communication between humans. Hearing also plays a very important role in human development. Marschark [2] even suggests that although deaf children have similar IQ results compared to other children, they do experience more learning difficulties in school. Hearing is useful for the integration aspect of intelligence, as it complements well other sensors such as vision by being omni-directional, capable of working in the dark and not limited by physical structures (such as walls). Therefore, it is important for robots to understand spoken language and respond to auditory events. The auditory capabilities will undoubtedly improve the intelligence manifested by autonomous robots.

The human hearing sense is very good at focusing on a single source of interest and following a conversation even when several people are speaking at the same time. We refer to this

situation as the *cocktail party effect*. In order to operate in human and natural settings, autonomous mobile robots should be able to do the same. This means that a mobile robot should be able to separate and recognise sound sources present in the environment at any time. This requires the robots not only to detect sounds, but also to locate their origin, separate the different sound sources (since sounds may occur simultaneously), and process all of this data to be able to extract useful information about the world.

While it is desirable for an artificial auditory system to achieve the same level of performance as the human auditory system, it is not necessary for the approach taken to mimic the human auditory system. Unlike humans, robots are not inherently limited to having only two ears (microphones) and do not have the human limitations due to psychoacoustic masking [3] or partial insensitivity to phase. On the other hand, the human brain is far more complex and powerful than what can be achieved today in terms of artificial intelligence. So it may be appropriate to compensate for this fact by adding more sensors. Using more than two microphones provides increased resolution in three-dimensional space. This also means increased robustness, since multiple signals greatly helps reduce the effects of noise and improve discrimination of multiple sound sources.

The primary objective of this thesis¹ is to give a mobile robot auditory capabilities using an array of microphones. We focus on three main capabilities:

1. Localising (potentially simultaneous) sound sources and being able to track them over time;
2. Separating simultaneous sound sources from each other so they can be analysed separately;
3. Performing speech recognition on separated sources.

While some of these aspects have already been studied in the field of signal processing, they are revisited here with a special focus on mobile robotics and its constraints:

¹Up-to-date information, as well as audio and video clips related to the project are available at <http://www.gel.usherb.ca/laborius/projects/Audible/>

- **Limited computational capabilities.** A mobile robot has only limited on-board computing power. For that reason, we impose that our system be able to run on a low-power, embedded PC computer.
- **Need for real-time processing with reasonable delay.** In order for the extracted auditory information to be useful, it must be available at the same time as the events are happening. For that reason, the processing delay must be kept small. A certain delay is still acceptable, but it depends on the particular information needed.
- **Weight and space constraints.** A mobile robot usually has strict weight and space constraints. The auditory system we propose must respect the constraints imposed by the robot and not the contrary. In practice, this means that the microphones must be placed on the robot wherever possible.
- **Noisy operating environment (both point source and diffuse sources, robot noise).** Mobile robots are set to evolve in a wide range of environments. Some of these environments are likely to be noisy and reverberant. The noise may take many different forms. It can be a stationary, diffuse noise, such as the room ventilation system or a number of machines in the room. Noise can also be in the form of people talking around the robot (not to the robot). In that case, the noise is non-stationary, usually a point source, and referred to as interference. Also, every environment is reverberant to a certain degree. While this is usually not a problem in small rooms, our system will certainly have to be robust to reverberation (the echo in a room) when a robot is to operate in larger, reverberant rooms.
- **Mobile sound sources.** A mobile robot usually evolves in a dynamically changing environment. That implies that sound sources around it will appear, disappear, and move around the robot.
- **Mobile reference system (robot can move).** Not only can sound sources move around the robot, but the robot itself should be able to move in its environment. The auditory

system must remain functional even when the robot is moving.

- **Adaptability.** It is highly desirable for the auditory system we develop to be easily adapted to any mobile robot. For this reason, there should be as few adjustments as possible that depend on the robot's shape.

1.1 Audition in Mobile Robotics

Artificial hearing for robots is a research topic still in its infancy, at least when compared to all the work already done on artificial vision in robotics. However, the field of artificial audition has been the subject of much research in recent years. In 2004, the IEEE/RSJ International Conference on Intelligent Robots and Systems (IROS) has for the first time included a special session on robot audition. Initial work on sound localisation by Irie [4] for the Cog [5] and Kismet robots can be found as early as 1995. The capabilities implemented were however very limited, partly because of the necessity to overcome hardware limitations.

The SIG robot² and its successor, SIG2³, both developed at Kyoto University, have integrated increasing auditory capabilities [6, 7, 8, 9, 10, 11, 12] over the years (from 2000 to now). Both robots are based on binaural audition, which is still the most common form of artificial audition on mobile robots. Original work by Nakadai *et al.* [6, 7] on active audition have made it possible to locate sound sources in the horizontal plane using binaural audition and active behaviour to disambiguate front from rear. Later work has focused more on sound source separation [10, 11] and speech recognition [13, 14].

The ROBITA robot, designed at Waseda University, uses two microphones to follow a conversation between two people, originally requiring each participant to wear a headset [15], although a more recent version uses binaural audition [16].

A completely different approach is used by Zhang and Weng [17] with the SAIL robot with the goal of making a robot develop auditory capabilities autonomously. In this case, the

²<http://winnie.kuis.kyoto-u.ac.jp/SIG/oldsig/>

³<http://winnie.kuis.kyoto-u.ac.jp/SIG/>

Q-learning unsupervised learning algorithm is used instead of supervised learning, which is most commonly used in the field of speech recognition. The approach is validated by making the robot learn simple voice commands. Although current speech recognition accuracy using conventional methods is usually higher than the results obtained, the advantage is that the robot learns words autonomously.

More recently, robots have started taking advantage of using more than two microphones. This is the case of the Sony QRIO SDR-4XII robot [18] that features seven microphones. Unfortunately, little information is available regarding the processing done with those microphones. A service robot by Choi *et al.* [19] uses eight microphones organised in a circular array to perform speech enhancement and recognition. The enhancement is provided by an adaptive beamforming algorithm. Work by Asano, Asoh, *et al.* [20, 21, 22] also uses a circular array composed of eight microphones on a mobile robot to perform both localisation and separation of sound sources. In more recent work [23], particle filtering is used to integrate vision and audition in order to track sound sources.

In general, human-robot interface is a popular area of audition-related research in robotics. Works on robot audition for human-robot interface has also been done by Prodanov *et al.* [24] and Theobalt *et al.* [25], based on a single microphone near the speaker. Even though human-robot interface is the most common goal of robot audition research, there is research being conducted for other goals. Huang *et al.* [26] use binaural audition to help robots navigate in their environment, allowing a mobile robot to move toward sound-emitting objects without colliding with those object. The approach even works when those objects are not visible (i.e., not in line of sight), which is an advantage over vision.

It is possible to use audition to determine the size and characteristics of a room, as proposed by Tesch and Zimmer [27]. The approach uses a single microphone and can be used for localisation purposes if the room has been visited before. The system works by emitting wideband noise and measuring reverberation characteristics.

Robot audition even has military applications, where a robot uses for instance an array of

eight microphones to detect impulsive noise events in order to locate a sniper weapon [28]. The approach is based on impulse time detection and the localisation is performed using Time Delay of Arrival (TDOA) estimates. The authors claim to be working on a 16-microphone version of their system.

Audition has also been applied to groups of robot⁴ at the Idaho National Engineering and Environmental Laboratory (INEEL). In that case, the robots use chirp sounds and audition to communicate with each other in a simple manner. The robots themselves have very limited auditory capabilities, but the goal is to include a large number of robots. Unfortunately, little information is available about the exact auditory capabilities of the robot.

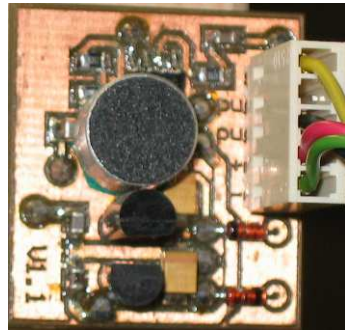
Although not strictly related to audition, work has been done to allow robots to show emotions when talking [29]. This is done by varying speech characteristics such as pitch, rate and intensity. If combined with auditory capabilities, this could enhance robot interactions with humans.

1.2 Experimental Setup

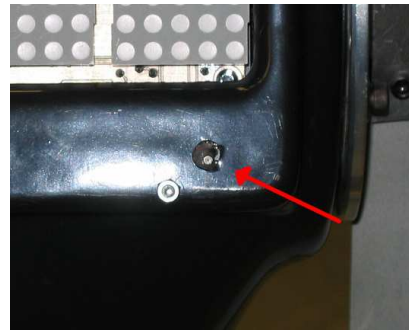
The proposed artificial auditory system is tested using an array of omni-directional microphones, each composed of an electret cartridge mounted on a simple custom pre-amplifier (as shown in Figure 1.1a). The number of microphones is set to eight, as it is the maximum number of analog input channels on commercially available soundcards. Two array configurations are used for the evaluation of the system. The first configuration (C1) is an open array and consists of inexpensive (\sim US\$1 each) microphones arranged on the vertices of a 16 cm cube mounted on top of the *Spartacus* robot (shown in Figure 1.2a). The second configuration (C2) is a closed array and uses smaller, middle-range (\sim US\$20 each) microphones, placed through holes (Figure 1.1b) at different locations on the body of the robot (shown in Figure 1.2b). Although we are mainly interested in the C2 configuration because it is the least intrusive, the C1 configuration is used

⁴<http://www.inel.gov/featurestories/12-01robots.shtml>

to demonstrate the validity of some of the hypotheses we make, as well as the adaptability of the system. It is reported that better localisation and separation results are obtained when maximising the distance between the microphones [30]. So, given the fact that we desire uniform performance regardless of the location of the sources, we spread the microphones evenly (and as far away from each other as possible) on the robot surface.



(a) Electret with pre-amplifier (C1)



(b) Electret installed directly on the robot frame (C2)

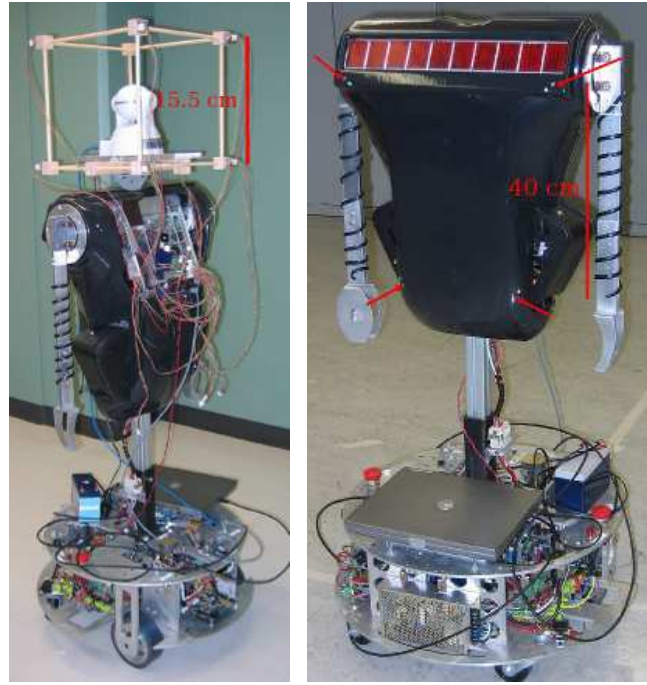
Figure 1.1: Microphones used on the Spartacus robot.

For both arrays, all channels are sampled simultaneously using an RME Hammerfall Multiface DSP connected to a notebook computer (Pentium-M 1.6 GHz CPU) through a CardBus interface. The software part is implemented within the FlowDesigner⁵ environment and is designed to be connected to other components of the robot through the MARIE⁶ framework, as described in [31].

Experiments are performed in two different environments. The first environment (E1) is a medium-size room (10 m \times 11 m, 2.5 m ceiling) with a reverberation time (-60 dB) of 350 ms and moderate noise (ventilation, computers). The second environment (E2) is a hall (16 m \times 17 m, 3.1 m ceiling, connected to other rooms) with a reverberation time of approximately 1.0 s and a high level of background noise. While E2 is a public area, we tried to minimise the noise (by not having people close to the experimental setup) made by other people in order to make the experiments repeatable.

⁵<http://flowdesigner.sourceforge.net/>

⁶<http://marie.sourceforge.net/>



(a) Open array configura- (b) Closed array configura-
tion (C1) (C2)

Figure 1.2: Spartacus robot in configurations.

1.3 Thesis Outline

This thesis is divided in three main parts, corresponding to the three auditory capabilities identified in the introduction: sound source localisation, sound source separation, and integration with speech recognition. A block diagram of the complete artificial auditory system is shown in Figure 1.3.

Chapter 2 describes the localisation subsystem. The method is based on a frequency-domain implementation of a steered beamformer along with a particle filter-based tracking algorithm. Results show that a mobile robot can localise and track in real-time multiple moving sources and can detect most sound sources reliably over a range of 7 meters. These new capabilities allow a mobile robot to interact with people in real life settings.

Chapter 3 presents a method for separating simultaneous sound sources for the separation subsystem. The microphone array and the sound localisation data are used in a real-time im-

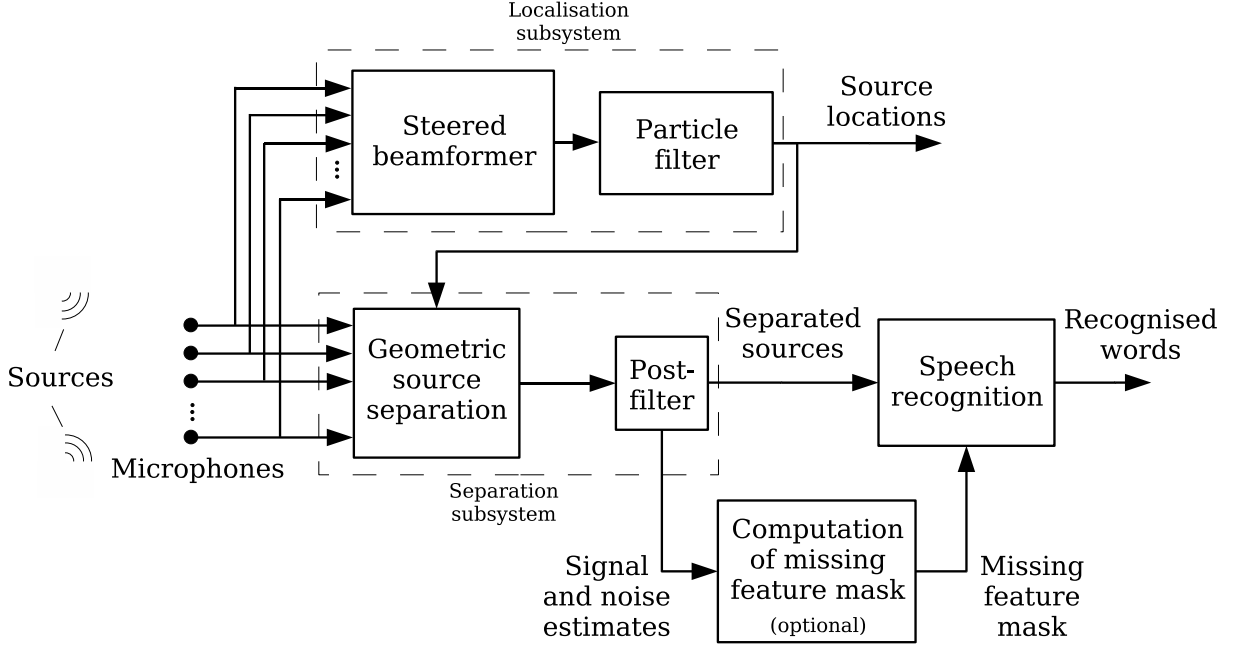


Figure 1.3: Overview of the proposed artificial auditory system.

plementation of the Geometric Source Separation [32] algorithm. A multi-source post-filter is also developed in order to further reduce interferences from other sources as well as background noise. The main advantage of our approach for mobile robots resides in the fact that both the frequency-domain Geometric Source Separation algorithm and the post-filter are able to adapt rapidly to new sources and non-stationarity. Separation results are presented for three simultaneous interfering speakers in the presence of noise. A reduction of log spectral distortion (LSD) and increase of signal-to-noise ratio (SNR) of approximately 8.9 dB and 13.7 dB are observed. When the source of interest is silent, background noise and interference is reduced by 24.5 dB.

Chapter 4 demonstrates the use of the sound separation system to give a mobile robot the ability to perform automatic speech recognition with simultaneous speakers. Two different configurations for speech recognition are tested. In one configuration, the separated audio is sent directly to an automatic speech recogniser (ASR). In the second configuration, the post-filter described in Chapter 3 is used to estimate the reliability of spectral features and compute a missing feature mask that provides the ASR with information about the reliability of spectral features. We show that it is possible to perform speech recognition for up to three simultaneous

speakers, even in a reverberant environment.

Chapter 5 concludes this thesis by summarising the results obtained, listing possible future work, and suggesting applications of this work to other fields.

Chapter 2

Sound Source Localisation

Sound source localisation is defined as the determination of the coordinates of sound sources in relation to a point in space. To perform sound localisation, our brain combines timing (more specifically delay or phase) and amplitude information from the sound perceived by our two ears [33], sometimes in addition to information from other senses. However, localising sound sources using only two inputs is a challenging task. The human auditory system is very complex and resolves the problem by accounting for the acoustic diffraction around the head and the ridges of the outer ear. Without this ability, localisation with two microphones is limited to azimuth only, along with the impossibility to distinguish if the sounds come from the front or the back. Also, obtaining high-precision readings when the sound source is in the same axis as the pair of microphones is more difficult.

One advantage with robots is that they do not have to inherit the same limitations as living creatures. Using more than two microphones allows reliable and accurate localisation in three dimensions (azimuth and elevation). Also, having multiple signals provides additional redundancy, reducing the uncertainty caused by the noise and non-ideal conditions such as reverberation and imperfect microphones. It is with this principle in mind that we have developed an approach allowing to localise sound sources using an array of microphones.

Our approach is based on a frequency-domain beamformer that is steered in all possible dir-

ections to detect sources. Instead of measuring TDOAs and then converting to a position, the localisation process is performed in a single step. This makes the system more robust, especially in the case where an obstacle prevents one or more microphones from properly receiving the signals. The results of the localisation process are then enhanced by probability-based post-processing, which prevents false detection of sources. This makes the system sensitive enough for simultaneous localisation of multiple moving sound sources. This approach is an extension of earlier work [34] and works for both far-field and near-field sound sources. Detection reliability, accuracy, and tracking capabilities of the approach are validated using the Spartacus robot platform, with different types of sound sources.

This chapter is organised as follows. Section 2.1 situates our work in relation to other research projects in the field. Section 2.2 presents a brief overview of the system. Section 2.3 describes our steered beamformer implemented in the frequency-domain. Section 2.4 explains how we enhance the results from the beamformer using a probabilistic post-processor. This is followed by experimental results in Section 2.5, showing how the system behaves under different conditions. Section 2.6 concludes the chapter and presents future work on sound localisation.

2.1 Related Work

Most of the work in relation to localisation of sound sources has been done using only two microphones. This is the case with the SIG robot that uses both inter-aural phase difference (IPD) and inter-aural intensity difference (IID) to locate sounds [12]. The binaural approach has limitations when it comes to evaluating elevation and usually, the front-back ambiguity cannot be resolved without resorting to active audition [35].

More recently, approaches using more than two microphones have been developed. One approach uses a circular array of eight microphones to locate sound sources using the MUSIC algorithm [22], a signal subspace approach. In our previous work also using eight microphones [36], we presented a method for localising a single sound source where time delay of arrival

(TDOA) estimation was separated from the direction of arrival (DOA) estimation. It was found that a system combining TDOA and DOA estimation in a single step improves the system's robustness, while allowing localisation (but not tracking) of simultaneous sources [34]. Kagami *et al.* [37] reports a system using 128 microphones for 2D sound localisation of sound sources. Similarly, Wang *et al.* [38] use 24 fixed microphones to track a moving robot in a room. However, it would not be practical to include such a large number of microphones on a mobile robot.

Most of the work so far on localisation of source sources does not address the problem of tracking moving sources. It is proposed in [39] to use a Kalman filter for tracking a moving source. However the proposed method assumes that a single source is present. In the past years, particle filtering [40] (a sequential Monte Carlo method) has been increasingly popular to resolve object tracking problems. Ward *et al.* [41, 42] and Vermaak [43] use this technique for tracking single sound sources. Asoh *et al.* [23] even suggested to use this technique for mixing audio and video data to track speakers. But again, the technique is limited to a single source due to the problem of associating the localisation observation data to each of the sources being tracked. We refer to that problem as the source-observation assignment problem. Some attempts are made at defining multi-modal particle filters in [44], and the use of particle filtering for tracking multiple targets is demonstrated in [45, 46, 47]. But so far, the technique has not been applied to sound source tracking. Our work demonstrates that it is possible to track multiple sound sources using particle filters by solving the source-observation assignment problem.

2.2 System Overview

The proposed localisation and tracking system, as shown in Figure 2.1, is composed of three parts:

- A microphone array;
- A memoryless localisation algorithm based on a steered beamformer;

- A particle filtering tracker.

The array is composed of up to eight omni-directional microphones mounted on the robot. Since the system is designed to be installed on any robot, there is no strict constraint on the position of the microphones: only their positions must be known in relation to each other (measured with ~ 0.5 cm accuracy). The microphone signals are used by a beamformer (spatial filter) that is steered in all possible directions in order to maximise the output energy. The initial localisation performed by the steered beamformer is then used as the input of a post-processing stage that uses particle filtering to simultaneously track all sources and prevent false detections. The output of the localisation system can be used to direct the robot attention to the source. It can also be used as part of a source separation algorithm to isolate the sound coming from a single source, as described in Chapter 3.

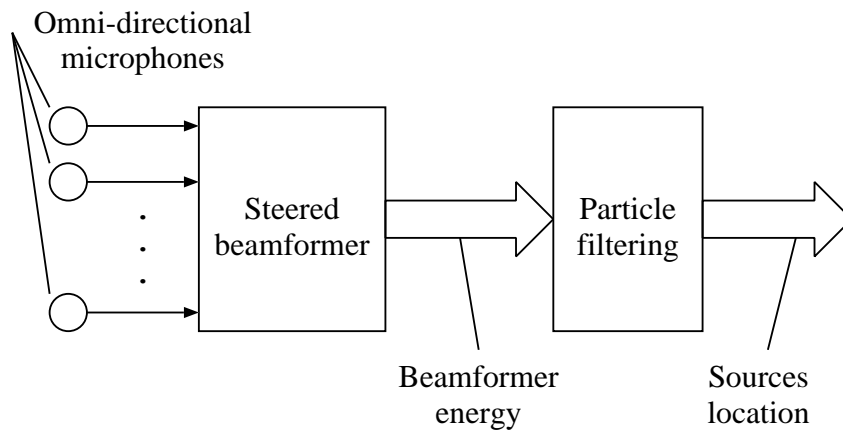


Figure 2.1: Overview of the Localisation subsystem.

2.3 Localisation Using a Steered Beamformer

The basic idea behind the steered beamformer approach to source localisation is to direct a beamformer in all possible directions and look for maximal output. This can be done by maximising the output energy of a simple delay-and-sum beamformer. The formulation in both time and frequency domain is presented in Section 2.3.1. Section 2.3.2 describes the frequency-

domain weighting performed on the microphone signals and Section 2.3.3 shows how the search is performed. A possible modification for improving the resolution is described in Section 2.3.4.

2.3.1 Delay-And-Sum Beamformer

The output $y(n_t)$ of an N -microphone delay-and-sum beamformer is defined as:

$$y(n_t) = \sum_{n=0}^{N-1} x_n(n_t - \tau_n) \quad (2.1)$$

where $x_n(n_t)$ is the signal from the n^{th} microphone and τ_n is the delay of arrival for that microphone. The output energy of the beamformer over a frame of length L is thus given by:

$$\begin{aligned} E &= \sum_{n_t=0}^{L-1} [y(n_t)]^2 \\ &= \sum_{n_t=0}^{L-1} [x_0(n_t - \tau_0) + \dots + x_{N-1}(n_t - \tau_{N-1})]^2 \end{aligned} \quad (2.2)$$

Assuming that only one sound source is present, we can see that E will be maximal when the delays τ_n are such that the microphone signals are in phase, and therefore add constructively.

One problem with this technique is that energy peaks are very wide [48], which means that the accuracy on τ_n is poor. Moreover, in the case where multiple sources are present, it is likely for the two or more energy peaks to overlap, making them impossible to distinguish. One way to narrow the peaks is to whiten the microphone signals prior to computing the energy [49]. Unfortunately, the coarse-fine search method as proposed in [48] cannot be used in that case because the narrow peaks can then be missed during the coarse search. Therefore, a full fine search is necessary, which requires increased computing power.

It is however possible to reduce the amount of computation by calculating the beamformer energy in the frequency domain. This also has the advantage of making the whitening of the signal easier. To do so, the beamformer output energy in Equation 2.2 can be expanded as:

$$\begin{aligned}
E &= \sum_{n=0}^{N-1} \sum_{n_t=0}^{L-1} x_n^2 (n_t - \tau_n) \\
&+ 2 \sum_{n_1=0}^{N-1} \sum_{n_2=0}^{n_1-1} \sum_{n_t=0}^{L-1} x_{n_1} (n_t - \tau_{n_1}) x_{n_2} (n_t - \tau_{n_2})
\end{aligned} \tag{2.3}$$

which in turn can be rewritten in terms of cross-correlations:

$$E = K + 2 \sum_{n_1=0}^{N-1} \sum_{n_2=0}^{n_1-1} R_{x_{n_1}, x_{n_2}} (\tau_{n_1} - \tau_{n_2}) \tag{2.4}$$

where $K = \sum_{n=0}^{N-1} \sum_{n_t=0}^{L-1} x_n^2 (n_t - \tau_n)$ is nearly constant with respect to the τ_m delays and can thus be ignored when maximising E . The cross-correlation function can be approximated in the frequency domain as:

$$R_{ij}(\tau) \approx \sum_{k=0}^{L-1} X_i(k) X_j(k)^* e^{j2\pi k\tau/L} \tag{2.5}$$

where $X_i(k)$ is the discrete Fourier transform of $x_i(n_t)$, $X_i(k)X_j(k)^*$ is the cross-spectrum of $x_i(n_t)$ and $x_j(n_t)$ and $(\cdot)^*$ denotes the complex conjugate. The power spectra and cross-power spectra are computed on overlapping windows (50% overlap) of $L = 1024$ samples at 48 kHz. The cross-correlations $R_{ij}(\tau)$ are computed by averaging the cross-power spectra $X_i(k)X_j(k)^*$ over a time period of 4 frames (40 ms). Once the $R_{ij}(\tau)$ are pre-computed, it is possible to compute E using only $N(N-1)/2$ lookup and accumulation operations, whereas a time-domain computation would require $2L(N+2)$ operations. For example, for $N = 8$ microphones and $N_g = 2562$ directions, it follows that the complexity of the search itself is reduced from 1.2 Gflops to only 1.7 Mflops. After counting all time-frequency transformations, the complexity is only 48.4 Mflops, 25 times less than a time domain search with the same resolution.

2.3.2 Spectral Weighting

In the frequency domain, the whitened cross-correlation (also known as the phase transform, or PHAT) is computed as:

$$R_{ij}^{(w)}(\tau) \approx \sum_{k=0}^{L-1} \frac{X_i(k)X_j(k)^*}{|X_i(k)||X_j(k)|} e^{j2\pi k\tau/L} \quad (2.6)$$

While it produces much sharper cross-correlation peaks, the whitened cross-correlation has one drawback: each frequency bin of the spectrum contributes the same amount to the final correlation, even if the signal at that frequency is dominated by noise. This makes the system less robust to noise, while making detection of voice (which has a narrow bandwidth) more difficult. In order to alleviate the problem, we introduce a weighting function that acts as a mask based on the signal-to-noise ratio (SNR). For microphone i , we define this weighting function as:

$$\zeta_i^\ell(k) = \frac{\xi_i^\ell(k)}{\xi_i^\ell(k) + 1} \quad (2.7)$$

where $\xi_i^\ell(k)$ is an estimate of the *a priori* SNR at the i^{th} microphone, at time frame ℓ , for frequency k . It is computed using the decision-directed approach proposed by Ephraim and Malah [50]:

$$\xi_i^\ell(k) = \frac{(1 - \alpha_d) [\zeta_i^{\ell-1}(k)]^2 |X_i^{\ell-1}(k)|^2 + \alpha_d |X_i^\ell(k)|^2}{\sigma_i^2(k)} \quad (2.8)$$

where $\alpha_d = 0.1$ is the adaptation rate and $\sigma_i^2(k)$ is the noise estimate for microphone i . It is easy to estimate $\sigma_i^2(k)$ using the Minima-Controlled Recursive Average (MCRA) technique [51], which adapts the noise estimate during periods of low energy.

It is also possible to make the system more robust to reverberation by modifying the weighting function to include a reverberation term $\lambda_i^{rev}(k, \ell)$ to the noise estimate at time frame ℓ . We use a simple reverberation model with exponential decay:

$$\lambda_i^{rev}(k, \ell) = \gamma \lambda_i^{rev}(k, \ell) + \frac{(1 - \gamma)}{\delta} |\zeta_i^\ell(k) X_i^{\ell-1}(k)|^2 \quad (2.9)$$

where γ represents the reverberation time (T_{60}) of the room ($\gamma = 10^{-6/T_{60}}$), δ is the Signal-to-Reverberant Ratio (SRR) and $\lambda_i^{rev}(k, -1) = 0$. In some sense, Equation 2.9 can be seen as modelling the *precedence effect* [52, 53] in order to give less weight to frequency bins where a loud sound was recently present. The resulting enhanced cross-correlation is defined as:

$$R_{ij}^{(e)}(\tau) = \sum_{k=0}^{L-1} \frac{\zeta_i(k) X_i(k) \zeta_j(k) X_j(k)^*}{|X_i(k)| |X_j(k)|} e^{j2\pi k\tau/L} \quad (2.10)$$

The spectral weighting described above has similarities with the maximum likelihood (ML) weighting described in [54], with two main differences. The first is that the weight we use requires a lower complexity because it can be applied directly to the spectrum of the signals. The second difference is that in high SNR conditions, the cross-correlation peak can take very large values, and is thus more difficult to use for evaluating the probability that a source is really present (see Section 2.4.2).

The advantage of our approach over the simpler PHAT lies in the fact that the PHAT does not take into account noise at all and assumes that the signal-to-reverberant ratio (SRR) is constant across frequency [54]. The latter assumption only holds when the signal being tracked is relatively stationary (i.e., no transients) compared to the reverberation time. For this reason, the PHAT cannot model the precedence effect. In practice, it was found that when the presence of a sound source is known, the localisation accuracy using our weighting is similar to that obtained using the PHAT. The main difference is that our weighting makes it easier to estimate if a source is really present. As far as we are aware, no other work focuses on sound source localisation when the number of sources present is unknown (and detection becomes important).

2.3.3 Direction Search on a Spherical Grid

In order to reduce the computation required and to make the system isotropic, we define a uniform triangular grid for the surface of a sphere. To create the grid, we start with an initial icosahedral grid [55]. Each triangle in the initial 20-element grid is recursively subdivided into

four smaller triangles, as shown in Figure 2.2. The resulting grid is composed of 5120 triangles and 2562 points. The beamformer energy is then computed for the hexagonal region associated with each of these points. Each of the 2562 regions covers a radius of about 2.5° around its centre, setting the resolution of the search.

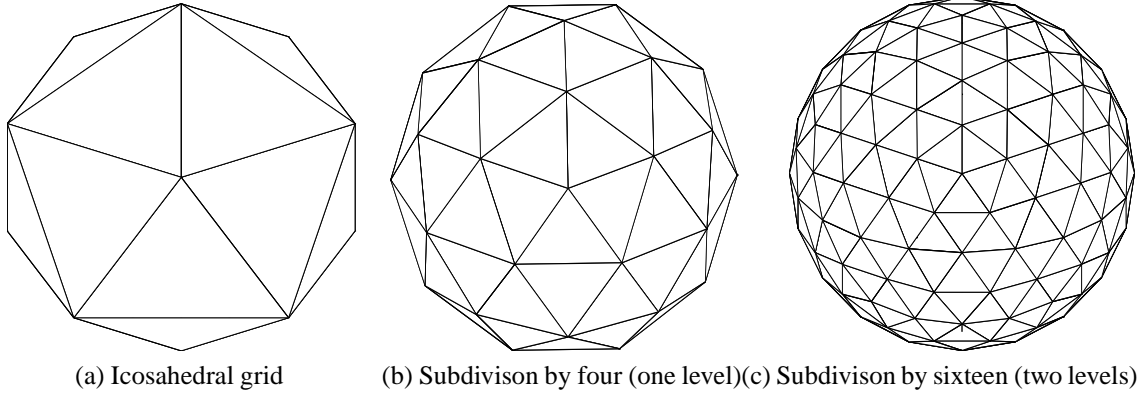


Figure 2.2: Recursive subdivision of a triangular element.

Algorithm 2.1 Steered beamformer direction search.

```

for all grid index  $k$  do
   $E_k \leftarrow 0$ 
  for all microphone pair  $ij$  do
     $\tau \leftarrow \text{lookup}(k, ij)$ 
     $E_k \leftarrow E_k + R_{ij}^{(e)}(\tau)$ 
  end for
end for
 $\text{direction of source} \leftarrow \text{argmax}_k (E_k)$ 

```

Once the cross-correlations $R_{ij}^{(e)}(\tau)$ are computed, the search for the best direction on the grid is performed as described by Algorithm 2.1. The *lookup* parameter is a pre-computed table of the time delay of arrival (TDOA) for each microphone pair and each direction on the sphere. Using the far-field assumption as illustrated in Figure 2.3, the TDOA in samples is computed using the cosine law [36]:

$$\cos \phi = \frac{c\tau_{ij}/F_s}{\|\vec{\mathbf{p}}_i - \vec{\mathbf{p}}_j\|} = \frac{(\vec{\mathbf{p}}_i - \vec{\mathbf{p}}_j) \cdot \vec{\mathbf{u}}}{\|\vec{\mathbf{p}}_i - \vec{\mathbf{p}}_j\| \|\vec{\mathbf{u}}\|} \quad (2.11)$$

where \vec{p}_i is the position of microphone i , \vec{u} is a unit-vector that points in the direction of the source, c is the speed of sound and F_s is the sampling rate. Isolating τ_{ij} from Equation 2.11 and knowing that \vec{u} is a unit vector, we obtain:

$$\tau_{ij} = \frac{F_s}{c} (\vec{p}_i - \vec{p}_j) \cdot \vec{u} \quad (2.12)$$

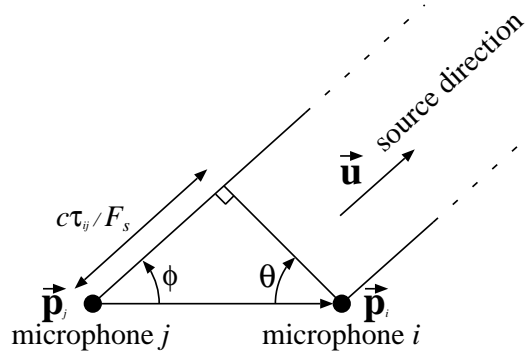


Figure 2.3: TDOA for the far field approximation.

Equation 2.12 assumes that the time delay is proportional to the distance between the source and microphone. This is only true when there is no diffraction involved. While this hypothesis is only verified for an “open” array (all microphones are in line of sight with the source), in practice we demonstrate experimentally (see Section 2.5) that the approximation is good enough for our system to work for a “closed” array (in which there are obstacles within the array).

For an array of N microphones and an N_g -element grid, the algorithm requires $N(N-1)N_g$ table memory accesses and $N(N-1)N_g/2$ additions. In the proposed configuration ($N_g = 2562$, $N = 8$), the accessed data can be made to fit entirely in a modern processor’s L2 cache.

Using Algorithm 2.1, our system is able to find the loudest source present by maximising the energy of a steered beamformer. In order to localise other sources that may be present, the process is repeated by removing the contribution of the first source to the cross-correlations, leading to Algorithm 2.2. Since we do not know how many sources are present, the number of sources to find is set to the constant Q . Therefore, Algorithm 2.2 finds the Q loudest sources

Algorithm 2.2 Localisation of multiple sources.

```

for  $q = 0$  to  $Q - 1$  do
   $D_q \leftarrow$  Steered beamformer direction search
  for all microphone pair  $ij$  do
     $\tau \leftarrow \text{lookup}(D_q, ij)$ 
     $R_{ij}^{(e)}(\tau) = 0$ 
  end for
end for

```

around the array. We determined empirically that the maximum number of sources our beamformer is able to locate at once is four. The fact that Algorithm 2.2 always finds four sources regardless of the number of sources present leads to a high rate of false detection, even when four or more sources are present. That problem is handled by the particle filter described in Section 2.4.

2.3.4 Direction Refining

When a source is located using Algorithm 2.1, the direction accuracy is limited by the size of the grid used. It is however possible, as an optional step, to further refine the source location estimate. In order to do so, we define a refined grid for the surrounding of the point where a source was found. To take into account the near-field effects, the grid is refined in three dimensions: horizontally, vertically and over distance. Using five points in each direction, we obtain a 125-point local grid with a maximum error of around 1° . For the near-field case, Equation 2.12 no longer holds, so it is necessary to compute the time differences as:

$$\tau_{ij} = \frac{F_s}{c} (\|d\vec{u} - \vec{p}_j\| - \|d\vec{u} - \vec{p}_i\|) \quad (2.13)$$

where d is the distance between the source and the centre of the array. Equation 2.13 is evaluated for five distances d (ranging from 50 cm to 5 m) in order to find the direction of the source with improved accuracy. Unfortunately, it was observed that the value of d found in the search is too unreliable to provide a good estimate of the distance between the source and the array. The

incorporation of the distance nonetheless allows improved accuracy for the near field case.

2.4 Particle-Based Tracking

The steered beamformer detailed in Section 2.3 provides only instantaneous, noisy information about sources being possibly present, and no information about the behaviour of the source in time (i.e. tracking). For that reason, it is desirable to use a probabilistic temporal integration to track the different sound sources based on all measurements available up to the current time.

It has been shown [41, 42, 23] that particle filters are an effective way of tracking sound sources. The choice of particle filtering is further motivated by the fact that earlier work using a fixed grid for tracking showed that the technique can not provide continuous tracking when moving sources had short periods of silence. This can be observed in Figure 2.4, taken from [34]. Particle filtering is also preferred to Kalman filtering because key aspects of the proposed algorithm, such as the handling of false detections and source-observation assignment (see Section 2.4.3), cannot be adequately modelled as a Gaussian process, as is assumed by the Kalman filter [39].

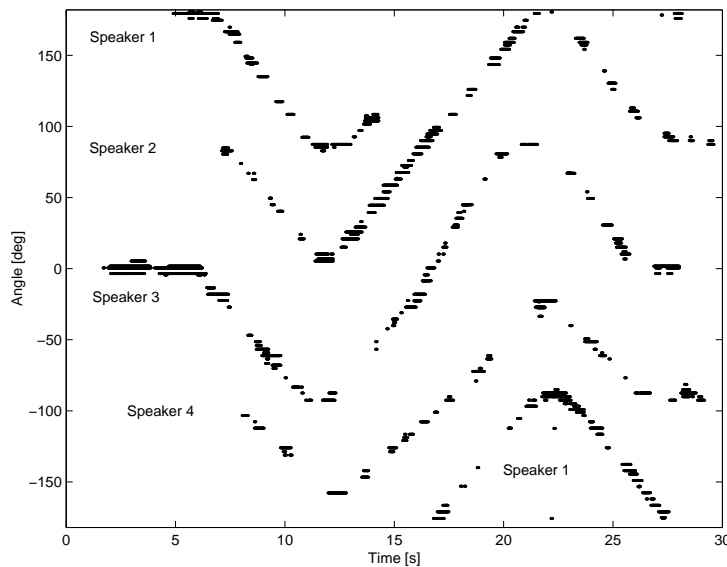


Figure 2.4: Probabilistic tracking of multiple sources using a fixed grid.

Let $\mathbf{S}_j^{(t)}$ be the state variable associated to source j ($j = 0, 1, \dots, M-1$) at time t , a particle filter approximates the probability density function (pdf) of $\mathbf{S}_j^{(t)}$ as:

$$p\left(\mathbf{S}_j^{(t)}\right) \approx \sum_{i=1}^{N_p} w_{j,i}^{(t)} \delta\left(\mathbf{S}_j^{(t)} - \mathbf{s}_{j,i}^{(t)}\right)$$

where $\delta\left(\mathbf{S}_j^{(t)} - \mathbf{s}_{j,i}^{(t)}\right)$ is the Dirac function for a particle of state $\mathbf{s}_{j,i}^{(t)}$, $w_{j,i}^{(t)}$ is the particle weight and N_p is the number of particles. With this approach, each particle can be viewed as representing a hypothesis about the location of a sound source and the weights assigned to the particles represent the probability for each hypothesis to be correct. The state vector for the particles is composed of six dimensions, three for the position $\mathbf{x}_{j,i}^{(t)}$ and three for its derivative:

$$\mathbf{s}_{j,i}^{(t)} = \begin{bmatrix} \mathbf{x}_{j,i}^{(t)} \\ \dot{\mathbf{x}}_{j,i}^{(t)} \end{bmatrix} \quad (2.14)$$

Figure 2.5 illustrates the particle representation of two sources. The source in red is located around 60 degrees azimuth and 15 degrees elevation while the source in green is located around -60 degrees azimuth and 20 degrees elevation. The spread of the particles is an indicator of the uncertainty on the source position.

Since the particle position is constrained to lie on a unit sphere and the speed is tangent to the sphere, there are only four degrees of freedom. The particle filtering algorithm is outlined in Algorithm 2.3 and generalises sound source tracking to an arbitrary and non-constant number of sources. The steps are detailed in Subsections 2.4.1 to 2.4.7. The particle weights are updated by taking into account observations obtained from the steered beamformer and by computing the assignment between these observations and the sources being tracked. From there, the estimated location of the source is the weighted mean of the particle positions.

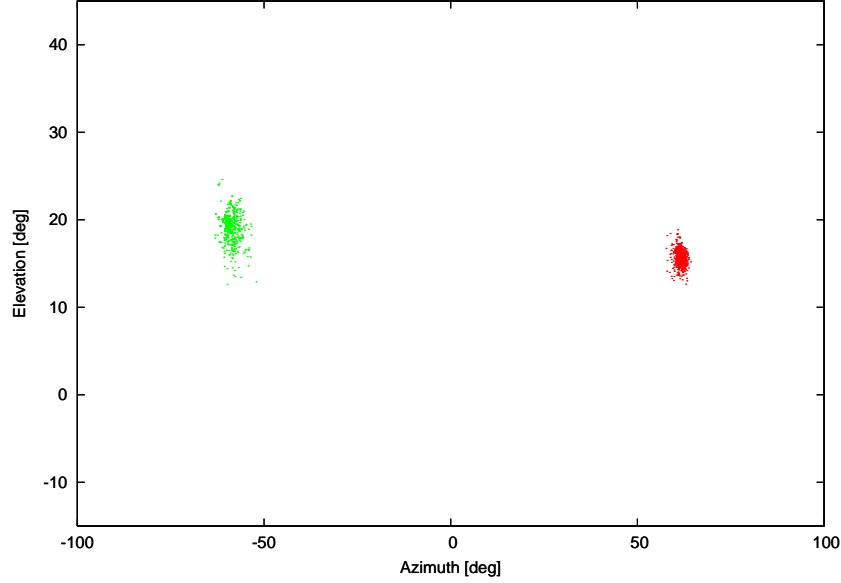


Figure 2.5: Example of two sources being represented by a particle filter.

Algorithm 2.3 Particle-based tracking algorithm. Steps 1 to 7 correspond to Subsections 2.4.1 to 2.4.7.

1. Predict the state $\mathbf{s}_j^{(t)}$ from $\mathbf{s}_j^{(t-1)}$ for each source j .
 2. Compute instantaneous direction probabilities associated with the steered beamformer response.
 3. Compute probabilities $P_{q,j}^{(t)}$ associating beamformer peaks to sources being tracked.
 4. Compute updated particle weights $w_{j,i}^{(t)}$.
 5. Add or remove sources if necessary.
 6. Compute source localisation estimate $\bar{\mathbf{x}}_j^{(t)}$ for each source.
 7. Resample particles for each source if necessary and go back to step 1.
-

2.4.1 Prediction

The prediction step in particle filtering plays a similar role as for the Kalman filter. However, instead of explicitly predicting the mean and variance of the model, the particles are subjected to a stochastic excitation with damping model as proposed in [42]:

$$\dot{\mathbf{x}}_{j,i}^{(t)} = a\dot{\mathbf{x}}_{j,i}^{(t-1)} + bF_{\mathbf{x}} \quad (2.15)$$

$$\mathbf{x}_{j,i}^{(t)} = \mathbf{x}_{j,i}^{(t-1)} + \Delta T \dot{\mathbf{x}}_{j,i}^{(t)} \quad (2.16)$$

where $a = e^{-\alpha\Delta T}$ controls the damping term, $b = \beta\sqrt{1 - a^2}$ controls the excitation term, $F_{\mathbf{x}}$ is a normally distributed random variable of unit variance and ΔT is the time interval between updates. In addition, we consider three possible states:

- Stationary source ($\alpha = 2, \beta = 0.04$);
- Constant velocity source ($\alpha = 0.05, \beta = 0.2$);
- Accelerated source ($\alpha = 0.5, \beta = 0.2$).

A normalisation step¹ ensures that $\mathbf{x}_i^{(t)}$ still lies on the unit sphere ($\|\mathbf{x}_{j,i}^{(t)}\| = 1$) after applying Equations 2.15 and 2.16.

2.4.2 Instantaneous Direction Probabilities from Beamformer Response

The steered beamformer described in Section 2.3 produces an observation $O^{(t)}$ for each time t . The observation $O^{(t)} = [O_0^{(t)} \dots O_{Q-1}^{(t)}]$ is composed of Q potential source locations \mathbf{y}_q found by Algorithm 2.2. We also denote $\mathbf{O}^{(t)}$, the set of all observations $O^{(t)}$ up to time t . We introduce the probability P_q that the potential source q is a true source (not a false detection). The value of P_q can be interpreted as our confidence in the steered beamformer output. For the first source ($q = 0$), we have observed that the higher the beamformer energy, the more likely that potential source is to be true. However, for the other potential sources ($q > 0$), false alarms are very frequent and independent of energy. With this in mind, for the four potential sources q ,

¹The normalisation is performed as $\mathbf{x}_i^{(t)} \leftarrow \mathbf{x}_i^{(t)} / \|\mathbf{x}_i^{(t)}\|$.

we define P_q empirically as:

$$P_q = \begin{cases} \nu^2/2, & q = 0, \nu \leq 1 \\ 1 - \nu^{-2}/2, & q = 0, \nu > 1 \\ 0.3, & q = 1 \\ 0.16, & q = 2 \\ 0.03, & q = 3 \end{cases} \quad (2.17)$$

with $\nu = E_0/E_T$, where E_T is a threshold that depends on the number of microphones, the frame size and the analysis window used (we empirically found that $E_T = 150$ is appropriate for eight microphones). Figure 2.6 shows an example of P_q values for potential sources found by the steered beamformer in a case with four moving sources². It is possible to distinguish four trajectories, but it can be seen that the observations from the steered beamformer are nonetheless very noisy.

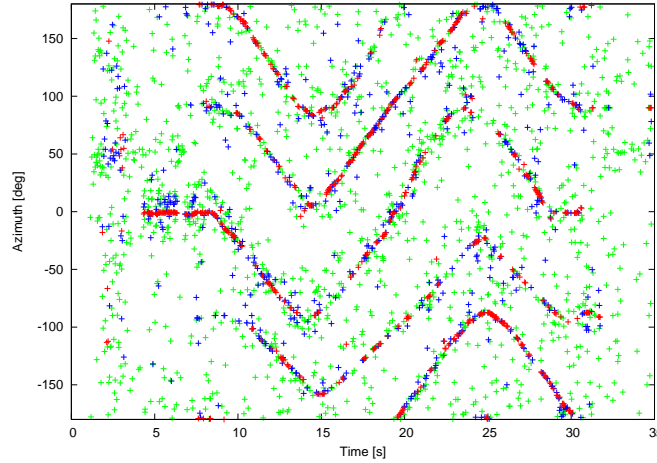


Figure 2.6: Beamformer output probabilities P_q for azimuth as a function of time. Observations with $P_q > 0.5$ shown in red, $0.2 < P_q < 0.5$ in blue, $P_q < 0.2$ in green.

At time t , the probability density of observing $O_q^{(t)}$ for a source located at particle position $\mathbf{x}_{j,i}^{(t)}$ is given by:

$$p\left(O_q^{(t)} \mid \mathbf{x}_{j,i}^{(t)}\right) = \mathcal{N}\left(\mathbf{y}_q; \mathbf{x}_{j,i}; \sigma^2\right) \quad (2.18)$$

²Only the azimuth part of \mathbf{y}_q is shown as a function of time.

where $\mathcal{N}(\mathbf{y}_q; \mathbf{x}_{j,i}; \sigma^2)$ is a normal distribution centred at $\mathbf{x}_{j,i}$ with variance σ^2 evaluated at \mathbf{y}_q , and models the localisation accuracy of the steered beamformer. We use $\sigma = 0.05$, which corresponds to an RMS error of 3 degrees for the location found by the steered beamformer.

2.4.3 Probabilities for Multiple Sources

Before we can derive the update rule for the particle weights $w_{j,i}^{(t)}$, we must first introduce the concept of source-observation assignment. For each potential source q detected by the steered beamformer, there are three possibilities:

- It is a false detection (H_0).
- It corresponds to one of the sources currently tracked (H_1).
- It corresponds to a new source that is not yet being tracked (H_2).

In the case of H_1 , we need to determine which tracked source j corresponds to potential source q . First, we assume that a potential source may correspond to at most one tracked source and that a tracked source can correspond to at most one potential source.

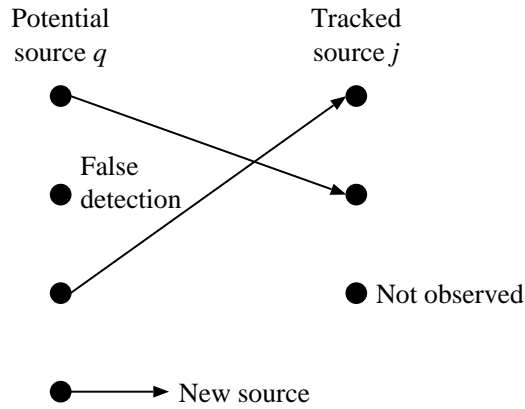


Figure 2.7: Assignment example where two of the tracked sources are observed, with one new source and one false detection. The assignment can be described as $f(\{0, 1, 2, 3\}) = \{1, -2, 0, -1\}$.

Let $f : \{0, 1, \dots, Q-1\} \longrightarrow \{-2, -1, 0, 1, \dots, M-1\}$ be a function assigning observation q to the source j (values -2 is used for false detection and -1 is used for a new source). Figure 2.7

illustrates a hypothetical case with four potential sources detected by the steered beamformer and their assignment to the tracked sources. Knowing $P(f | O^{(t)})$ (the probability that f is the correct assignment given observation $O^{(t)}$) for all possible f , we can derive $P_{q,j}$, the probability that the tracked source j corresponds to the potential source q as:

$$P_{q,j}^{(t)} = \sum_f \delta_{j,f(q)} P(f | O^{(t)}) \quad (2.19)$$

$$P_q^{(t)}(H_0) = \sum_f \delta_{-2,f(q)} P(f | O^{(t)}) \quad (2.20)$$

$$P_q^{(t)}(H_2) = \sum_f \delta_{-1,f(q)} P(f | O^{(t)}) \quad (2.21)$$

where $\delta_{i,j}$ is the Kronecker delta. Equation 2.19 is in fact the sum of the probabilities of all f that assign potential source q to tracked source j and similarly for Equations 2.20 and 2.21.

Omitting t for clarity, the probability $P(f|O)$ is given by:

$$P(f|O) = \frac{p(O|f)P(f)}{p(O)} \quad (2.22)$$

Knowing that there is only one correct assignment ($\sum_f P(f|O) = 1$), we can avoid computing the denominator $p(O)$ by using normalisation. Assuming conditional independence of the observations given the mapping function, we can decompose $p(O|f)$ into individual components:

$$p(O|f) = \prod_q p(O_q|f(q)) \quad (2.23)$$

We assume that the distribution of the false detections (H_0) and the new sources (H_2) are uniform, while the distribution for tracked sources (H_1) is the pdf approximated by the particle distribution convolved with the steered beamformer error pdf:

$$p(O_q|f(q)) = \begin{cases} 1/4\pi, & f(q) = -2 \\ 1/4\pi, & f(q) = -1 \\ \sum_i w_{f(q),i} p(O_q|\mathbf{x}_{j,i}), & f(q) \geq 0 \end{cases} \quad (2.24)$$

The *a priori* probability of f being the correct assignment is also assumed to come from independent individual components, so that:

$$P(f) = \prod_q P(f(q)) \quad (2.25)$$

with:

$$P(f(q)) = \begin{cases} (1 - P_q) P_{false}, & f(q) = -2 \\ P_q P_{new} & f(q) = -1 \\ P_q P \left(Obs_j^{(t)} \mid \mathbf{O}^{(t-1)} \right) & f(q) \geq 0 \end{cases} \quad (2.26)$$

where P_{new} is the *a priori* probability that a new source appears and P_{false} is the *a priori* probability of false detection. The probability $P \left(Obs_j^{(t)} \mid \mathbf{O}^{(t-1)} \right)$ that source j is observable (i.e., that it exists and is active) at time t is given by:

$$P \left(Obs_j^{(t)} \mid \mathbf{O}^{(t-1)} \right) = P \left(E_j \mid \mathbf{O}^{(t-1)} \right) P \left(A_j^{(t)} \mid \mathbf{O}^{(t-1)} \right) \quad (2.27)$$

where E_j is the event that source j actually exists and $A_j^{(t)}$ is the event that it is active (but not necessarily detected) at time t . By active, we mean that the signal it emits is non-zero (for example, a speaker who is not making a pause). The probability that the source exists is given by:

$$P \left(E_j \mid \mathbf{O}^{(t-1)} \right) = P_j^{(t-1)} + \left(1 - P_j^{(t-1)} \right) \frac{P_o P \left(E_j \mid \mathbf{O}^{(t-2)} \right)}{1 - (1 - P_o) P \left(E_j \mid \mathbf{O}^{(t-2)} \right)} \quad (2.28)$$

where P_o is the *a priori* probability that a source is not observed (i.e., undetected by the steered beamformer) even if it exists (with $P_o = 0.2$ in our case) and $P_j^{(t)} = \sum_q P_{q,j}^{(t)}$ is the probability that source j is observed (assigned to any of the potential sources).

Assuming a first order Markov process, we can write the following about the probability of source activity:

$$\begin{aligned} P \left(A_j^{(t)} \mid \mathbf{O}^{(t-1)} \right) &= P \left(A_j^{(t)} \mid A_j^{(t-1)} \right) P \left(A_j^{(t-1)} \mid \mathbf{O}^{(t-1)} \right) \\ &\quad + P \left(A_j^{(t)} \mid \neg A_j^{(t-1)} \right) \left[1 - P \left(A_j^{(t-1)} \mid \mathbf{O}^{(t-1)} \right) \right] \end{aligned} \quad (2.29)$$

with $P\left(A_j^{(t)} \mid A_j^{(t-1)}\right)$ the probability that an active source remains active (set to 0.95), and $P\left(A_j^{(t)} \mid \neg A_j^{(t-1)}\right)$ the probability that an inactive source becomes active again (set to 0.05). Assuming that the active and inactive states are equiprobable, the activity probability is computed using Bayes' rule and usual probability manipulations:

$$P\left(A_j^{(t)} \mid \mathbf{O}^{(t)}\right) = \frac{1}{1 + \frac{[1 - P(A_j^{(t)} \mid \mathbf{O}^{(t-1)})][1 - P(A_j^{(t)} \mid O^{(t)})]}{P(A_j^{(t)} \mid \mathbf{O}^{(t-1)})P(A_j^{(t)} \mid O^{(t)})}} \quad (2.30)$$

2.4.4 Weight Update

At times t , the new particle weights for source j are defined as:

$$w_{j,i}^{(t)} = p\left(\mathbf{x}_{j,i}^{(t)} \mid \mathbf{O}^{(t)}\right) \quad (2.31)$$

Assuming that the observations are conditionally independent given the source position, and knowing that for a given source j , $\sum_{i=1}^{N_p} w_{j,i}^{(t)} = 1$, we obtain through Bayesian inference:

$$\begin{aligned} w_{j,i}^{(t)} &= \frac{p\left(\mathbf{O}^{(t)} \mid \mathbf{x}_{j,i}^{(t)}\right) p\left(\mathbf{x}_{j,i}^{(t)}\right)}{p\left(\mathbf{O}^{(t)}\right)} \\ &= \frac{p\left(O^{(t)} \mid \mathbf{x}_{j,i}^{(t)}\right) p\left(\mathbf{O}^{(t-1)} \mid \mathbf{x}_{j,i}^{(t)}\right) p\left(\mathbf{x}_{j,i}^{(t)}\right)}{p\left(\mathbf{O}^{(t)}\right)} \\ &= \frac{p\left(\mathbf{x}_{j,i} \mid O^{(t)}\right) p\left(\mathbf{x}_{j,i}^{(t)} \mid \mathbf{O}^{(t-1)}\right) p\left(O^{(t)}\right) p\left(\mathbf{O}^{(t-1)}\right)}{p\left(\mathbf{O}^{(t)}\right) p\left(\mathbf{x}_{j,i}^{(t)}\right)} \\ &= \frac{p\left(\mathbf{x}_{j,i}^{(t)} \mid O^{(t)}\right) w_{j,i}^{(t-1)}}{\sum_{i=1}^{N_p} p\left(\mathbf{x}_{j,i}^{(t)} \mid O^{(t)}\right) w_{j,i}^{(t-1)}} \end{aligned} \quad (2.32)$$

Let $I_j^{(t)}$ denote the event that source j is observed at time t and knowing that $P\left(I_j^{(t)}\right) = P_j^{(t)} = \sum_q P_{q,j}^{(t)}$, we have:

$$p\left(\mathbf{x}_{j,i}^{(t)} \mid O^{(t)}\right) = \left(1 - P_j^{(t)}\right) p\left(\mathbf{x}_{j,i}^{(t)} \mid O^{(t)}, \neg I_j^{(t)}\right) + P_j^{(t)} p\left(\mathbf{x}_{j,i}^{(t)} \mid O^{(t)}, I_j^{(t)}\right) \quad (2.33)$$

In the case where no observation matches the source, all particles have the same probability, so we obtain:

$$p\left(\mathbf{x}_{j,i}^{(t)} \mid O^{(t)}\right) = \left(1 - P_j^{(t)}\right) \frac{1}{N_p} + P_j \frac{\sum_{q=1}^Q P_{q,j}^{(t)} p\left(O_q^{(t)} \mid \mathbf{x}_{j,i}^{(t)}\right)}{\sum_{i=1}^N \sum_{q=1}^Q P_{q,j}^{(t)} p\left(O_q^{(t)} \mid \mathbf{x}_{j,i}^{(t)}\right)} \quad (2.34)$$

where the denominator on the right side of Equation 2.34 provides normalisation for the $I_j^{(t)}$ case, so that $\sum_{i=1}^N p\left(\mathbf{x}_{j,i}^{(t)} \mid O^{(t)}, I_j^{(t)}\right) = 1$.

2.4.5 Adding or Removing Sources

In a real environment, sources may appear or disappear at any moment. If, at any time, $P_q(H_2)$ is higher than a threshold empirically set³ to 0.3, we consider that a new source is present. In that case, a set of particles is created for source q . Even when a new source is created, it is only assumed to exist if its probability of existence $P\left(E_j \mid \mathbf{O}^{(t)}\right)$ reaches a certain threshold, which we empirically set⁴ to 0.98. At this point, the probability of existence is set to 1 and ceases to be updated.

In the same way, we set a time limit (typically two seconds) on sources. If the source has not been observed ($P_j^{(t)} < T_{obs}$) for a certain amount of time, we consider that it no longer exists. In that case, the corresponding particle filter is no longer updated nor considered in future calculations. The value of T_{obs} only determines whether a discontinuous source will be considered as one or two sources.

³The value must be small enough for all sources to be detected, but large enough to prevent a large number of false alarms from being tracked.

⁴The exact value does not have a significant impact on the performance of the system

2.4.6 Parameter Estimation

The estimated position $\hat{\mathbf{x}}_j^{(t)}$ of each source is the mean of the pdf and can be obtained as a weighted average of its particles position:

$$\hat{\mathbf{x}}_j^{(t)} = \sum_{i=1}^{N_p} w_{j,i}^{(t)} \mathbf{x}_{j,i}^{(t)} \quad (2.35)$$

It is however possible to obtain better accuracy simply by adding a delay to the algorithm. This can be achieved by augmenting the state vector by past position values. At time t , the position at time $t - T$ is thus expressed as:

$$\hat{\mathbf{x}}_j^{(t-T)} = \sum_{i=1}^{N_p} w_{j,i}^{(t)} \mathbf{x}_{j,i}^{(t-T)} \quad (2.36)$$

Using the same example as in Figure 2.6, Figure 2.8 represents how the particle filter is able to remove the noise and produce smooth trajectories. The added delay produces an even smoother result.

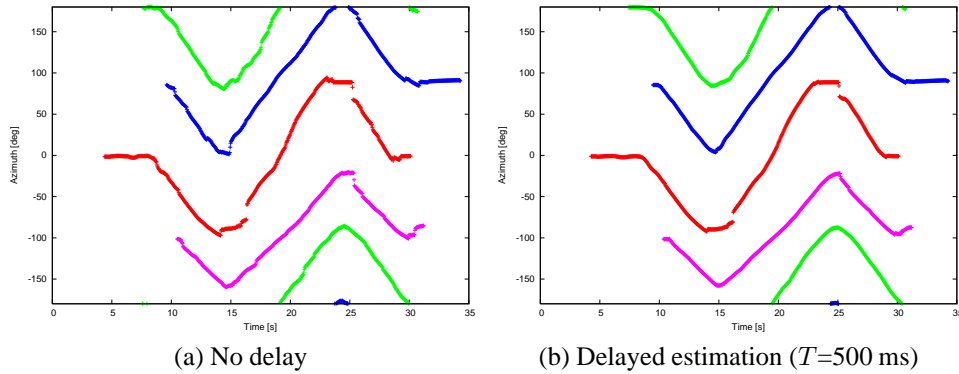


Figure 2.8: Tracking of four moving sources, showing azimuth as a function of time.

2.4.7 Resampling

Resampling is necessary in order to prevent the filter from degenerating to a single particle of weight 1. During the resampling stage N_p “new” particles are drawn from the original

N_p particles with the probability of a particle being selected being proportional to its weight $w_{j,i}^{(t)}$. After resampling, all particle weights are reset to $1/N_p$, preserving the original pdf. The resampling step in particle filtering can be viewed as survival of the fittest, where the particles with a large weight are more likely to be selected (and can be selected multiple times) than the particles with a small weight.

Also, resampling is performed only when $N_{eff} \approx \left(\sum_{i=1}^N w_{j,i}^2 \right)^{-1} < N_{min}$ [56] with $N_{min} = 0.7N$. That criterion ensures that resampling only occurs when new data is available for a certain source. Otherwise, this would cause unnecessary reduction in particle diversity, due to some particles randomly disappearing.

2.5 Results

Results for the localisation are obtained using the robot described in Section 1.2 with the C1 and C2 configurations in the E1 and E2 environments. Running the localisation system in real-time currently requires 30% of a 1.6 GHz Pentium-M CPU. Due to the low complexity of the particle filtering algorithm, we are able to use 1000 particles per source without noticeable increase in complexity. This also means that the CPU time does not increase significantly with the number of sources present. For all tasks, configurations and environments, all parameters have the same value, except for the reverberation decay γ , which is set to 0.65 ($T_{60} = 350$ ms) in the E1 environment and 0.85 ($T_{60} = 910$ ms) in the E2 environment. In both cases, the Signal-to-Reverberant Ratio (SRR) δ is set to 3.3 (5.2 dB).

2.5.1 Characterisation

The system is characterised in environment E1 in terms of detection reliability and accuracy. Detection reliability is defined as the capacity to detect and localise sounds to within 10 degrees, while accuracy is defined as the localisation error for sources that are detected. We use three different types of sound: a hand clap, the test sentence (“Spartacus, come here”), and a burst of

white noise lasting 100 ms. The sounds are played from a speaker placed at different locations around the robot and at three different heights: 0.1 m, 1 m, 1.4 m.

2.5.1.1 Detection Reliability

Detection reliability is tested at distances (measured from the centre of the array) ranging from 1 m (a normal distance for close interaction) to 7 m (limitations of the room). Three indicators are computed: correct localisation (within 10 degrees), reflections (incorrect elevation due to floor and ceiling), and other errors (repeated detection or large error). For all indicators, we compute the number of occurrences divided by the number of sounds played. This test includes 1440 sounds at a 22.5° interval for 1 m and 3 m, and 360 sounds at a 90° interval for 5 m and 7 m).

Results are shown in Table 2.1 for both C1 and C2 configurations⁵. In configuration C1, results show near-perfect reliability even at seven meter distance. For C2, we noted that the reliability depends on the sound type, so detailed results for different sounds are provided in Table 2.2, showing that only hand clap sounds cannot be reliably detected passed one meter. We expect that a human would have achieved a score of 100% for this reliability test.

Like most localisation algorithms, our system is unable to detect pure tones. This behaviour is explained by the fact that sinusoids occupy only a very small region of the spectrum and thus have a very small contribution to the cross-correlations with the proposed weighting. It must be noted that tones tend to be more difficult to localise than wideband signals even for the human auditory system⁶.

2.5.1.2 Localisation Accuracy

In order to measure the accuracy of the localisation system, we use the same setup as for measuring reliability, with the exception that only distances of 1 m and 3 m are tested (1440

⁵The total for a configuration does not have to be equal to 100% percent because there are cases where nothing is detected and other cases where an error occurs in addition to correct localisation.

⁶Observed from personal experience.

Table 2.1: Detection reliability for C1 and C2 configurations.

Distance	Correct (%)		Reflection (%)		Other error (%)	
	C1	C2	C1	C2	C1	C2
1 m	100	94.2	0.0	7.3	0.0	1.3
3 m	99.4	80.6	0.0	21.0	0.3	0.1
5 m	98.3	89.4	0.0	0.0	0.0	1.1
7 m	100	85.0	0.6	1.1	0.6	1.1

Table 2.2: Correct localisation rate as a function of sound type and distance for C2 configuration.

Distance	Hand clap (%)	Speech (%)	Noise burst (%)
1 m	88.3	98.3	95.8
3 m	50.8	97.9	92.9
5 m	71.7	98.3	98.3
7 m	61.7	95.0	98.3

sounds at a 22.5° interval) due to limited space available in the testing environment. Neither distance nor sound type has significant impact on accuracy. The root mean square accuracy results are shown in Table 2.3 for configurations C1 and C2. Both azimuth and elevation are shown separately. According to [57, 58], human sound localisation accuracy ranges between two and four degrees in similar conditions. The localisation accuracy of our system is thus equivalent or better than human localisation accuracy.

Table 2.3: Localisation accuracy (root mean square error).

Localisation error	C1 (deg)	C2 (deg)
Azimuth	1.10	1.44
Elevation	0.89	1.41

2.5.2 Source Tracking

We measure the tracking capabilities of the system for multiple sound sources. These are performed using the C2 configuration in both E1 and E2 environments. In all cases, the distance between the robot and the sources is approximately two meters. The azimuth is shown as a function of time for each source. The elevation is not shown as it is almost the same for all sources during these tests. The trajectories of the sources in the three experiments are shown in Figure 2.9. For each of the three cases, only one experiment was performed so that no selection would have to be made about which trial to display.

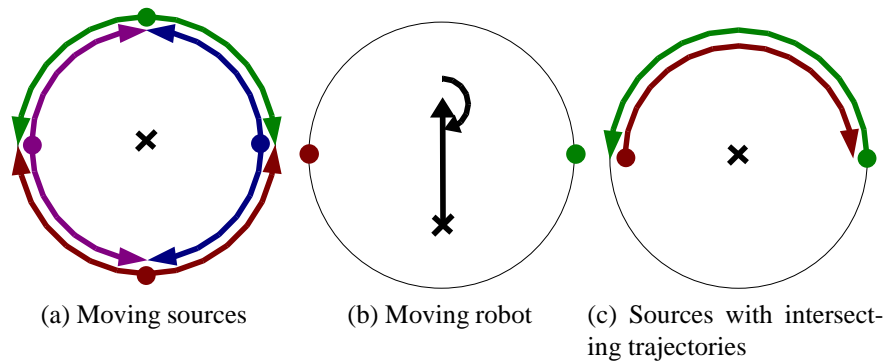


Figure 2.9: Source trajectories (robot represented as an X, sources represented with dots).

2.5.2.1 Moving Sources

In a first set of trials, four people were told to talk continuously (reading a text with normal pauses between words) to the robot while moving, as shown on Figure 2.9a. Each person walked 90 degrees towards the left of the robot before walking 180 degrees towards the right.

Results are presented in Figure 2.10 for delayed estimation ($T=500$ ms). In both environments, the source estimated trajectories are consistent with the trajectories of the four speakers and only one false detection was present for a short period of time.

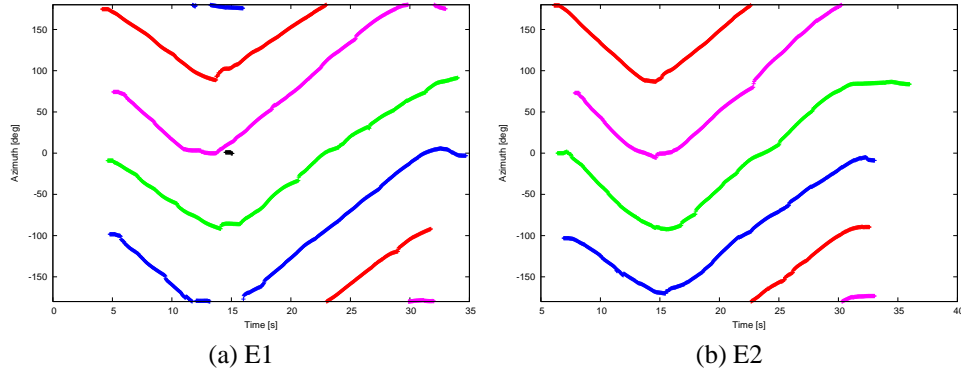


Figure 2.10: Four speakers moving around a stationary robot. False detection shown in black (around $t = 15$ s in E1).

2.5.2.2 Moving Robot

Tracking capabilities of our system are also evaluated in the context where the robot is moving, as shown on Figure 2.9b. In this experiment, two people are talking continuously to the robot as it is passing between them. The robot then makes a half-turn to the left. Results are presented in Figure 2.11 for delayed estimation ($T=500$ ms). Once again, the estimated source trajectories are consistent with the trajectories of the sources relative to the robot for both environments. Only one false detection was present for a short period of time.

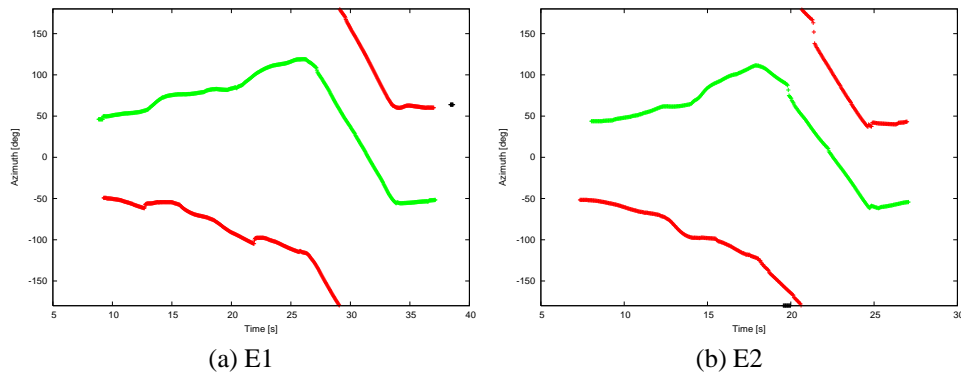


Figure 2.11: Four speakers moving around a stationary robot. Two stationary speakers with the robot moving. False detection shown in black (around $t = 38$ s in E1 and around $t = 20$ s in E2).

2.5.2.3 Sources with Intersecting Trajectories

In this experiment, two moving speakers are talking continuously to the robot, as shown on Figure 2.9c. They start from each side of the robot, intersecting in front of the robot before reaching the other side. Results for delayed estimation ($T=500$ ms) are presented in Figure 2.12 and show that the particle filter is able to keep track of each source. This result is possible because the prediction step (Section 2.4.1) imposes some inertia to the sources.

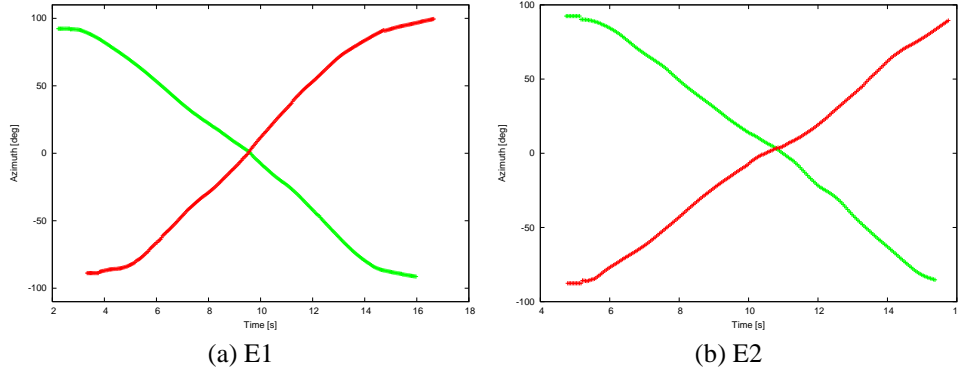


Figure 2.12: Two speakers intersecting in front of the robot.

2.5.2.4 Number of Microphones

These results evaluate how the number of microphones used affect the system capabilities. To do so, we use the same recording as in 2.5.2.1 for C2 in E1 with only a subset of the microphone signals to perform localisation. Since a minimum of four microphones are necessary for localising sounds without ambiguity⁷, we evaluate the system for four to seven microphones (selected arbitrarily as microphones number 1 through N). Comparing results of Figure 2.13 to those obtained in Figure 2.10 for E1, it can be observed that tracking capabilities degrade gracefully as microphones are removed. While using seven microphones makes little difference compared to the baseline of eight microphones, the system is unable to reliably track more than

⁷With three microphones, it is not possible to distinguish sources on either side of the plane formed by the microphones.

two of the sources when only four microphones are used. Although there is no theoretical relationship between the number of microphones and the maximum number of sources that can be tracked, this clearly shows how the redundancy added by using more microphones can help in the context of sound source localisation.

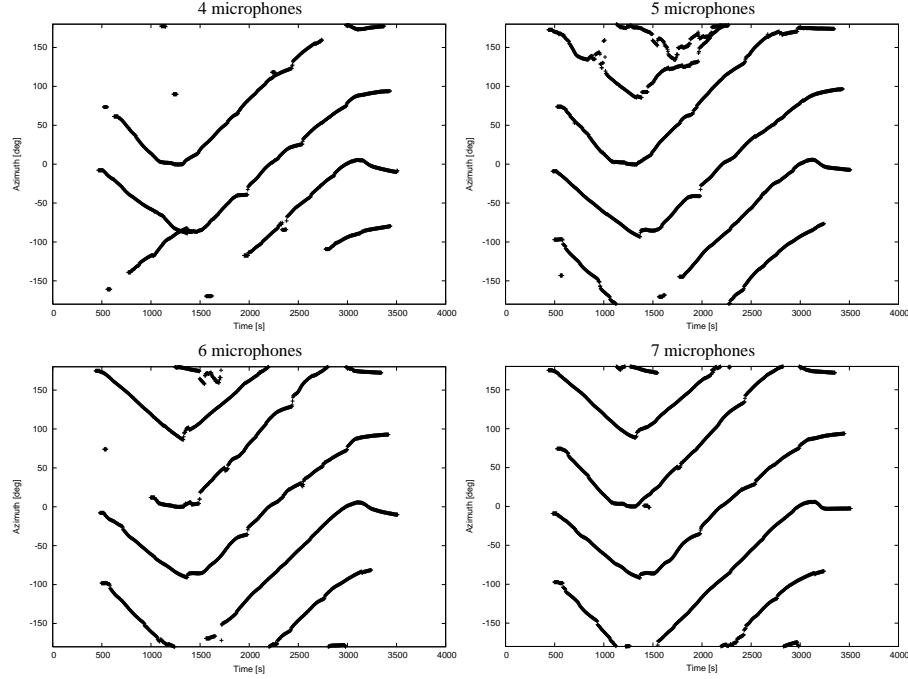


Figure 2.13: Tracking of four sources using C2 in the E1 environment, using 4 to 7 microphones (E_T adjusted to be proportional to the number of microphone pairs, $T = 500$ ms).

2.5.2.5 Audio Bandwidth

We evaluate the impact of audio bandwidth on the tracking capabilities using the same recording as in 2.5.2.1 for C2 in E1. The input signal is low-pass filtered at different frequencies, while the rest of the processing is still performed at 48 kHz, so that the cross-correlations are computed at higher resolution. Figure 2.14 presents tracking results corresponding to 8 kHz sampling rate and 16 kHz sampling rate, since those sampling rate have been used in other work [22, 39, 41, 54]. It can be observed that results are significantly degraded when compared to Figure 2.10, especially in the case of 8 kHz sampling, where only two of the four sources could be tracked.

This can be explained by the fact that the spectrum of speech extends beyond 8 kHz and that those higher frequencies can still contribute to the localisation process. Figure 2.14 justifies our use of the full 20 kHz audio bandwidth.

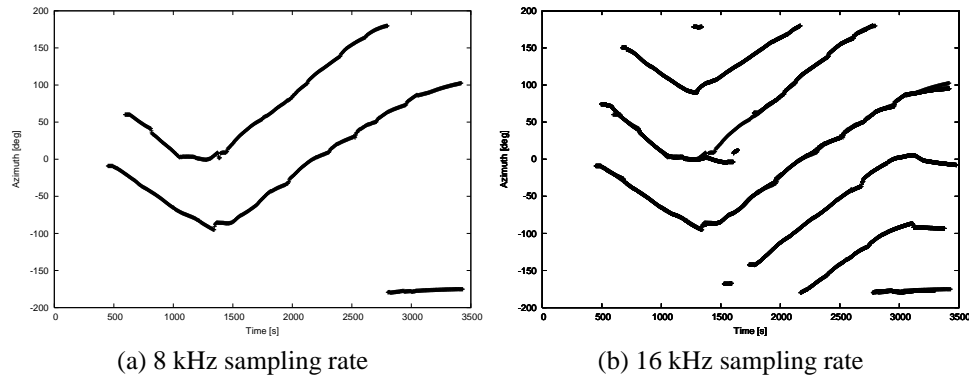


Figure 2.14: Tracking of four sources using C2 in the E1 environment for reduced audio bandwidth.

2.5.3 Localisation and Tracking for Robot Control

This experiment is performed in real-time and consists of making the robot follow the person speaking to it. At any time, only the source present for the longest time is considered. When the source is detected in front (within 10 degrees) of the robot, it is made to go forward. At the same time, regardless of the angle, the robot turns toward the source in such a way as to keep the source in front. Using this simple control system, it is possible to control the robot simply by talking to it, even in noisy and reverberant environments.

This has been tested by controlling the robot going from environment E1 to environment E2, having to go through corridors and an elevator, speaking to the robot with normal intensity at a distance ranging from one meter to three meters. The system worked in real-time⁸, providing tracking data at a rate of 25 Hz with no additional delay ($T=0$) on the estimator. The robot reaction time is limited mainly by the inertia of the robot. One problem we encountered during the experiment is that when going through corridors, the robot would sometimes detect reflections

⁸A video of the experiment can be downloaded from <http://www.gel.usherb.ca/laborius/projects/Audible/JMLocalization.mov>

on the walls in addition to the real sources. Fortunately, the fact that the robot considers only the oldest source present reduces problems from both reflections and noise sources.

2.6 Discussion

Using an array of eight microphones, we have implemented a system that is able to localise and track simultaneous moving sound sources in the presence of noise and reverberation, at distances up to seven meters. We have also demonstrated that the system can successfully control the motion of a robot in real-time, using only the direction of sounds. The tracking capabilities demonstrated result from combining our frequency-domain steered beamformer with a particle filter tracking multiple sources. Moreover, the solution we found to the source-observation assignment problem is also applicable to other multiple objects tracking problems, like visual tracking.

A robot using the proposed system has access to a rich, robust and useful set of information derived from its acoustic environment. This can certainly affect its ability of making autonomous decisions in real life settings, and show higher intelligent behaviour. Also, because the system is able to localise multiple sound sources, it can be exploited by a sound separation algorithm and enable speech recognition to be performed. This allows to identify the sound sources so that additional relevant information can be obtained from the acoustic environment.

The main aspect of the localisation algorithm that could be improved is robustness to sound reflections on hard surfaces (such as the floor, the walls and the ceiling) that sometimes cause a source to be detected at multiple locations at the same time. For this, it may be possible to use knowledge of the environment to eliminate impossible hypotheses (such as a speech source coming from below the floor).

Chapter 3

Sound Source Separation

In this chapter, we address the problem of separating individual sound sources from a mixture of sounds. The human hearing sense is very good at focusing on a single source of interest despite all kinds of interferences. We generally refer to this situation as the *cocktail party effect*, where a human listener is able to follow a conversation even when several people are speaking at the same time. For a mobile robot, it means being able to separate each sound source present in the environment at any moment.

Working toward that goal, we have developed a two-step approach for performing sound source separation on a mobile robot equipped with an array of eight microphones. The first step consists of linear separation based on a simplified version of the Geometric Source Separation (GSS) approach, proposed by Parra and Alvino [32], with a faster stochastic gradient estimation and shorter time frames estimations. The second step is a generalisation of beamformer post-filtering for multiple sources and uses adaptive spectral estimation of background noise and interfering sources to enhance the signal produced during the initial separation. The novelty of this post-filter resides in the fact that, for each source of interest, the noise estimate is decomposed into stationary, reverberation, and transient components assumed to be due to leakage between the outputs of the initial separation stage.

The chapter is organised as follows. Section 3.1 presents prior art in multi-microphone

separation of sound sources. Section 3.2 gives an overview of the complete separation algorithm. Section 3.3 presents the linear separation algorithm and Section 3.4 describes the proposed post-filter. Results are presented in Section 3.5, followed by a discussion in Section 3.6.

3.1 Related Work

There are several approaches to sound source separation from multiple microphones. Most fall either into the Blind Source Separation (BSS) or beamforming categories. Blind Source Separation and Independent Component Analysis (ICA) are ways to recover the original (unmixed) sources with no prior knowledge, other than the fact that all sources are statistically independent. Several criteria exist for expressing the independence of the sources, either based on information theory (e.g., Kullback-Leiber divergence) [59] or based on statistics (e.g., maximum likelihood) [60]. Blind source separation has been applied to audio [61, 62], often in the form of frequency domain ICA [63, 64, 65]. Recently, Araki *et al.* [66] have applied ICA to the separation of three sources using only two microphones.

One drawback of BSS and ICA techniques is that they require assumptions to be made about the statistics of the sources to be separated. These assumptions are usually contained in the contrast function [67] or other simplifying hypotheses [68]. Also, while the weak assumptions made by BSS and ICA can be considered as an advantage of the method for certain applications, we consider it to be a weakness in the context of microphone array sound source separation because these techniques do not use the knowledge about the location of the sound sources.

A more “classical” way of isolating a source coming from a certain direction is beamforming. Unlike BSS, beamforming assumes that the transfer function between the source of interest and the different microphones is known approximately. It is thus possible to optimise the beamformer parameters in such a way as to minimise noise while conserving perfect response for the signal of interest. This is known as the Minimum Variance Distortionless Response (MVDR) criterion [69].

The beamforming technique most widely used today is the Generalised Sidelobe Canceller (GSC), originally proposed by Griffiths and Jim [70]. The GSC algorithm uses a fixed beamformer (delay and sum) to produce an initial estimation of the source of interest. Also, a blocking matrix is used to produce noise reference signals (that do not contain the source of interest) than can be used by a multiple-input canceller to further reduce noise at the output of the fixed beamformer. The GSC algorithm can be implemented in the frequency domain [71] where its components are matrices, or in the time domain [72] where the components are adaptive filters.

Recently, a method has been proposed to combine the advantages of both the BSS and the beamforming approach. The Geometric Source Separation (GSS) approach proposed by Parra and Alvino [32] uses the assumption that all sources are independent, while using information about source position through a geometric constraint. Unlike most variants of BSS, the GSS algorithm uses only second order statistics as its independence criterion, making it simpler and more robust. The GSS has been extended to take into account the Head-Related Transfer Function (HRTF) in order to improve separation [73]. However, we choose not to apply this technique because of the complexity involved and the fact that it would make the system more difficult to adapt to different robots (i.e., different configurations for placing the microphones).

All methods previously listed can be called Linear Source Separation (LSS) methods, in that once the demixing parameters are fixed, each output is a Linear Time Invariant (LTI) transformation from the microphone inputs. In real-life environments with background noise, reverberation and imperfect microphones, it is not possible to achieve perfect separation using LSS methods, so further noise reduction is required. Several techniques have been developed to remove background noise, including spectral subtraction [74] and optimal spectral amplitude estimation [50, 75, 51]. Techniques have also been developed specifically to reduce noise at the output of LSS algorithms, generally beamformers. Most of these post-filtering techniques address reduction of stationary background noise [76, 77, 78]. Recently, a multi-channel post-filter taking into account non-stationary interferences was proposed by Cohen [79].

3.2 System Overview

The proposed sound separation algorithm, as shown in Figure 3.1, is composed of three parts:

1. A microphone array;
2. A linear source separation algorithm (LSS) implemented as a variant of the Geometric Source Separation (GSS) algorithm;
3. A multi-source post-filter.

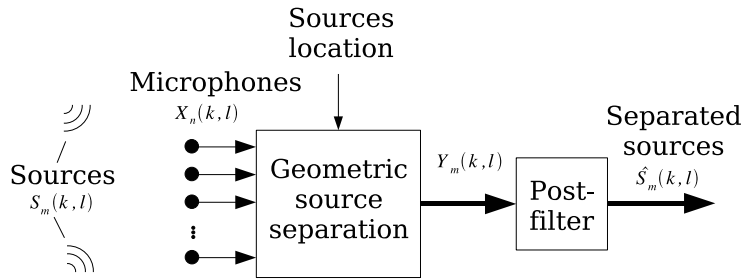


Figure 3.1: Overview of the separation system.

The microphone array is composed of a number of omni-directional elements mounted on the robot. The microphone signals are combined linearly in a first-pass separation algorithm. The output of this initial separation is then enhanced by a (non-linear) post-filter designed to optimally attenuate the remaining noise and interference from other sources.

We assume that these sources are detected and that their position is estimated by the localisation and tracking algorithm described in Chapter 2. We also assume that sources may appear, disappear or move at any time. It is thus necessary to maximise the adaptation speed for both the LSS and the multi-source post-filter.

3.3 Linear Source Separation

The LSS algorithm we propose in this section is based on the Geometric Source Separation (GSS) approach proposed by Parra and Alvino [32]. Unlike the Linearly Constrained Minimum

Variance (LCMV) beamformer that minimises the output power subject to a distortionless constraint, GSS explicitly minimises cross-talk, leading to faster adaptation. The method is also interesting for use in the mobile robotics context because it allows easy addition and removal of sources. Using some approximations described in Subsection 3.3.2.1, it is also possible to implement separation with relatively low complexity (i.e., complexity that grows linearly with the number of microphones), as described in [80].

3.3.1 Geometric Source Separation

The method operates in the frequency domain on overlapped frames of 21 ms (1024 samples at 48 kHz). Let $S_m(k, \ell)$ be the real (unknown) sound source m at time frame ℓ and for discrete frequency k . We denote as $\mathbf{s}(k, \ell)$ the vector corresponding to the sources $S_m(k, \ell)$ and matrix $\mathbf{A}(k)$ is the transfer function leading from the sources to the microphones. The signal received at the microphones is thus given by:

$$\mathbf{x}(k, \ell) = \mathbf{A}(k)\mathbf{s}(k, \ell) + \mathbf{n}(k, \ell) \quad (3.1)$$

where $\mathbf{n}(k, \ell)$ is the non-coherent background noise received at the microphones. The matrix $\mathbf{A}(k)$ can be estimated using the result of a sound localisation algorithm. Assuming that all transfer functions have unity gain, the elements of $\mathbf{A}(k)$ can be expressed as:

$$a_{ij}(k) = e^{-j2\pi k\delta_{ij}} \quad (3.2)$$

where δ_{ij} is the time delay (in samples) to reach microphone i from source j .

The separation result is then defined as $\mathbf{y}(k, \ell) = \mathbf{W}(k, \ell)\mathbf{x}(k, \ell)$, where $\mathbf{W}(k, \ell)$ is the separation matrix that must be estimated. This is done by providing two constraints (the index ℓ is omitted for the sake of clarity):

1. Decorrelation of the separation algorithm outputs, expressed as $\mathbf{R}_{\mathbf{yy}}(k) - \text{diag}[\mathbf{R}_{\mathbf{yy}}(k)] =$

$\mathbf{0}^1$.

2. The geometric constraint $\mathbf{W}(k)\mathbf{A}(k) = \mathbf{I}$, which ensures unity gain in the direction of the source of interest and places zeros in the direction of interferences.

In theory, constraint 2) could be used alone for separation (the method is referred to as LS-C2 in [32]), but in practice, the method does not take into account reverberation or errors in localisation. It is also subject to instability if $\mathbf{A}(k)$ is not invertible at a specific frequency. When used together, constraints 1) and 2) are too strong. For this reason, we use a “soft” constraint (referred to as GSS-C2 in [32]) combining 1) and 2) in the context of a gradient descent algorithm.

Two cost functions are created by computing the square of the error associated with constraints 1) and 2). These cost functions are respectively defined as:

$$J_1(\mathbf{W}(k)) = \|\mathbf{R}_{yy}(k) - \text{diag}[\mathbf{R}_{yy}(k)]\|^2 \quad (3.3)$$

$$J_2(\mathbf{W}(k)) = \|\mathbf{W}(k)\mathbf{A}(k) - \mathbf{I}\|^2 \quad (3.4)$$

where the matrix norm is defined as $\|\mathbf{M}\|^2 = \text{trace}[\mathbf{M}\mathbf{M}^H]$ and is equal to the sum of the square of all elements in the matrix. The gradient of the cost functions with respect to $\mathbf{W}(k)$ is equal to [32]:

$$\frac{\partial J_1(\mathbf{W}(k))}{\partial \mathbf{W}^*(k)} = 4\mathbf{E}(k)\mathbf{W}(k)\mathbf{R}_{xx}(k) \quad (3.5)$$

$$\frac{\partial J_2(\mathbf{W}(k))}{\partial \mathbf{W}^*(k)} = 2[\mathbf{W}(k)\mathbf{A}(k) - \mathbf{I}]\mathbf{A}^H(k) \quad (3.6)$$

where $\mathbf{E}(k) = \mathbf{R}_{yy}(k) - \text{diag}[\mathbf{R}_{yy}(k)]$.

¹ Assuming non-stationary sources, second order statistics are sufficient for ensuring independence of the separated sources.

The separation matrix $\mathbf{W}(k)$ is then updated as follows:

$$\mathbf{W}^{n+1}(k) = \mathbf{W}^n(k) - \mu \left[\alpha(k) \frac{\partial J_1(\mathbf{W}(k))}{\partial \mathbf{W}^*(k)} + \frac{\partial J_2(\mathbf{W}(k))}{\partial \mathbf{W}^*(k)} \right] \quad (3.7)$$

where $\alpha(f)$ is an energy normalisation factor equal to $\|\mathbf{R}_{xx}(k)\|^{-2}$ and μ is the adaptation rate. We use $\mu = 0.01$, which performs adequately for both stationary and moving sources.

3.3.2 Proposed Improvements to the GSS algorithm

We propose two improvements to the GSS algorithm as it is described in [32]. The first modification simplifies the computation of the correlation matrices $\mathbf{R}_{xx}(k)$ and $\mathbf{R}_{yy}(k)$, while the second one introduces regularisation to prevent large values to appear in the demixing matrix during the adaptation process.

3.3.2.1 Stochastic Gradient Adaptation

Instead of estimating the correlation matrices $\mathbf{R}_{xx}(k)$ and $\mathbf{R}_{yy}(k)$ on several seconds of data, our approach uses instantaneous estimations. This is analogous to the approximation made in the Least Mean Square (LMS) adaptive filter [69]. We thus assume that:

$$\mathbf{R}_{xx}(k) = \mathbf{x}(k)\mathbf{x}(k)^H \quad (3.8)$$

$$\mathbf{R}_{yy}(k) = \mathbf{y}(k)\mathbf{y}(k)^H \quad (3.9)$$

It is then possible to rewrite the gradient of Equation 3.5 as:

$$\frac{\partial J_1(\mathbf{W}(k))}{\partial \mathbf{W}^*(k)} = 4 [\mathbf{E}(k) \mathbf{W}(k) \mathbf{x}(k)] \mathbf{x}(k)^H \quad (3.10)$$

which only requires matrix-by-vector products, greatly reducing the complexity of the algorithm. The normalisation factor $\alpha(k)$ can also be simplified as $[\|\mathbf{x}(k)\|^2]^{-2}$. Although we use instantaneous estimation, the fact that the update rate is small means that many frames of data

are still necessary for adapting the demixing matrix, so the averaging is performed implicitly. We have observed that the modification did not cause significant degradation in performance, while it greatly facilitates real-time implementation.

3.3.2.2 Regularisation Term

Another modification we propose to the GSS algorithm is the addition of a regularisation. Since it is desirable for the demixing matrix to be as small as possible (while still respecting the other constraints), we define the regularisation term as the cost:

$$J_R(\mathbf{W}(k)) = \lambda \|\mathbf{W}(k)\|^2 \quad (3.11)$$

The gradient of the regularisation cost is equal to:

$$\frac{\partial J_R(\mathbf{W}(k))}{\partial \mathbf{W}^*(k)} = \lambda \mathbf{W}(k) \quad (3.12)$$

so we can rewrite Equation 3.7 as:

$$\mathbf{W}^{n+1}(k) = \mathbf{W}^n(k) - \mu \left[\alpha(k) \frac{\partial J_1(\mathbf{W}(k))}{\partial \mathbf{W}^*(k)} + \frac{\partial J_2(\mathbf{W}(k))}{\partial \mathbf{W}^*(k)} + \frac{\partial J_R(\mathbf{W}(k))}{\partial \mathbf{W}^*(k)} \right] \quad (3.13)$$

or:

$$\mathbf{W}^{n+1}(k) = (1 - \lambda\mu) \mathbf{W}^n(k) - \mu \left[\alpha(k) \frac{\partial J_1(\mathbf{W}(k))}{\partial \mathbf{W}^*(k)} + \frac{\partial J_2(\mathbf{W}(k))}{\partial \mathbf{W}^*(k)} \right] \quad (3.14)$$

where we set the regularisation parameter λ to 0.5.

3.3.3 Initialisation

The fact that sources can appear or disappear at any time imposes constraints on the initialisation of the separation matrix $\mathbf{W}(k)$. The initialisation must provide the following:

- The initial weights for a new source;

- Acceptable separation (before adaptation).

Furthermore, when a source appears or disappears, other sources must be unaffected.

One easy way to satisfy both constraints is to initialise the column of $\mathbf{W}(k)$ corresponding to the new source m as:

$$w_{m,i}(k) = \frac{a_{i,m}^*(k)}{N} \quad (3.15)$$

where N is the number of microphones. This weight initialisation corresponds to a delay-and-sum beamformer, referred to as the I1 initialisation method [32]. Such initialisation ensures that prior to adaptation, the performances are at worst equivalent to a delay-and-sum beamformer.

3.4 Multi-Source Post-Filter

In order to enhance the output of the GSS algorithm presented in Section 3.3, we derive a frequency-domain post-filter that is based on the optimal estimator originally proposed by Ephraim and Malah [50, 75] and further improved by Cohen and Berdugo [51, 79, 81]. The novelty of our approach, as proposed in [82, 80], resides in the fact that, for a given output of the GSS, the transient components of the corrupting sources is assumed to be due to leakage from the other channels during the GSS process. Furthermore, for a given source, the stationary and the transient components are combined into a single noise estimator used for noise suppression, as shown in Figure 3.2.

For this post-filter, we consider that all interferences (except the background noise) are localised (detected) sources and we assume that the leakage between outputs is constant. This leakage is due to reverberation, localisation error, differences in microphone frequency responses, near-field effects, etc. In addition, the post-filter is tuned in such a way as to maximise speech recognition accuracy, as opposed to perceptual quality or objective quality measurement.

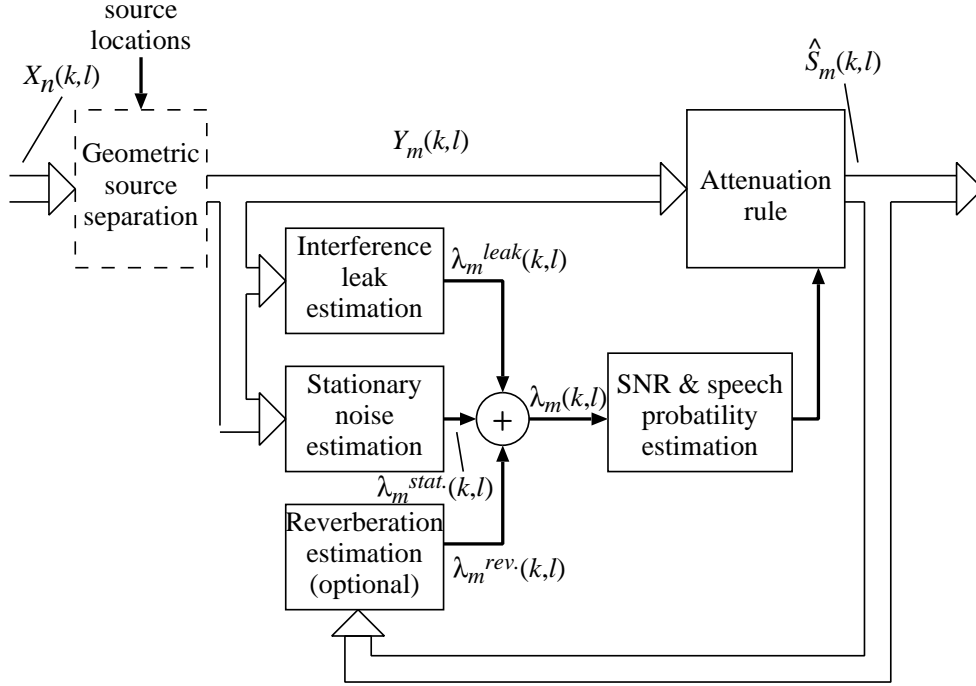


Figure 3.2: Overview of the complete separation system.

$X_n(k, \ell), n = 0 \dots N - 1$: Microphone inputs, $Y_m(k, \ell), m = 0 \dots M - 1$: Inputs to the post-filter, $\hat{S}_m(k, \ell) = G_m(k, \ell)Y_m(k, \ell), m = 0 \dots M - 1$: Post-filter outputs.

3.4.1 Noise Estimation

This section describes the estimation of noise variances that are used to compute the weighting function $G_m(k, \ell)$ by which the outputs $Y_m(k, \ell)$ of the LSS is multiplied to generate a cleaned signal whose spectrum is denoted $\hat{S}_m(k, \ell)$. The noise variance estimation $\lambda_m(k, \ell)$ is expressed as:

$$\lambda_m(k, \ell) = \lambda_m^{stat.}(k, \ell) + \lambda_m^{leak}(k, \ell) \quad (3.16)$$

where $\lambda_m^{stat.}(k, \ell)$ is the estimate of the stationary component of the noise for source m at frame ℓ for frequency k , and $\lambda_m^{leak}(k, \ell)$ is the estimate of source leakage. We compute the stationary noise estimate $\lambda_m^{stat.}(k, \ell)$ using the Minima Controlled Recursive Average (MCRA) technique proposed by Cohen and Berdugo [51].

To estimate $\lambda_m^{leak}(k, \ell)$, we assume that the interference from other sources is reduced by a factor η (typically $-10 \text{ dB} \leq \eta \leq -5 \text{ dB}$) by the separation algorithm (LSS). The leakage

estimate is thus expressed as:

$$\lambda_m^{leak}(k, \ell) = \eta \sum_{i=0, i \neq m}^{M-1} Z_i(k, \ell) \quad (3.17)$$

where $Z_m(k, \ell)$ is the smoothed spectrum of the m^{th} source $Y_m(k, \ell)$, and is recursively defined (with $\alpha_s = 0.2$, from informal listening tests) as:

$$Z_m(k, \ell) = \alpha_s Z_m(k, \ell - 1) + (1 - \alpha_s) |Y_m(k, \ell)|^2 \quad (3.18)$$

In the case where reverberation is present, we can add a third term to Equation 3.16, so that:

$$\lambda_m(k, \ell) = \lambda_m^{stat.}(k, \ell) + \lambda_m^{leak}(k, \ell) + \sum_{i=0}^{M-1} \lambda_i^{rev}(k, \ell) \quad (3.19)$$

where the reverberation estimate $\lambda_i^{rev}(k, \ell)$ for source i is given by (similarly to Equation 2.9):

$$\lambda_i^{rev}(k, \ell) = \gamma \lambda_i^{rev}(k, \ell - 1) + \frac{(1 - \gamma)}{\delta} \left| \hat{S}_i(k, \ell - 1) \right|^2 \quad (3.20)$$

This method of taking into account reverberation is similar to the work by Wu and Wang [83] but it is used in such a way that reverberation from the source of interest and from the interfering sources is considered at the same time. Unlike the work of Wu and Wang, we do not need inverse filtering to compensate for spectral coloration because artificial speech recognition (ASR) engines typically normalise the channel response using cepstral mean subtraction (CMS).

3.4.2 Suppression Rule in the Presence of Speech

We now derive the suppression rule under H_1 , the hypothesis that speech is present. From here on, unless otherwise stated, the m and ℓ arguments are omitted for clarity and the equations are given for each m and for each ℓ . The proposed noise suppression rule is based on minimum mean-square error (MMSE) estimation of the log-spectral amplitude. Although earlier work [82,

80] proposed an optimal estimator in the loudness domain ($|S(k)|^{1/2}$) to maximise perceptual quality, the choice of the log-domain here is based on optimal speech recognition accuracy.

Assuming that speech is present (H_1), the amplitude estimator $\hat{A}_{H_1}(k)$ is defined as:

$$\hat{A}_{H_1}(k) = \exp(E[\log |S(k)| | Y(k), H_1]) = G_{H_1}(k) |Y(k)| \quad (3.21)$$

where $G_{H_1}(k)$ is the spectral gain assuming that speech is present.

The optimal spectral gain is given in [75]:

$$G_{H_1}(k) = \frac{\xi(k)}{1 + \xi(k)} \left\{ \frac{1}{2} \int_{v(k)}^{\infty} \frac{e^{-t}}{t} dt \right\} \quad (3.22)$$

where $\gamma(k) \triangleq |Y(k)|^2 / \lambda(k)$ and $\xi(k) \triangleq E[|X(k)|^2] / \lambda(k)$ are respectively the *a posteriori* SNR and the *a priori* SNR, and $v(k) \triangleq \gamma(k)\xi(k) / (\xi(k) + 1)$ [50, 75].

Using the modifications proposed in [51] to take into account speech presence uncertainty, the *a priori* SNR $\xi(k)$ is estimated recursively as:

$$\hat{\xi}(k, \ell) = (1 - \alpha_p) G_{H_1}^2(k, \ell - 1) \gamma(k, \ell - 1) + \alpha_p \max\{\gamma(k, \ell) - 1, 0\} \quad (3.23)$$

where the update rate α_p is dependent on the *a priori* SNR as proposed by Cohen [81]:

$$\alpha_p = \left(\frac{\hat{\xi}(k, \ell)}{1 + \hat{\xi}(k, \ell)} \right)^2 + \alpha_{pmin} \quad (3.24)$$

with $\alpha_{pmin} = 0.07$ determined from informal listening tests to force a minimal amount of adaptation.

3.4.3 Optimal Gain Modification Under Speech Presence Uncertainty

In order to take into account the probability of speech presence, we derive the estimator for the log-domain:

$$\hat{A}(k) = \exp (E [\log |S(k)| | Y(k)]) \quad (3.25)$$

Considering H_1 , the hypothesis that speech is present for a source (source index m and frame index ℓ are omitted for clarity), and H_0 , the hypothesis that speech is absent (as defined in [51]), we obtain:

$$\begin{aligned} E [\log A(k) | Y(k)] &= p(k) E [\log A(k) | H_1, Y(k)] \\ &+ [1 - p(k)] E [\log A(k) | H_0, Y(k)] \end{aligned} \quad (3.26)$$

where $p(k)$ is the probability of speech at frequency k .

The optimally modified gain is thus given by:

$$G(k) = \exp [p(k) \log G_{H_1}(k) + (1 - p(k)) \log G_{min}] \quad (3.27)$$

where $G_{H_1}(k)$ is defined in Equation 3.22, and G_{min} is the minimum gain allowed when speech is absent, which is set to -20 dB (similarly as in [51]) to limit distortion to the signal. Equation 3.27 further simplifies as:

$$G(k) = \{G_{H_1}(k)\}^{p(k)} \cdot G_{min}^{1-p(k)} \quad (3.28)$$

The probability of speech presence is computed as:

$$p(k) = \left\{ 1 + \frac{\hat{q}(k)}{1 - \hat{q}(k)} (1 + \xi(k)) \exp (-v(k)) \right\}^{-1} \quad (3.29)$$

where $\hat{q}(k)$ is the *a priori* probability of speech absence for frequency k and is defined as [51]:

$$\hat{q}(k) = \min (1 - P_{local}(k)P_{global}(k)P_{frame}, 0.9) \quad (3.30)$$

where $P_{local}(k)$, $P_{global}(k)$ and P_{frame} are speech presence probabilities computed respectively on a local frequency window, a large frequency window and on the whole frame.

The computation of $P_{local}(k)$, $P_{global}(k)$ and P_{frame} is inspired from Cohen and Berdugo [51] and Choi [84] so that:

$$P_{\psi}(k) = \frac{1}{1 + \left(\frac{\theta}{\zeta_{\psi}(k)}\right)^2} \quad (3.31)$$

where ψ can be either *local*, *global* or *frame*, θ is a soft-decision threshold that we set to -5 dB, and $\zeta_{\psi}(k)$ is a recursive average of the estimated *a priori* SNR:

$$\zeta_{\psi}(k) = (1 - \alpha_{\zeta}) \zeta(k) + \alpha_{\zeta} \sum_{j=-w_1}^{w_2} h_{\psi}(j) \hat{\xi}(k+j) \quad (3.32)$$

with $\alpha_{\zeta} = 0.3$ (determined from listening tests). In Equation 3.32, $h_{\psi}(j)$ is a Hanning window covering 140 Hz for P_{local} , 1400 Hz for P_{global} and the full band for P_{frame} .

3.4.4 Post-filter Initialisation

When a new source appears, post-filter state variables need to be initialised. Most of these variables may safely be set to zero. The exception is $\lambda_m^{stat.}(k, \ell_0)$, the initial stationary noise estimation for source m . The MCRA algorithm requires several seconds to produce its first estimate for source m , so it is necessary to find another way to estimate the background noise until a better estimate is available. This initial estimate is thus computed using noise estimations at the microphones. Assuming the delay-and-sum initialisation of the weights from Equation 3.15, the initial background noise estimate is thus:

$$\lambda_m^{stat.}(k, \ell_0) = \frac{1}{N^2} \sum_{n=0}^{N-1} \sigma_{x_n}^2(k) \quad (3.33)$$

where $\sigma_{x_n}^2(k)$ is the noise estimation for microphone n .

3.5 Results

The separation system is tested using the robot described in Section 1.2 in both C1 and C2 configurations. In order to test the system, three streams of voice were recorded separately, in a quiet environment. The speech consists of 251 sequences of four connected digits taken from the AURORA database [85] played from speakers located at 90 degrees to the left, in front, and 135 degrees to the right of the robot. The background noise is recorded on the robot and includes the room ventilation and the internal robot fans. All four signals are recorded using the same microphone array and subsequently mixed together. This procedure is required in order to compute the distance measures (such as SNR) presented in this section. It is worth noting that although the signals were mixed artificially, the result still represents real conditions with background noise, interfering sources, and reverberation. Because a clean reference signal is required, only the E1 environment is considered (it is not possible to make clean recordings in the E2 environment).

In evaluating our source separation system, we use the conventional signal-to-noise ratio (SNR) and the log spectral distortion (LSD), that is defined as:

$$\text{LSD} = \frac{1}{L} \sum_{\ell=0}^{L-1} \left[\frac{1}{K} \sum_{k=0}^{K-1} \left(10 \log_{10} \frac{\max(|S(k, \ell)|^2, \epsilon(k))}{\max(|\hat{S}(k, \ell)|^2, \epsilon(k))} \right)^2 \right]^{\frac{1}{2}} \quad (3.34)$$

where L is the number of frames, K is the number of frequency bins and $\epsilon(k)$ is meant to prevent extreme values for spectral regions of low energy. In both cases, the reference signal is estimated by applying the GSS algorithm on multi-channel recording containing only the source of interest. Because the reference signal is only available with reverberation, the reverberation suppression algorithm is not used in these tests. Only the narrowband part of the signal (300 Hz to 3400 Hz) is considered since most of the speech information is contained in that band.

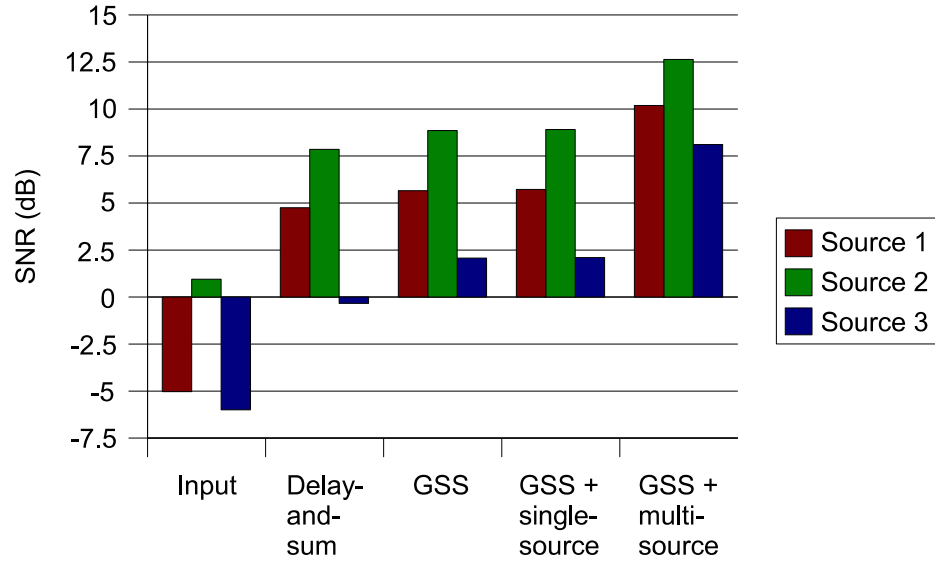
Measurements are made for the following processing:

- unprocessed microphone inputs;
- delay-and-sum (fixed) beamformer;
- separation with GSS only;
- separation with GSS followed by a conventional single-source post-filter (removing the interference estimation from our post-filter);
- separation with GSS followed by the proposed multi-source post-filter.

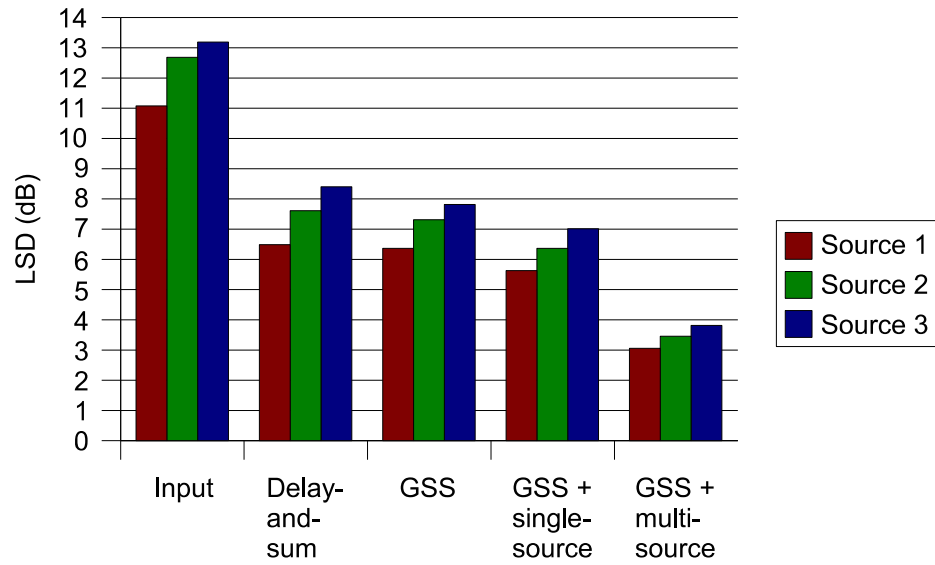
The SNR and LSD results for each source and for each processing is shown in Figure 3.3. These results demonstrate that when three sources are present, the complete source separation system we propose provides an average SNR improvement of 13.7 dB and an average LSD improvement 8.9 dB. It can be observed that both the GSS algorithm and the post-filter play an important role in the separation and that our proposed multi-source post-filter performs significantly better than single-source noise removal. When combined together, the GSS algorithm and the post-filter require 25% of a 1.6 GHz Pentium-M to run in real-time when three sources are present.

There are two factors that affect the SNR and LSD measures: the amount of residual noise and interference, and the distortion caused to the signal of interest. It is not possible to separate those two factors. For that reason, we measured the attenuation (relative to the input signal) of the noise and interference in the direction of each source when it is silent. Attenuation for the different processing is shown in Figure 3.4 (the input signal has 0 dB attenuation by definition). The GSS algorithm alone provides an average attenuation of 9 dB, while our proposed multi-source post-filter further attenuates the noise and interference by 15.5 dB (compared to GSS alone), for a total average attenuation of 24.5 dB.

The results in SNR, LSD and attenuation show that the delay-and-sum algorithm performs reasonably well when compared to the GSS algorithm. Because our implementation of the GSS is initialised in a manner equivalent to a delay-and-sum beamformer, this indicates that we can



(a) Signal-to-noise ratio (SNR)



(b) Log-spectral distance (LSD)

Figure 3.3: Signal-to-noise ratio (SNR) and log-spectral distortion (LSD) for each source of interest.

expect the separation algorithm to work well even when adaptation is incomplete. Also, it shows that the delay-and-sum beamformer could be used instead of GSS in a case where very limited computing power is available.

Time-domain signal plots for the first source are shown in Figure 3.5 and spectrograms

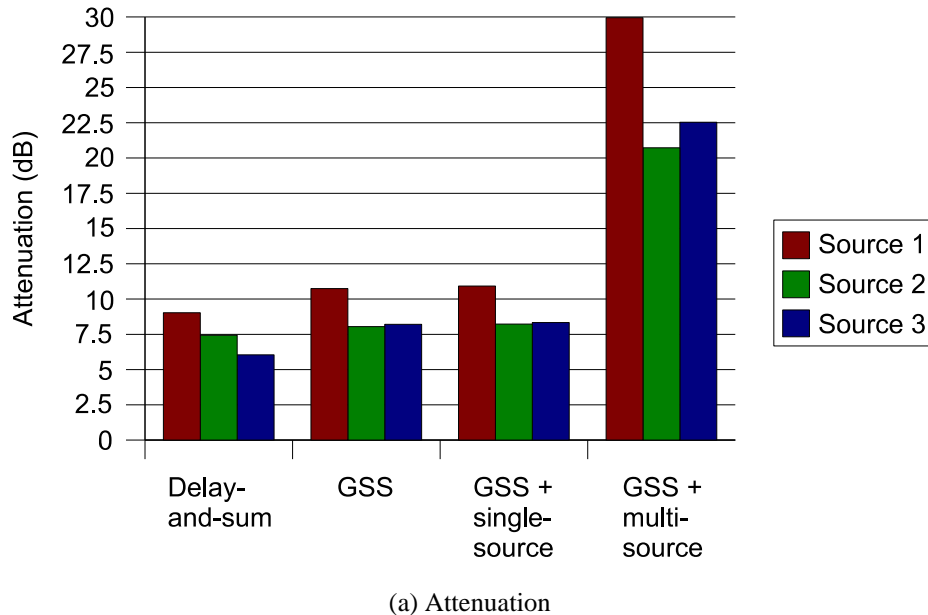


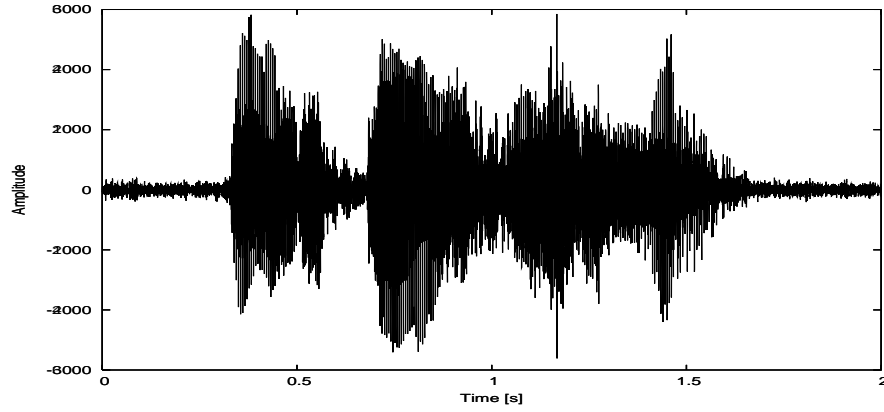
Figure 3.4: Attenuation of noise and interference in the direction of each source of interest.

are shown in Figure 3.6. Even though the task involves non-stationary interference with the same frequency content as the signal of interest, it can be observed that our proposed post-filter (unlike the single-source post-filter) is able to remove most of the interference, while not causing excessive distortion to the signal of interest. Informal subjective evaluation confirms that the post-filter has a positive impact on both quality and intelligibility of the speech².

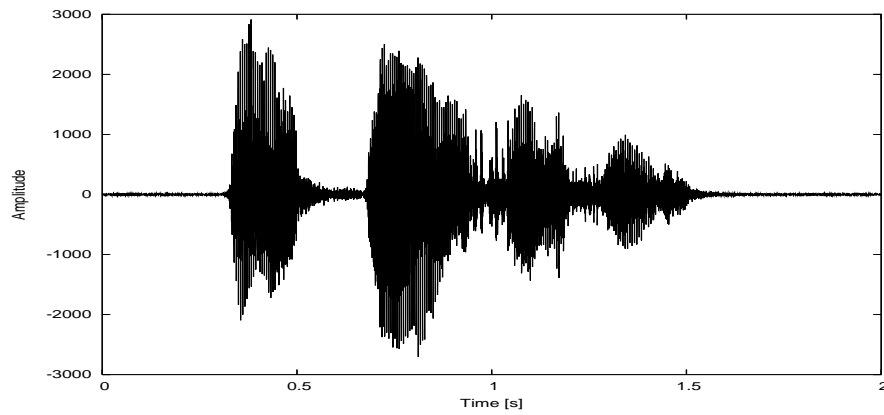
3.6 Discussion

In this chapter, we described a microphone array linear source separator and a post-filter in the context of multiple and simultaneous sound sources. The linear source separator is based on a simplification of the geometric source separation algorithm that performs regularisation and instantaneous estimation of the correlation matrix $\mathbf{R}_{xx}(k)$. The post-filter is based on an optimal log-spectral MMSE estimator where the noise estimate is computed as the sum of a stationary noise estimate, an estimation of leakage from the geometric source separation algorithm, and a

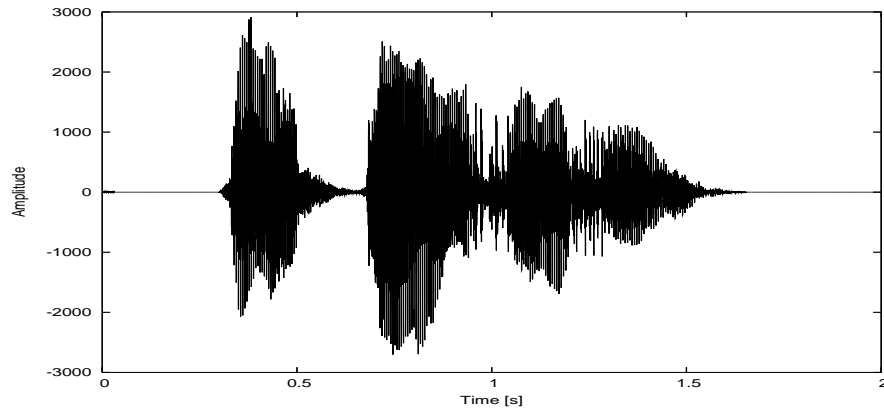
²Audio signals and spectrograms for all three sources are available at: <http://www.gel.usherb.ca/laborius/projects/Audible/separation/>



(a) Signal captured by one microphone



(b) Separated signal



(c) Reference signal

Figure 3.5: Temporal signals for separation of first source.

reverberation estimate.

Experimental results show an average reduction in log spectral distortion of 8.9 dB and an

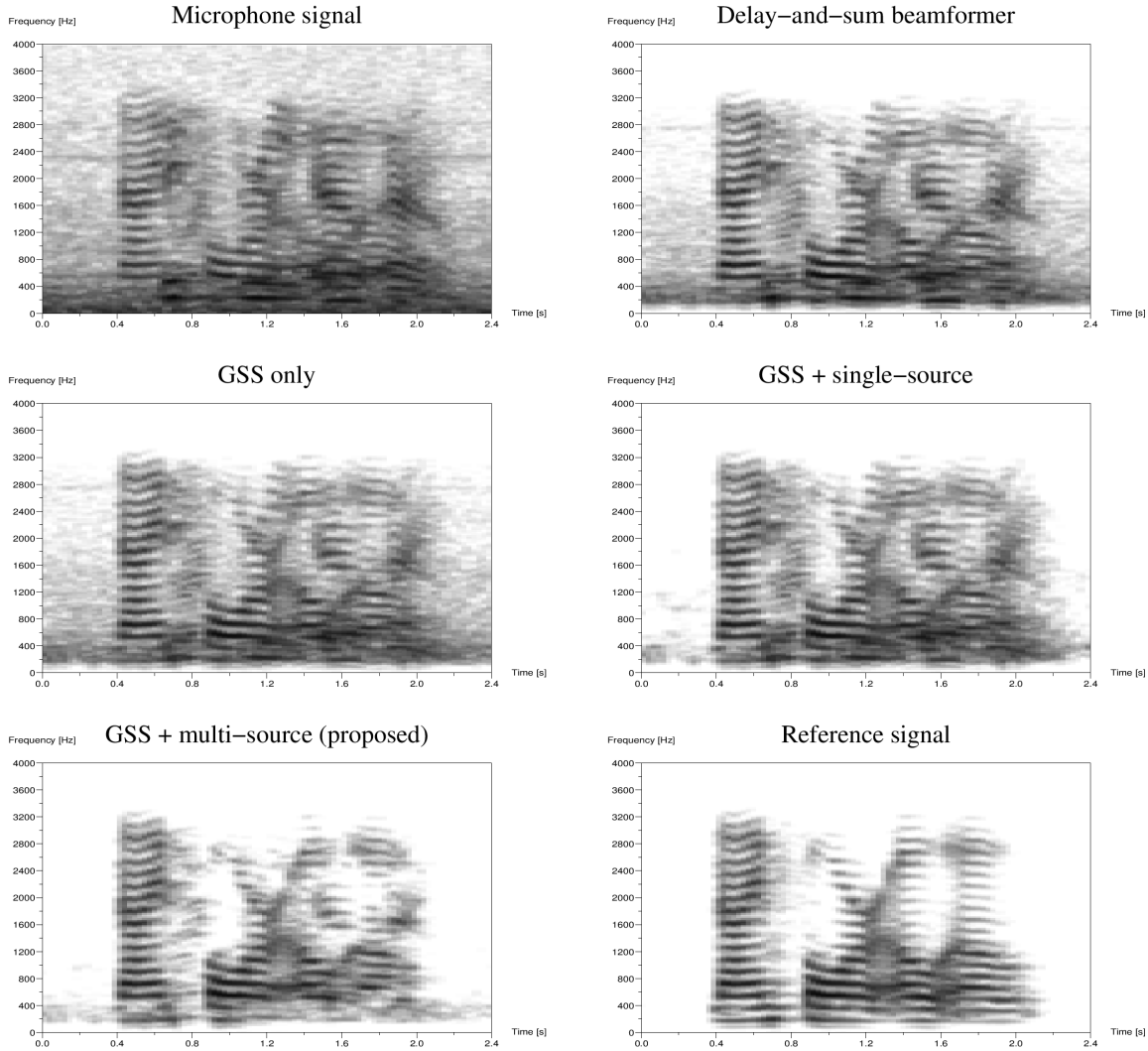


Figure 3.6: Spectrograms for separation of first source comparing different processing.

average increase of the signal-to-noise ratio of 13.7 dB compared to the noisy signal inputs. This is significantly better than all other methods evaluated. A significant part of that improvement is due to our multi-source post-filter, which is shown to perform better than a traditional single-source post-filter. Informal evaluation and visual inspection of spectrograms indicate that the distortion introduced by the system is acceptable to most listeners.

A possible improvement to the algorithm would be to derive a method that computes reverberation parameters so that the system can automatically adapt to changing environments. It would also be interesting to explore the use of the signal phase as an additional source of

information to the post-filter, as proposed by Aarabi and Shi [86]. Finally, the multi-source post-filter we have developed makes few assumptions about the nature of the signals or the linear separation algorithm used. It may thus be applicable to other multi-sensor systems.

Chapter 4

Speech Recognition of Separated Sound Sources

Robust speech recognition usually assumes source separation and/or noise removal from the audio or feature vectors. When several people speak at the same time, each separated speech signal is severely distorted in spectrum from its original signal.

We propose two different approaches for speech recognition on a mobile robot. Both approaches make use of the separated sources computed by the algorithm presented in Chapter 3. The first is a conventional approach and consists of sending the separated audio directly to a speech recognition engine for further processing. This is the most common method for speech recognition using a microphone array [87] and, in some variants, the acoustic models are adapted to the separated speech [88].

The second approach provides closer integration between the sound source separation algorithm and the speech recognition engine by estimating the reliability of spectral features, and providing that information to the speech recognition engine so it can be used during recognition [89, 90]. This second approach, as originally described in [91], was developed in collaboration with Kyoto University and builds on an original proof-of-concept by Yamamoto [13, 14]. Unlike the original proof-of-concept, which required access to the clean speech data, the system

we now propose can be used in a real environment by computing the missing feature mask only from the data available to the robot. This is done by using interference information provided by the multi-source post-filter described in Section 3.4.

This chapter is organised as follows. Section 4.1 discusses the state of the art and limitations of speech enhancement and missing feature-based speech recognition. Section 4.2 gives an overview of the system. Speech recognition integration and computation of the missing feature mask are addressed in Section 4.3. Results are presented in Section 4.4, followed by a discussion.

4.1 Related Work in Robust Speech Recognition

Robustness against noise in conventional¹ automatic speech recognition (ASR) is being extensively studied, particularly in the AURORA project [85]. In order to realise noise-robust speech recognition, *multi-condition training* (training on a mixture of clean speech and noises) has been studied [92, 93]. This is currently the most common method for vehicle and telephone applications. Because an acoustic model obtained by multi-condition training reflects the noise in a specific condition, ASR's use of the acoustic model is effective as long as the noise is stationary. This assumption holds for background noise in a vehicle and on a telephone. However, multi-condition training may not be effective for mobile robots, since those usually work in dynamically changing noisy environments. Source separation and speech enhancement algorithms for robust recognition is another potential alternative for ASR on mobile robots. However, this method is not always effective, since most source separation and speech enhancement techniques add some distortion to the separated signals and consequently degrade features, reducing the recognition rate, even if the signal is perceived to be cleaner by naïve listeners [94]. The work of Seltzer *et al.* [95] on microphone arrays addresses the problem of optimising the array processing specifically for speech recognition.

¹We use conventional in the sense of speech recognition for applications where a single microphone is used in a static environment such as a vehicle or an office.

Although the source separation and speech enhancement system in Chapter 3 are designed for optimal speech recognition, it is desirable to make speech recognition more robust to uncertain or distorted features.

4.1.1 Missing Feature Theory Overview

Research of confidence islands in the time-frequency plane representation has been shown to be effective in various applications and can be implemented with different strategies. One of the most effective is the missing feature strategy. Cooke *et al.* [96, 97] propose a probabilistic estimation of a mask in regions of the time-frequency plane where the information is not reliable. Then, after masking, the parameters for speech recognition are generated and can be used in conventional speech recognition systems. Using this method, it is possible to obtain a significant increase in recognition rates without any modelling of the noise [98]. In this scheme, the mask is essentially based on the signal-to-interference ratio (SIR) and a probabilistic estimation of the mask is used.

A missing feature theory-based ASR uses a Hidden Markov Model (HMM) where acoustic model probabilities are modified to take into account only the reliable features. According to the work by Cooke *et al.* [97], HMMs are trained on clean data. Density in each state S is modelled using mixtures of M_g Gaussians with diagonal-only covariance.

Let $f(\mathbf{x}|S)$ be the output probability density of feature vector \mathbf{x} in state S , and $P(j|S)$ represent the weight of mixture j expressed as a probability. The output probability density is given by:

$$f(\mathbf{x}|S) = \sum_{j=1}^{M_g} P(j|S) f(\mathbf{x}|j, S) \quad (4.1)$$

Cooke *et al.* [97] propose to transform Equation 4.1 to take into consideration the only reliable features from \mathbf{x} and to remove unreliable features. This is equivalent to use the marginalisation probability density functions $f(x_r|j, S)$ instead of $f(\mathbf{x}|j, S)$ by simply implementing a binary mask. Consequently, only reliable features are used in the probability calculation, and

the recogniser can avoid undesirable effects due to unreliable features.

Conventional ASR usually uses Mel Frequency Cepstral Coefficients (MFCC) [99] that capture the characteristics of speech. However, the missing feature mask is usually computed in the spectral domain and it is not easy to convert to the cepstral domain. Automatic generation of missing feature mask needs prior information about which spectral regions of a separated sound are distorted. This information can be obtained by our sound source separation and post-filter system [80, 82]. We use the post-filter gains to automatically generate the missing feature mask. Since we use a vector of 48 spectral features, the missing feature mask is a vector comprising the 48 corresponding values. The value may be discrete (1 for reliable, or 0 for unreliable) or continuous between 0 and 1.

4.1.2 Applications of Missing Feature Theory

Hugo Van hamme [100] formulates the missing feature approach for speech recognisers using conventional parameters such as MFCC. He uses data imputation according to Cooke [97] and proposes a suitable transformation to be used with MFCC for missing features. The acoustic model evaluation of the unreliable features is modified to express that their clean values are unknown or confined within bounds. In a more recent paper, Hugo Van hamme [101] presents speech recognition results by integrating harmonicity in the signal to noise ratio for noise estimation. He uses only static MFCC as, according to him, dynamic MFCC do not increase sufficiently the speech recognition rate when used in the context of missing features framework. The needs to estimate pitch and voiced regions in the time-space representation is a limit to this approach. In a similar approach, Raj, Seltzer and Stern [102] propose to modify the spectral representation to derive cepstral vectors. They present two missing feature algorithms that reconstruct spectrograms from incomplete noisy spectral representations (*masked* representations). Cepstral vectors can be derived from the reconstructed spectrograms for missing feature recognition. Seltzer *et al.* [103] propose the use of a Bayesian classifier to determine the reliability of spectrographic elements. Ming, Jancovic and Smith [104, 105] propose the

probabilistic union model as an alternative to the missing feature framework. According to the authors, methods based on the missing feature framework usually require the identification of the noisy bands. This identification can be difficult for noise with unknown, time-varying spectral characteristics. They designed an approach for speech recognition involving partial, unknown corrupted frequency-bands. In their approach, they combine the local frequency-band information based on the union of random events, to reduce the dependence of the model on information about the noise. Cho and Oh [106] apply the *union model* to improve robust speech recognition based on frequency bands selection. From this selection, they generate “channel-attentive” Mel frequency cepstral coefficients. Even if the use of missing features for robust recognition is relatively recent, many applications have already been designed.

In order to avoid the use of multi-condition training, we propose to merge a multi-microphone source separation and speech enhancement system with the missing feature approach. Very little work has been done with arrays of microphones in the context of missing feature theory. To our knowledge, only McCowan *et al.* [107] applies the missing feature framework to microphone arrays. The proposed approach defines a missing feature mask based on the input-to-output ratio of a post-filter. The approach is however only validated on stationary noise.

4.2 ASR on Separated Sources

In the first proposed approach, the sources separated using the algorithm described in Chapter 3 are sent directly to a speech recognition engine, as shown in Figure 4.1.

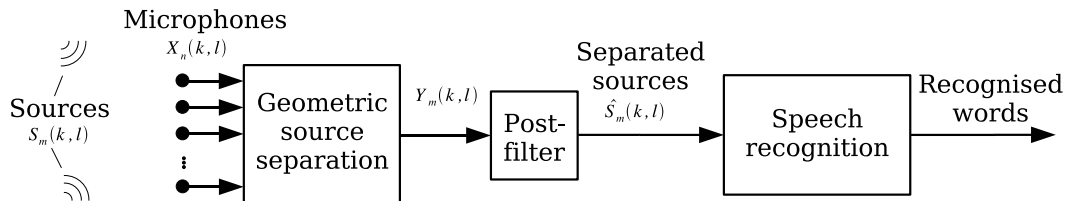


Figure 4.1: Direct integration of speech recognition.

The second approach, illustrated in Figure 4.2, aims to integrate the different steps of source separation, speech enhancement and speech recognition as closely as possible in order to maximise recognition accuracy by using as much of the available information as possible. The missing feature mask is generated in the time-frequency plane since the separation module and the post-filter already use this signal representation.

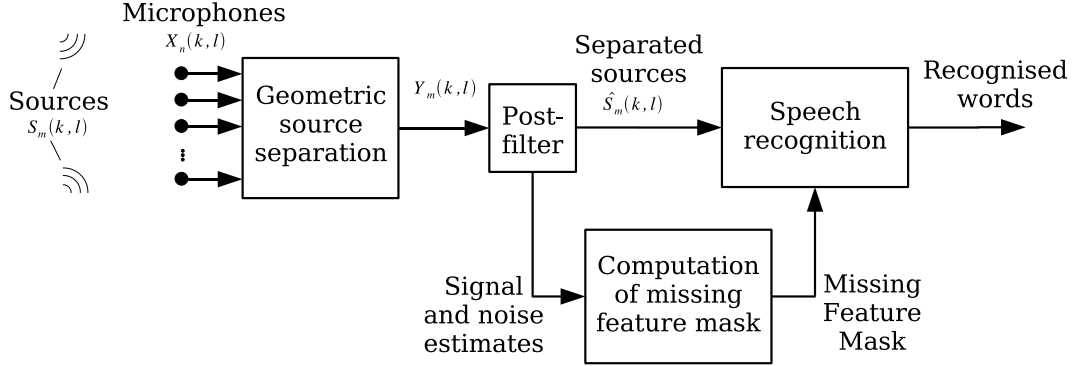


Figure 4.2: Speech recognition integration using missing feature theory

Not only can the multi-source post-filter reduce the amount of noise and interference, but its behaviour provides useful information that can be used to evaluate the reliability of different regions of the time-frequency plane for the separated signals. That information is used to compute a missing feature mask, which the ASR can use to further improve accuracy. This also has the advantage that acoustic models trained on clean data can be used (no multi-condition training is required).

Some missing feature mask techniques can also require the estimation of prior characteristics of the corrupting sources or noise. They usually assume that the noise or interference characteristics vary slowly with time. This is not possible in the context of a mobile robot. We propose to estimate quasi-instantaneously the mask (without preliminary training) by exploiting the post-filter outputs along with the local gains (in the time-frequency plane representation) of the post-filter. These local gains are used to generate the missing feature mask. Thus, the ASR with clean acoustic models can adapt to the distorted sounds by consulting the post-filter feature missing masks. This approach is also a partial solution to the automatic generation of

simultaneous missing feature masks (one for each speaker). It allows the use of simultaneous speech recognisers (one for each separated sound source) with their own mask.

4.3 Missing Feature Recognition

The post-filter uses adaptive spectral estimation of background noise, interfering sources and reverberation to enhance the signal produced during the initial separation. The main idea lies in the fact that, for each source of interest, the noise estimate is decomposed into stationary and transient components assumed to be due to leakage between the output channels of the initial separation stage. It also provides useful information concerning the amount of noise present at a certain time, at a particular frequency. Hence, we use the post-filter to estimate a missing feature mask that indicates how reliable each region of the spectrum is when performing recognition.

4.3.1 Computation of Missing Feature Masks

The missing feature mask is a matrix representing the reliability of each feature in the time-frequency plane. More specifically, this reliability is computed for each frame and for each Mel-frequency band. This reliability can be either a continuous value from 0 to 1, or a discrete value of 0 or 1. In this work, discrete masks are used.

It is worth mentioning that computing the mask in the Mel-frequency bank domain means that it is not possible to use MFCC features, since the effect of the Discrete Cosine Transform (DCT) cannot be applied to the missing feature mask. For this reason, the log-energy of the Mel-frequency bands are used directly as features.

Each Mel-frequency band is considered reliable if the ratio of the output energy over the input energy is greater than a threshold T_m . The reason for this choice is that it is assumed that the more noise present in a certain frequency band, the lower the post-filter gain will be for that band.

We proceed in two steps. For each frame ℓ and for each MEL frequency band i , do:

1. Compute a continuous mask $m_\ell(i)$ that reflects the reliability of the band:

$$m_\ell(i) = \frac{S_\ell^{out}(i) + N_\ell(i)}{S_\ell^{in}(i)} \quad (4.2)$$

where $S_\ell^{in}(i)$ and $S_\ell^{out}(i)$ are respectively the post-filter input and output energy for frame ℓ at Mel-frequency band i , and $N_\ell(i)$ is the background noise estimate (summation of the $\lambda_m^{stat.}(k, \ell)$ for band i).

2. Deduce a binary mask $M_\ell(i)$ used to remove the unreliable MEL frequency bands at frame ℓ :

$$M_\ell(i) = \begin{cases} 1, & m_\ell(i) > T_m \\ 0, & \text{otherwise} \end{cases} \quad (4.3)$$

where T_m is an arbitrary threshold (we use $T_m = 0.25$ based on speech recognition experiments).

In comparison to McCowan *et al.* [107], the use of the multi-source post-filter allows a better reliability estimation by distinguishing between interference and background noise. We include the background noise estimate $N_\ell(i)$ in the numerator of Equation 4.2 to ensure that the missing feature mask equals 1 when no speech source is present (as long as there is no interference). Without this condition, all of the features would be considered unreliable in the case where no speech is present for the source of interest. This would, in turn, prevent the silence model of the ASR from performing adequately (this has been observed in practice). Using a more conventional post-filter as proposed by McCowan *et al.* [107] and Cohen *et al.* [79] would not allow the mask to preserve silence features, which is known to degrade ASR accuracy. The distinction between background noise and interference also reflects the fact that background noise cancellation is generally much better than interference cancellation.

An example of missing feature masks with the corresponding separated signals after post-filtering is shown in Figure 4.8. It is observed that the mask indeed preserves the silent periods

and considers unreliable regions of the spectrum as dominated by other sources. The missing feature mask for delta-features (time derivative of the Mel spectral features) is computed using the mask for the static features. The dynamic mask $\Delta M_\ell(i)$ is computed as:

$$\Delta M_\ell(i) = \prod_{k=-2}^2 M_{\ell-k}(i) \quad (4.4)$$

and is non-zero only when all the MEL features used to compute the delta-features are deemed reliable.

4.3.2 Speech Analysis for Missing Feature ASR

Since MFCC cannot be easily used directly with a missing feature mask and as the post-filter gains are expressed in the time–frequency plane, we use spectral features that are derived from MFCC features with the Inverse Discrete Cosine Transform (IDCT). The detailed steps for feature generation are as follows:

1. [FFT] The speech signal sampled at 16 kHz is analysed using an FFT with a 400-point window and a 160 frame shift.
2. [Mel] The spectrum is analysed by a Mel-scale filter bank to obtain the Mel-scale spectrum of the 24th order.
3. [Log] The Mel-scale spectrum of the 24th order is converted to log-energies.
4. [DCT] The log Mel-scale spectrum is converted by Discrete Cosine Transform to the cepstrum.
5. [Lifter] Cepstral features 0 and 13-23 are set to zero so as to make the spectrum smoother.
6. [CMS] Convolutional effects are removed using Cepstral Mean Subtraction.
7. [IDCT] The normalised cepstrum is transformed back to the log Mel-scale spectral domain by means of an Inverse DCT.

8. [Differentiation] The features are differentiated in the time domain. Thus, we obtain 24 log spectral features as well as their first-order time derivatives.

The [CMS] step is necessary in order to remove the effect of convolutive noise, such as reverberation and microphone frequency response.

The same features are used for training and evaluation. Training is performed on clean speech, without any effect from the post-filter. In practice, this means that the acoustic model does not need to be adapted in any way to our method and the only difference with a conventional ASR is the use of the missing feature mask as represented in Equation 4.1.

4.3.3 Automatic Speech Recognition Using Missing Feature Theory

Once the ASR features and the missing feature mask are computed, the last step consists of making use of the missing feature mask in the probability model of the ASR. Let $f(x|s)$ be the output probability density of feature vector x in state S . The output probability density is defined by Equation 4.1 and becomes:

$$f(\mathbf{x}|S) = \sum_{j=1}^{M_g} P(j|S) f(\mathbf{x}_r|j, S) \quad (4.5)$$

where $\mathbf{x}_r = \{x_i | M(i) = 1\}$ contains only the reliable features of \mathbf{x} . This means that only reliable features are used in probability calculation, and thus the recogniser can avoid undesirable effects due to unreliable features.

4.4 Results

In this section, we present speech recognition results for the two coupling methods: direct, and using missing feature theory. The testing conditions include recognition of two and three stationary simultaneous speakers, as well as recognition on two moving speakers.

4.4.1 Direct Coupling

For the case where speech recognition is performed directly on the separated speech, we use the same setup as described in Section 1.2. We use the Nuance² speaker-independent commercial speech recognition engine, which only accepts speech sampled at 8 kHz. The test data is composed of 251 utterances of four connected English digits (male and female) selected from the AURORA clean database³. In each test, the utterances are played from two or three speakers at the same time. In the condition where three speakers are used, one speaker is placed at 90 degrees on the left, one is in front of the robot, and the other is placed 90 degrees to the right. In the case of two speakers, only the speakers in front and on the right are used.

Three processing conditions are compared:

1. Use of the GSS algorithm only with no post-filtering;
2. Use of the GSS with post-filter, but without enabling reverberation cancellation (no dereverb., Equation 3.16);
3. The proposed system with GSS, post-filtering including reverberation cancellation (Equation 3.19).

No tests are presented using only one microphone because in this case, the system would have no directional information at all to distinguish between the speakers (it would recognise the same digits for all sources).

Results for two simultaneous speakers are shown in Figure 4.3, while results for three simultaneous speakers are shown in Figure 4.4. The average recognition rate (word correct averaged over all sources) is 83% for three simultaneous speakers and 90% for two simultaneous speakers. In all cases, the proposed system provides a significant improvement over the use of the GSS algorithm alone. The average reduction in word error rate is 51% relative⁴ and is fairly

²<http://www.nuance.com/>

³Files were taken from the `testa/clean1/` to `testa/clean4/` directories.

⁴The relative improvement is computed as the difference in error rates, divided by the error rate for the reference condition.

constant across microphone configuration, environment (reverberation conditions) and number of speakers. The results with no reverberation cancellation show that reverberation cancellation is responsible for half of the post-filter improvement in the E2 environment (1 second reverberation time), but has no significant effect on the E1 environment (350 ms reverberation time), even though individual results vary slightly.

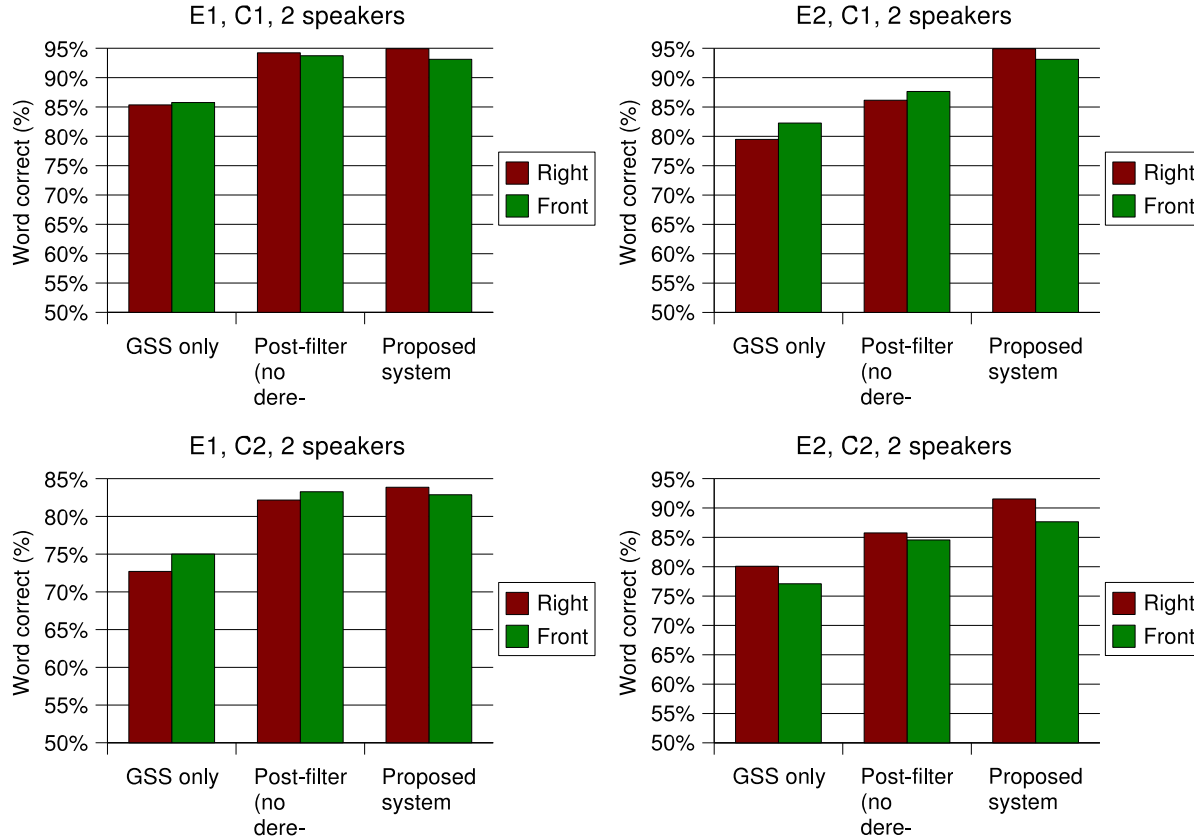


Figure 4.3: Speech recognition results for two simultaneous speakers.

4.4.1.1 Human Capabilities

Just for the sake of comparison, we compare the auditory capabilities developed to human capabilities in a *cocktail party* context. This is done by repeating the previous experiment with a person in the place of the robot. Five different listeners placed in the E1 environment were told to transcribe the digits from the front speaker only. We did not ask the listeners to transcribe all directions because humans can usually only focus their attention on a single source of interest.

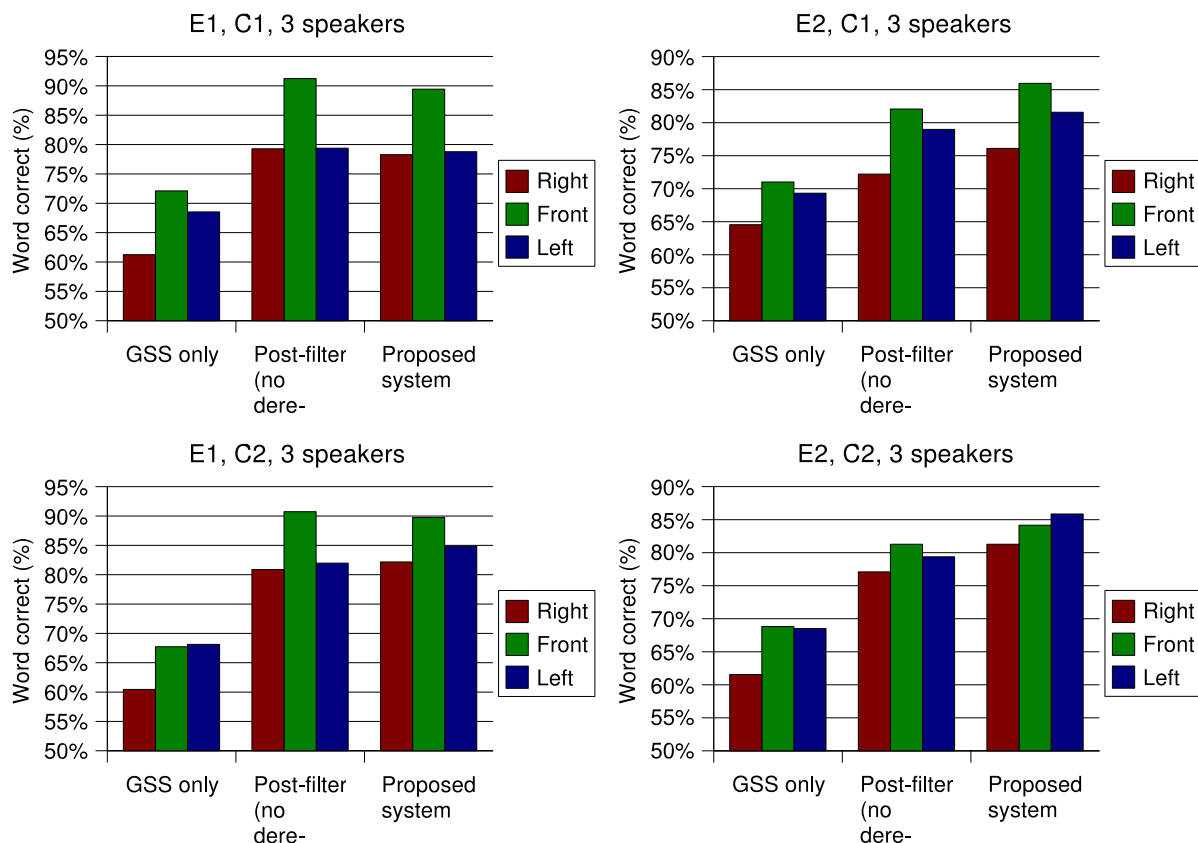


Figure 4.4: Speech recognition results for three simultaneous speakers.

The use of connected digits for the test is convenient because for this, humans cannot make use of higher level language knowledge. Moreover, the listeners were all non-native English speakers. It is shown in [108] that in noisy conditions, non-native listeners tend to obtain recognition accuracy results similar to those obtained by an ASR. This indicates that our tests would be comparing mainly the lower-level auditory capabilities (audio analysis) of humans to our robot.

The results in Figure 4.5 comparing human accuracy show an important variability between speakers. Those results indicate that in difficult *cocktail party* conditions, our system performs equally or better than humans. In fact, the best listener obtained only 0.5% (absolute) better accuracy, while the worst listener had 11% lower accuracy (absolute). We do not however expect these results to hold for the case of real conversations, since in this case, humans have an advantage over an ASR's language model (we are good at “guessing” what words will come

next in a conversation). On the other hand, our system is able to listen to several conversations simultaneously, while our listeners could not recognise much of what originated from the other sources.

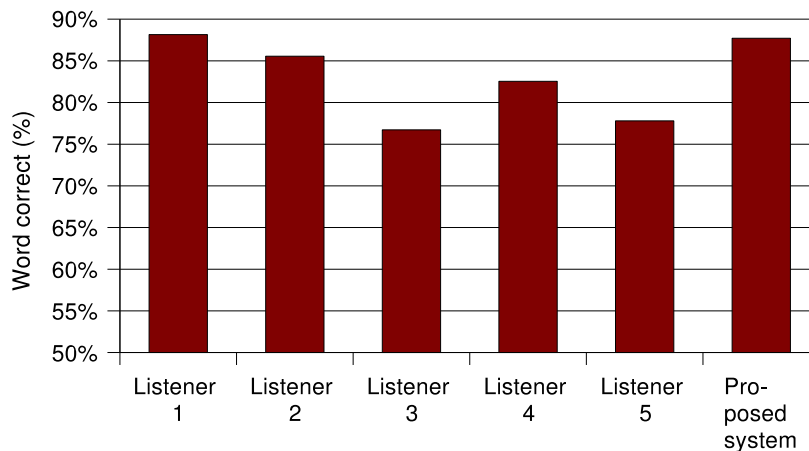


Figure 4.5: Human versus machine speech recognition accuracy.

4.4.1.2 Moving Sources

We performed an experiment to measure speech recognition accuracy when speakers are moving. Unfortunately, the fact that the AURORA data used in the previous experiment is only available at 8 kHz makes accurate tracking impossible because most of the speech bandwidth is not available (see Section 2.5.2.5). For that reason, the digit strings were spoken out loud in the E1 environment, while wandering around the robot at a distance varying between one and two metres. The estimated trajectories of both speakers are shown in Figure 4.6. Over a period of three minutes, only two false detections were found, one of which can be explained as being the sound of a speaker's feet. The speech recognition accuracy (word correct) is 96.0% for the first speaker (trajectory shown in green) and 85.1% for the second speaker (trajectory shown in red). The difference between the two results can be explained by the fact that the first speaker's voice is louder.

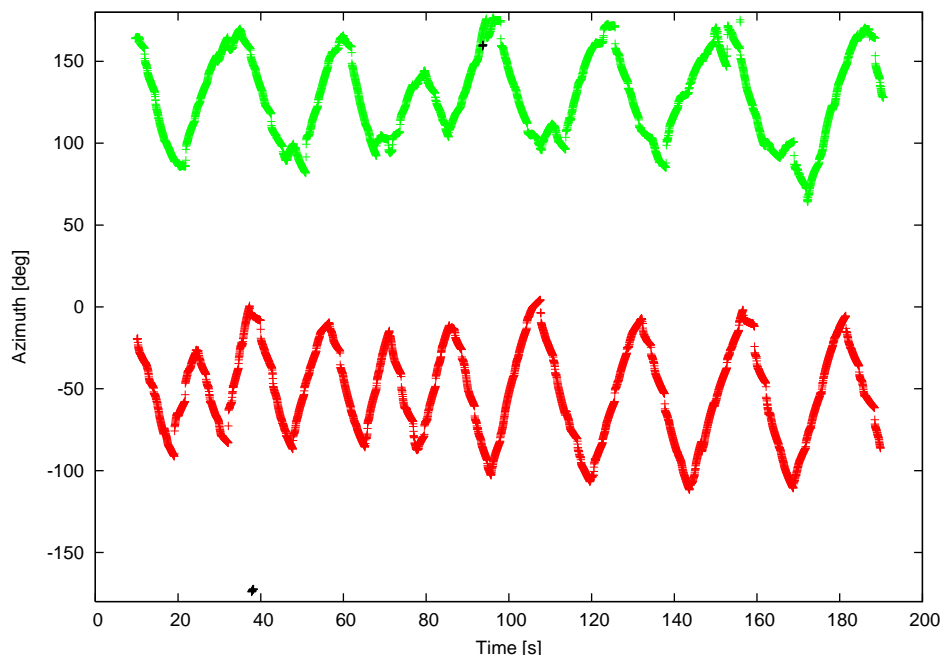


Figure 4.6: Source trajectories (azimuth as a function of time): recognition on two moving speakers. Two false detections are shown in black (around $t = 40$ s and $t = 100$ s).

4.4.2 Missing Feature Theory Coupling

Unlike other experiments, the work on speech recognition integration using missing feature theory is evaluated on the SIG2 humanoid robot on which eight microphones were installed, as shown in Figure 4.7. These results were obtained during a collaboration with Kyoto University and, while they reflect a slightly older version of the separation algorithm, we believe they are nonetheless valid and interesting.

Because the ASR needs to be modified to support MFT, it was not possible to use Nuance as in Section 4.4.1 because it is not distributed with the source code. The speech recognition engine used is based on the CASA Tool Kit (CTK) [98] hosted at Sheffield University, U.K.⁵, and uses 16 kHz audio as input. The same work was also applied to the Julius [109] Japanese ASR⁶, but since preliminary experiments comparing both recognisers showed better recognition accuracy using CTK, only these results are reported.

⁵<http://www.dcs.shef.ac.uk/research/groups/spandh/projects/respice/ctk/>

⁶<http://julius.sourceforge.jp/>

In order to test the system, three Japanese voices (two males, one female) are played simultaneously: one in front, one on the left, and one on the right. In three different experiments, the angle between the centre speaker and the side speakers are set to 30, 60, and 90 degrees. The speakers are placed two meters away from the robot. The room in which the experiment took place has a reverberation time of approximately 300 ms. The post-filter uses short-term spectral amplitude (STSA) estimation [50] since it was found to maximise speech recognition accuracy. Speech recognition complexity is not reported as it usually varies greatly between different engine and settings. Japanese isolated word recognition is performed using speaker-independent triphone [110] acoustic models.

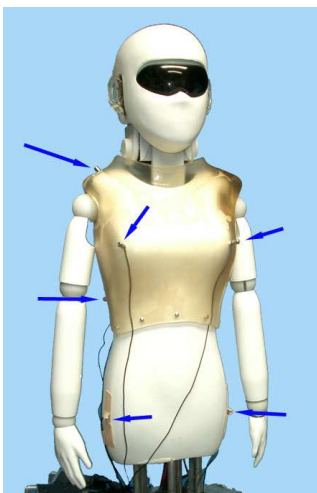


Figure 4.7: SIG 2 robot with eight microphones (two are occluded).

4.4.2.1 Separated Signals

Spectrograms showing separation of the three speakers⁷ are shown in Figure 4.8, along with the corresponding mask for static features. Even though the task involves non-stationary interference with the same frequency content as the signal of interest, we observe that our post-filter is able to remove most of the interference. Informal subjective evaluation has confirmed that

⁷Audio signals and spectrograms for all three sources are available at: <http://www.gel.usherb.ca/laborius/projects/Audible/separation/sap/>

the post-filter has a positive impact on both quality and intelligibility of the speech. This is also confirmed by improved recognition results.

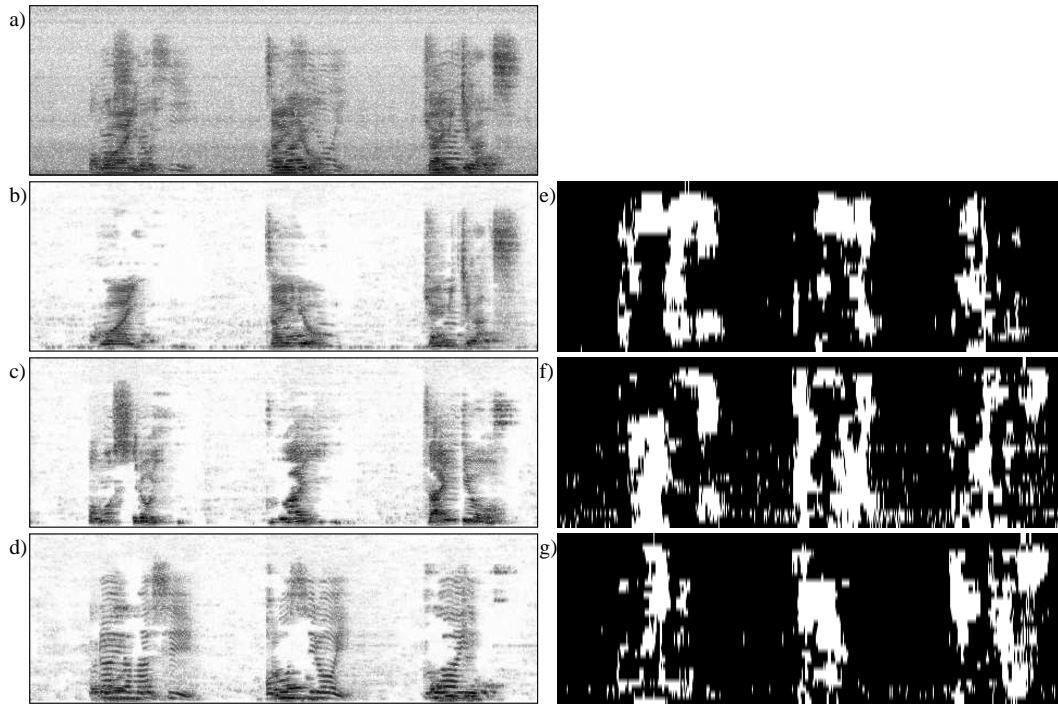


Figure 4.8: Missing feature masks for separation of three speakers, 90° apart with post-filter: a) signal as captured at microphone #1; b) separated right speaker; c) separated centre speaker; d) separated left speaker; e) – g) corresponding mel-frequency missing feature mask for static features with reliable features ($M_\ell(i) = 1$) shown in black. Time is represented on the x-axis and frequency (0-8kHz) on the y-axis.

4.4.2.2 Speech Recognition Accuracy

We present speech recognition accuracy results obtained in three different conditions:

1. Geometric Source Separation (GSS) only;
2. GSS separation plus post-filter;
3. GSS separation plus post-filter and missing feature mask.

Again, no tests are presented using only one microphone because in this case, the system would have no directional information at all to distinguish between the speakers (it would recognise

the same digits for all sources). The speech recognition accuracy on the clean (non-mixed) data is usually very high (>95%), so it is not reported either.

The test set contains 200 isolated common Japanese words spoken simultaneously by two male speakers and one female speaker. There is no overlap with the training set. Results are presented in Figures 4.9, 4.10 and 4.11. The relatively poor results with GSS only are mainly due to the highly non-stationary interference coming from the two other speakers and the fact that the microphones placement is constrained by the robot dimensions. The post-filter brings an average reduction in relative error rate⁸ of 10% over use of GSS alone. When the post-filter is combined with missing feature theory, the total improvement becomes 38%. The important difference in recognition accuracy as a function of direction (left, centre, right) is mainly due to differences in playback level, resulting in different SNR levels after GSS. It can also be observed from the results that accuracy decreases as the separation between sources decreases. This can be explained by the fact that it is more difficult to find a demixing matrix for narrow angles, making the GSS step less efficient. Note that these results cannot be compared to those obtained in Section 4.4.1 because the task and experimental setup are completely different.

4.5 Discussion

In this chapter, we demonstrate a complete multi-microphone speech recognition system that integrates all stages of source separation and recognition so as to maximise accuracy in the context of simultaneous speakers. We also demonstrate that the multi-source post-filter described in Section 3.4 can be optionally used to enhance speech recognition accuracy by providing feature reliability information (in the form of a missing feature mask) to a missing feature theory-based ASR. This optional missing feature mask is designed so that only spectral regions dominated by interference are marked as unreliable.

When the separation system is coupled directly to the ASR without the use of a missing

⁸The relative error rate is computed as the difference in errors divided by the number of errors in the reference setup.

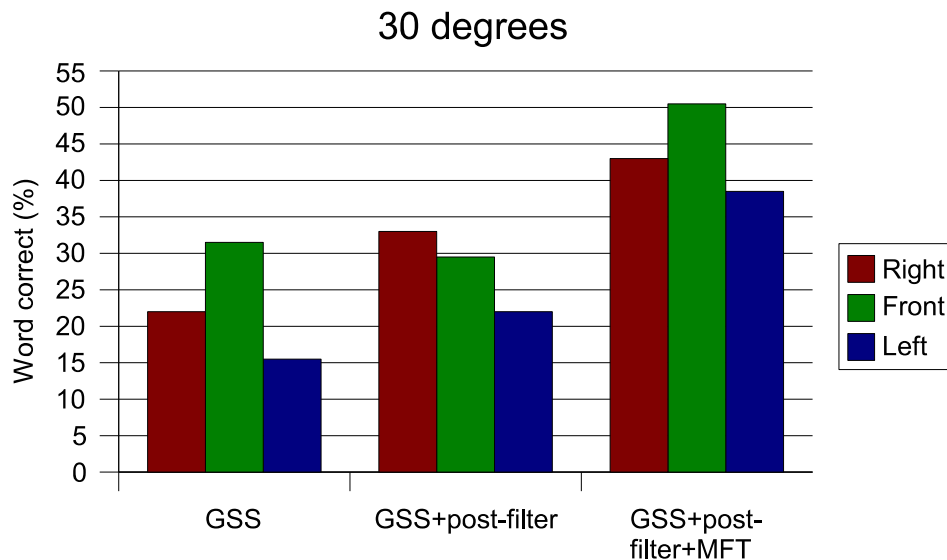


Figure 4.9: Speech recognition accuracy results for 30° separation between speakers.

feature mask, the speech recognition rate is on average 83% for three simultaneous speakers and 90% for two simultaneous speakers. The result also clearly demonstrates the importance of the post-filter and reverberation cancellation for reverberant environments. Moreover, the results obtained are equal or better than those obtained by human listeners in the same conditions. Good results are also obtained when the speakers are moving.

When using a missing feature theory-based ASR, we have obtained a reduction of 38% (relative) in error rate compared to separation with GSS only. In this case, the post-filter alone contributes to a 10% reduction in error rate. This shows that speech recognition on simultaneous speakers can be enhanced when using the missing feature framework in conjunction with a multi-source post-filter.

In the future, we believe it is possible for the technique to be generalised to the use of cepstral features (which provide better accuracy) instead of spectral features. One way to achieve this would be to go one step further to increase speech recognition robustness by explicitly considering the uncertainty in the feature values. Instead of considering features as reliable or unreliable, the acoustic model would take into consideration both the estimated features and their variance, as proposed in [111, 112].

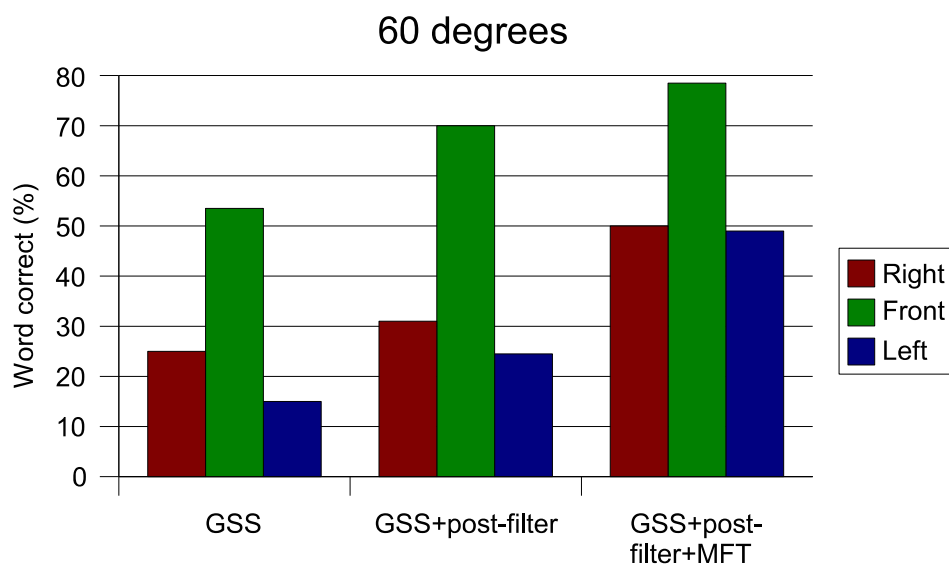


Figure 4.10: Speech recognition accuracy results for 60° separation between speakers.

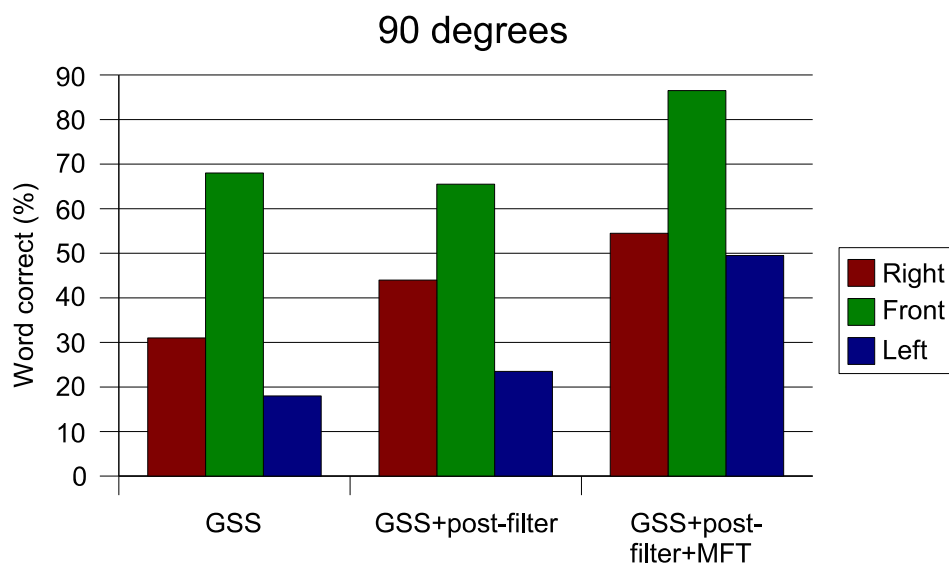


Figure 4.11: Speech recognition accuracy results for 90° separation between speakers.

Chapter 5

Conclusion

In this thesis, a complete auditory system for a mobile robot is presented. The system is composed of subsystems for localising sources, separating the different sources, as well as performing speech recognition. The sound localisation system is composed of two parts: a steered beamformer implemented in the frequency domain that is able to “listen” for sources in all possible directions; a particle filter using a probabilistic model to track multiple sound sources by combining past and present estimations from the steered beamformer.

The sound source separation algorithm is also composed of two parts. The first part is an implementation of the Geometric Source Separation (GSS) algorithm that provides partial separation using the microphone array audio data and the location of the sources. The sources separated by the GSS algorithm are then sent to the second part, a multi-source post-filter, that uses a log-domain spectral estimator to further remove noise, interference and reverberation. The novelty of our post-filter is that it estimates the spectrum of interferences by using the other separated sources.

The output of the sound source separation subsystem is used for performing speech recognition. The audio can be sent directly to an ASR for recognition. Optionally, it is possible to use internal values from the post-filter to compute a missing feature mask, representing the reliability of the spectral features. That mask can then be sent to the ASR so as to ignore unreliable

features and increase recognition rate.

We can now comment on the original mobile robotics constraints imposed on the system, as outlined in Chapter 1:

- **Limited computational capabilities.** The system is able to function in real-time consuming between 40% and 70% (depending on the number of sources present) of the CPU cycles on a Pentium-M 1.6 GHz. Using machine-dependant optimisations could probably help to further reduce the computational requirements.
- **Need for real-time processing with reasonable delay.** The delay added by the localisation system is 50 ms, which is small enough for any application (and no longer than typical human reflexes). The delay for the separation is even less, so it is only limited by the delay in localisation information. In cases where it is needed, an additional delay of 500 ms to the localisation algorithm also provides smoother tracking, while still making the (rougher) short-delay estimations available for source separation and fast reflex actions.
- **Weight and space constraints.** The additional weight of the system is composed only of the eight microphones (very light), the soundcard and the embedded computer. Of these, the soundcard and computer could be made even smaller by the use of a DSP card. The space constraints are also respected, since each microphone is a 2.5 cm square (could be even further reduced by using smaller components) and can be placed directly on the surface of the robot's frame, without having to modify the robot in any way.
- **Noisy operating environment (both point source, diffuse sources, robot noise).** We have shown that the system works in noisy environments, with several people talking at the same time. Also, the system is shown to perform reliably even in a room where the reverberation time is 1 second.
- **Mobile sound sources.** The system is tested in conditions where the sound sources are moving and is still able to perform both tracking and separation on those sources.

- **Mobile reference system (robot can move).** We demonstrate that the system functions when the robot is moving. Also, because no absolute reference is used, this case is equivalent to the case where all sources are moving (the system does not know whether the robot or the sources are moving).
- **Adaptability.** The system is demonstrated in two different configurations on the Spartacus robot. Also, a collaboration with Kyoto University has shown that the system could work on the SIG2 robot without any modification.

In light of this, we can say that all the goals set for a mobile robot auditory system are successfully achieved.

5.1 Future Work

An important aspect of speech-based human-robot interaction that has not been addressed in this thesis is dialog management. While it is important for a robot to be able to recognise speech in real-life environments, it is equally important for the robot to know what to say and what to expect as a response. The latter means that the robot should be able to update its speech recognition context (vocabulary, grammar and/or language model) dynamically. Also, it would be desirable for a robot to have good conversational and socialising skills. As part of a more complete dialog system, it would be interesting for the robot to still be able to listen even when it is speaking. This would require using echo cancellation to subtract the speech from the robot from the signal captured at the microphones.

Since the current system is able to recognise what is being said by a speaker, the logical extension would be to recognise who the speaker is. This would involve running speaker identification algorithms on the separated outputs. Also, it would be useful to recognise non-speech sounds occurring in the environment. These include people walking, doors closing, phones ringing, etc. This could be used to direct the attention of the robot, e.g. by directing a camera to events occurring in its surroundings.

Another area of research in mobile robot audition would be to apply human-inspired audition techniques with the use of a microphone array. This includes making use of the head-related transfer function (HRTF) along with interaural intensity difference (IID) to obtain additional information about the signals. In the same spirit, it would be interesting to adapt computational auditory scene analysis (CASA) and neural based techniques [113] to the use of microphone arrays.

Finally, on a more practical aspect, a useful improvement would consist of implementing the system described in this thesis on a DSP platform. This would allow integration with a larger variety of robots by alleviating the size and computational requirements.

5.2 Perspectives

While the system developed for this thesis is especially targeted at mobile robotics, many of the advancements made are also applicable to other fields or research areas. First, the localisation algorithm developed can be easily adapted to a video-conferencing application. It would thus allow the camera to automatically follow the person speaking, even if that person is moving, as is done by Mungamuru and Aarabi [54].

The sound separation system can also be applied to different fields. The robustness to noise would make it suitable for use in noisy environments (such as automobiles) in order to improve speech recognition accuracy. The ability to perform recognition simultaneously on different speakers would also make it possible to generate a real-time text version of a meeting (e.g., for deaf participants), as well as performing automatic generation of meeting minutes or lecture transcription. Also, the localisation information combined with speech recognition results would allow automatic annotation of audio content and could be used in conjunction with the Annodex¹ annotation format [114].

Now that we have demonstrated that it is possible for a mobile robot to have auditory

¹<http://www.annodex.net/>

capabilities close to that of humans (and in some cases maybe better), we believe that mobile robots will be able to interact more naturally with humans in an unconstrained environments. This assertion will soon be verified in practice as the Spartacus robot will attend the 2005 AAAI conference as part of the AAAI challenge².

²<http://palantir.swarthmore.edu/aaai05/robotChallenge.htm>

Bibliography

- [1] R. A. Brooks, C. Breazeal, R. Irie, C. Kemp, M. Marjanovic, B. Scassellati, and M. Williamson, “Alternate essences of intelligence,” in *Proceedings National Conference on Artificial Intelligence*, 1998, pp. 961–976.
- [2] M. Marschark, *Raising and Educating a Deaf Child*. Oxford University Press, 1998, <http://www.rit.edu/memrtl/course/interpreting/modules/modulelist.htm>.
- [3] R. H. Ehmer, “Masking patterns of tones,” *Journal of the Acoustical Society of America*, vol. 31, no. 8, 1959.
- [4] R. Irie, “Robust sound localization: An application of an auditory perception system for a humanoid robot,” Master’s thesis, MIT Department of Electrical Engineering and Computer Science, 1995.
- [5] R. Brooks, C. Breazeal, M. Marjanovic, B. Scassellati, and M. Williamson, “The Cog project: Building a humanoid robot,” in *Computation for Metaphors, Analogy, and Agents*, C. Nehaniv, Ed. Spriver-Verlag, 1999, pp. 52–87.
- [6] K. Nakadai, T. Lourens, H. G. Okuno, and H. Kitano, “Active audition for humanoid,” in *Proceedings National Conference on Artificial Intelligence*, 2000, pp. 832–839.
- [7] K. Nakadai, T. Matsui, H. G. Okuno, and H. Kitano, “Active audition system and humanoid exterior design,” in *Proceedings IEEE/RSJ International Conference on Intelligent Robots and Systems*, 2000, pp. 1453–1461.
- [8] K. Nakadai, K. Hidai, H. G. Okuno, and H. Kitano, “Real-time multiple speaker tracking by multi-modal integration for mobile robots,” in *Proceedings Eurospeech*, 2001, pp. 1193–1196.
- [9] H. G. Okuno, K. Nakadai, K.-I. Hidai, H. Mizoguchi, and H. Kitano, “Human-robot interaction through real-time auditory and visual multiple-talker tracking,” in *Proceedings IEEE/RSJ International Conference on Intelligent Robots and Systems*, 2001, pp. 1402–1409.
- [10] K. Nakadai, H. G. Okuno, and H. Kitano, “Real-time sound source localization and separation for robot audition,” in *Proceedings IEEE International Conference on Spoken Language Processing*, 2002, pp. 193–196.

- [11] —, “Exploiting auditory fovea in humanoid-human interaction,” in *Proceedings National Conference on Artificial Intelligence*, 2002, pp. 431–438.
- [12] K. Nakadai, D. Matsuura, H. G. Okuno, and H. Kitano, “Applying scattering theory to robot audition system: Robust sound source localization and extraction,” in *Proceedings IEEE/RSJ International Conference on Intelligent Robots and Systems*, 2003, pp. 1147–1152.
- [13] S. Yamamoto, K. Nakadai, H. Tsujino, T. Yokoyama, and H. Okuno, “Improvement of robot audition by interfacing sound source separation and automatic speech recognition with missing feature theory,” in *Proceedings IEEE International Conference on Robotics and Automation*, 2004, pp. 1517–1523.
- [14] S. Yamamoto, K. Nakadai, H. Tsujino, and H. Okuno, “Assessment of general applicability of robot audition system by recognizing three simultaneous speeches,” in *Proceedings IEEE/RSJ International Conference on Intelligent Robots and Systems*, 2004, pp. 2111–2116.
- [15] Y. Matsusaka, T. Tojo, S. Kubota, K. Furukawa, D. Tamiya, K. Hayata, Y. Nakano, and T. Kobayashi, “Multi-person conversation via multi-modal interface - A robot who communicate with multi-user,” in *Proceedings Eurospeech*, 1999, pp. 1723–1726.
- [16] Y. Matsusaka, S. Fujie, and T. Kobayashi, “Modeling of conversational strategy for the robot participating in the group conversation,” in *Proceedings Eurospeech*, 2001.
- [17] Y. Zhang and J. Weng, “Grounded auditory development by a developmental robot,” in *Proceedings INNS/IEEE International Joint Conference of Neural Networks*, 2001, pp. 1059–1064.
- [18] M. Fujita, Y. Kuroki, T. Ishida, and T. Doi, “Autonomous behavior control architecture of entertainment humanoid robot SDR-4X,” in *Proceedings IEEE/RSJ International Conference on Intelligent Robots and Systems*, 2003, pp. 960–967.
- [19] C. Choi, D. Kong, J. Kim, and S. Bang, “Speech enhancement and recognition using circular microphone array for service robots,” in *Proceedings IEEE/RSJ International Conference on Intelligent Robots and Systems*, 2003, pp. 3516–3521.
- [20] H. Asoh, S. Hayamizu, I. Hara, Y. Motomura, S. Akaho, and T. Matsui, “Socially embedded learning of the office-conversant mobile robot *jijo-2*,” in *Proceedings International Joint Conference on Artificial Intelligence*, vol. 1, 1997, pp. 880–885.
- [21] F. Asano, H. Asoh, and T. Matsui, “Sound source localization and signal separation for office robot *jijo-2*,” in *Proceedings International Conference on Multisensor Fusion and Integration for Intelligent Systems*, 1999, pp. 243–248.
- [22] F. Asano, M. Goto, K. Itou, and H. Asoh, “Real-time source localization and separation system and its application to automatic speech recognition,” in *Proceedings Eurospeech*, 2001, pp. 1013–1016.

- [23] H. Asoh, F. Asano, K. Yamamoto, T. Yoshimura, Y. Motomura, N. Ichimura, I. Hara, and J. Ogata, "An application of a particle filter to bayesian multiple sound source tracking with audio and video information fusion," in *Proceedings International Conference on Information Fusion*, 2004, pp. 805–812.
- [24] P. J. Prodanov, A. Drygajlo, G. Ramel, M. Meisser, and R. Siegwart, "Voice enabled interface for interactive tour-guided robots," in *Proceedings IEEE/RSJ International Conference on Intelligent Robots and Systems*, 2002, pp. 1332–1337.
- [25] C. Theobalt, J. Bos, T. Chapman, A. Espinosa-Romero, M. Fraser, G. Hayes, E. Klein, T. Oka, and R. Reeve, "Talking to Godot: Dialogue with a mobile robot," in *Proceedings IEEE/RSJ International Conference on Intelligent Robots and Systems*, 2002, pp. 1338–1343.
- [26] J. Huang, T. Supaongprapa, I. Terakura, F. Wang, N. Ohnishi, and N. Sugie, "A model-based sound localization system and its application to robot navigation," *Robots and Autonomous Systems*, vol. 27, no. 4, pp. 199–209, 1999.
- [27] G. Tesch and U. Zimmer, "Acoustic-based room discrimination for the navigation of autonomous mobile robots," in *Proceedings IEEE International Symposium on Computational Intelligence in Robotics and Automation*, 1999, pp. 274–281.
- [28] S. H. Young and M. V. Scanlon, "Detection and localization with an acoustic array on a small robotic platform in urban environments," U.S. Army Research Laboratory, Tech. Rep., 2003.
- [29] C. Breazeal, "Emotive qualities in robot speech," in *Proceedings IEEE/RSJ International Conference on Intelligent Robots and Systems*, 2001, pp. 1389–1394.
- [30] D. Rabinkin, "Optimum sensor placement for microphone arrays," Ph.D. dissertation, Graduate School – New Brunswick Rutgers, The State University of New Jersey, 1998.
- [31] C. Côté, D. Létourneau, F. Michaud, J.-M. Valin, Y. Brosseau, C. Raïevsky, M. Lemay, and V. Tran, "Code reusability tools for programming mobile robots," in *Proceedings IEEE/RSJ International Conference on Intelligent Robots and Systems*, 2004.
- [32] L. C. Parra and C. V. Alvino, "Geometric source separation: Merging convolutive source separation with geometric beamforming," *IEEE Transactions on Speech and Audio Processing*, vol. 10, no. 6, pp. 352–362, 2002.
- [33] W. M. Hartmann, "How we localize sounds," *Physics Today*, vol. 47, pp. 29–34, 1999.
- [34] J.-M. Valin, F. Michaud, B. Hadjou, and J. Rouat, "Localization of simultaneous moving sound sources for mobile robot using a frequency-domain steered beamformer approach," in *Proceedings IEEE International Conference on Robotics and Automation*, vol. 1, 2004, pp. 1033–1038.
- [35] K. Nakadai, T. Lourens, H. G. Okuno, and H. Kitano, "Active audition for humanoid," in *Proceedings National Conference on Artificial Intelligence*, 2000, pp. 832–839.

- [36] J.-M. Valin, F. Michaud, J. Rouat, and D. Létourneau, "Robust sound source localization using a microphone array on a mobile robot," in *Proceedings IEEE/RSJ International Conference on Intelligent Robots and Systems*, 2003, pp. 1228–1233.
- [37] S. Kagami, Y. Tamai, H. Mizoguchi, and T. Kanade, "Microphone array for 2D sound localization and capture," in *Proceedings IEEE International Conference on Robotics and Automation*, 2004, pp. 703–708.
- [38] Q. Wang, T. Ivanov, and P. Aarabi, "Acoustic robot navigation using distributed microphone arrays," *Information Fusion (Special Issue on Robust Speech Processing)*, vol. 5, no. 2, pp. 131–140, 2004.
- [39] D. Bechler, M. Schlosser, and K. Kroschel, "System for robust 3D speaker tracking using microphone array measurements," in *Proceedings IEEE/RSJ International Conference on Intelligent Robots and Systems*, 2004, pp. 2117–2122.
- [40] M. S. Arulampalam, S. Maskell, N. Gordon, and T. Clapp, "A tutorial on particle filters for online nonlinear/non-gaussian bayesian tracking," *IEEE Transactions on Signal Processing*, vol. 50, no. 2, pp. 174–188, 2002.
- [41] D. B. Ward and R. C. Williamson, "Particle filtering beamforming for acoustic source localization in a reverberant environment," in *Proceedings IEEE International Conference on Acoustics, Speech, and Signal Processing*, vol. II, 2002, pp. 1777–1780.
- [42] D. B. Ward, E. A. Lehmann, and R. C. Williamson, "Particle filtering algorithms for tracking an acoustic source in a reverberant environment," *IEEE Transactions on Speech and Audio Processing*, vol. 11, no. 6, pp. 826–836, 2003.
- [43] J. Vermaak and A. Blake, "Nonlinear filtering for speaker tracking in noisy and reverberant environments," in *Proceedings IEEE International Conference on Acoustics, Speech, and Signal Processing*, vol. 5, 2001, pp. 3021–3024.
- [44] J. Vermaak, A. Doucet, and P. Pérez, "Maintaining multi-modality through mixture tracking," in *Proceedings International Conference on Computer Vision*, 2003, pp. 1950–1954.
- [45] J. MacCormick and A. Blake, "A probabilistic exclusion principle for tracking multiple objects," *International Journal of Computer Vision*, vol. 39, no. 1, pp. 57–71, 2000.
- [46] C. Hue, J.-P. L. Cadre, and P. Perez, "A particle filter to track multiple objects," in *Proceedings IEEE Workshop on Multi-Object Tracking*, 2001, pp. 61–68.
- [47] J. Vermaak, S. Godsill, and P. Pérez, "Monte Carlo filtering for multi-target tracking and data association," *IEEE Transactions on Aerospace and Electronic Systems*, 2005. (To appear).
- [48] R. Duraiswami, D. Zotkin, and L. Davis, "Active speech source localization by a dual coarse-to-fine search," in *Proceedings IEEE International Conference on Acoustics, Speech, and Signal Processing*, 2001, pp. 3309–3312.

- [49] M. Omologo and P. Svaizer, "Acoustic event localization using a crosspower-spectrum phase based technique," in *Proceedings IEEE International Conference on Acoustics, Speech, and Signal Processing*, 1994, pp. II-273-II-276.
- [50] Y. Ephraim and D. Malah, "Speech enhancement using minimum mean-square error short-time spectral amplitude estimator," *IEEE Transactions on Acoustics, Speech and Signal Processing*, vol. ASSP-32, no. 6, pp. 1109-1121, 1984.
- [51] I. Cohen and B. Berdugo, "Speech enhancement for non-stationary noise environments," *Signal Processing*, vol. 81, no. 2, pp. 2403-2418, 2001.
- [52] J. Huang, N. Ohnishi, and N. Sugie, "Sound localization in reverberant environment based on the model of the precedence effect," *IEEE Transactions on Instrumentation and Measurement*, vol. 46, no. 4, pp. 842-846, 1997.
- [53] J. Huang, N. Ohnishi, X. Guo, and N. Sugie, "Echo avoidance in a computational model of the precedence effect," *Speech Communication*, vol. 27, no. 3-4, pp. 223-233, 1999.
- [54] B. Mungamuru and P. Aarabi, "Enhanced sound localization," *IEEE Transactions on Systems, Man, and Cybernetics Part B*, vol. 34, no. 3, pp. 1526-1540, 2004.
- [55] F. Giraldo, "Lagrange-Galerkin methods on spherical geodesic grids," *Journal of Computational Physics*, vol. 136, pp. 197-213, 1997.
- [56] A. Doucet, S. Godsill, and C. Andrieu, "On sequential Monte Carlo sampling methods for bayesian filtering," *Statistics and Computing*, vol. 10, pp. 197-208, 2000.
- [57] W. M. Hartmann, "Localization of sounds in rooms," *Journal of the Acoustical Society of America*, vol. 74, pp. 1380-1391, 1983.
- [58] B. Rakerd and W. M. Hartmann, "Localization of noise in a reverberant environment," in *Proceedings International Congress on Acoustics*, 2004.
- [59] S. Haykin, *Neural Networks, a Comprehensive Foundation*, 2nd ed. Prentice Hall, 1999.
- [60] J.-F. Cardoso, "Blind signal separation: Statistical principles," in *Proceedings IEEE*, vol. 9, no. 10, 1998, pp. 2009-2025.
- [61] H. Saruwatari, T. Kawamura, and K. Shikano, "Blind source separation for speech based on fast-convergence algorithm with ica and beamforming," in *Proceedings Eurospeech*, 2001, pp. 2603-2606.
- [62] A. Koutras, E. Dermatas, and G. Kokkinakis, "Improving simultaneous speech recognition in real room environments using overdetermined blind source separation," in *Proceedings Eurospeech*, 2001, pp. 1009-1012.
- [63] S. Araki, S. Makino, R. Mukai, and H. Saruwatari, "Equivalence between frequency domain blind source separation and frequency domain adaptive null beamformers," in *Proceedings Eurospeech*, 2001, pp. 2595-2598.

- [64] R. Mukai, S. Araki, and S. Makino, "Separation and dereverberation performance of frequency domain blind source separation for speech in a reverberant environment," in *Proceedings Eurospeech*, 2001, pp. 2599–2602.
- [65] S. Rickard, R. Balan, and J. Rosca, "Real-time time-frequency based blind source separation," in *Proceedings International Conference on Independent Component Analysis and Blind Source Separation*, 2001, pp. 651–656.
- [66] S. Araki, S. Makino, A. Blin, R. Mukai, and H. Sawada, "Underdetermined blind separation for speech in real environments with sparseness and ica," in *Proceedings IEEE International Conference on Acoustics, Speech, and Signal Processing*, 2004, pp. 881–884.
- [67] S.-I. Amari, A. Cichocki, and H. H. Yang, "Blind signal separation and extraction: Neural and information-theoretic approaches," in *Unsupervised Adaptive Filtering volume I, Blind Source Separation*, ser. Adaptive and Learning Systems for Signal Processing. Wiley-Interscience, 2000, ch. 3, pp. 63–138.
- [68] P. Comon and P. Chevalier, "Blind source separation: Models, concepts, algorithms, and performance," in *Unsupervised Adaptive Filtering Volume I, Blind Source Separation*, ser. Adaptive and Learning Systems for Signal Processing. Wiley-Interscience, 2000, ch. 5, pp. 191–235.
- [69] S. Haykin, *Adaptive Filter Theory*, 4th ed. Prentice Hall, 2002.
- [70] L. J. Griffiths and C. W. Jim, "An alternative approach to linearly constrained adaptive beamforming," *IEEE Transactions on Antennas and Propagation*, vol. AP-30, no. 1, pp. 27–34, 1982.
- [71] S. Gannot, D. Burshtein, and E. Weinstein, "Signal enhancement using beamforming and nonstationarity with application to speech," *IEEE Transactions on Signal Processing*, vol. 49, no. 8, pp. 1614–1626, 2001.
- [72] O. Hoshuyama, A. Sugiyama, and A. Hirano, "A robust adaptive beamformer for microphone arrays with a blocking matrix using constrained adaptive filters," *IEEE Transactions on Signal Processing*, vol. 47, no. 10, pp. 2677–2684, 1999.
- [73] M. S. Pedersen and L. K. Hansen, "Semi-blind source separation using head-related transfer functions," in *Proceedings IEEE International Conference on Acoustics, Speech, and Signal Processing*, vol. V, 2004, pp. 713–716.
- [74] S. F. Boll, "A spectral subtraction algorithm for suppression of acoustic noise in speech," in *Proceedings IEEE International Conference on Acoustics, Speech, and Signal Processing*, 1979, pp. 200–203.
- [75] Y. Ephraim and D. Malah, "Speech enhancement using minimum mean-square error log-spectral amplitude estimator," *IEEE Transactions on Acoustics, Speech and Signal Processing*, vol. ASSP-33, no. 2, pp. 443–445, 1985.

- [76] R. Zelinski, "A microphone array with adaptive post-filtering for noise reduction in reverberant rooms," in *Proceedings IEEE International Conference on Acoustics, Speech, and Signal Processing*, vol. 5, 1988, pp. 2578–2581.
- [77] I. McCowan, C. Marro, and L. Mauuary, "Robust speech recognition using near-field superdirective beamforming with post-filtering," in *Proceedings IEEE International Conference on Acoustics, Speech, and Signal Processing*, 2000, p. 1723.
- [78] I. McCowan and H. Bourlard, "Microphone array post-filter for diffuse noise field," in *Proceedings IEEE International Conference on Acoustics, Speech, and Signal Processing*, vol. 1, 2002, pp. 905–908.
- [79] I. Cohen and B. Berdugo, "Microphone array post-filtering for non-stationary noise suppression," in *Proceedings IEEE International Conference on Acoustics, Speech, and Signal Processing*, 2002, pp. 901–904.
- [80] J.-M. Valin, J. Rouat, and F. Michaud, "Enhanced robot audition based on microphone array source separation with post-filter," in *Proceedings IEEE/RSJ International Conference on Intelligent Robots and Systems*, 2004, pp. 2123–2128.
- [81] I. Cohen, "On the decision-directed estimation approach of Ephraim and Malah," in *Proceedings IEEE International Conference on Acoustics, Speech, and Signal Processing*, 2004, pp. 293–296.
- [82] J.-M. Valin, J. Rouat, and F. Michaud, "Microphone array post-filter for separation of simultaneous non-stationary sources," in *Proceedings IEEE International Conference on Acoustics, Speech, and Signal Processing*, 2004.
- [83] M. Wu and D. Wang, "A two-stage algorithm for enhancement of reverberant speech," in *Proceedings IEEE International Conference on Acoustics, Speech, and Signal Processing*, 2005, pp. 1085–1088.
- [84] M. S. Choi and H. G. Kang, "An improved estimation of a priori speech absence probability for speech enhancement : in perspective of speech perception," in *Proceedings IEEE International Conference on Acoustics, Speech, and Signal Processing*, 2005, pp. 1117–1120.
- [85] D. Pearce, "Developing the ETSI Aurora advanced distributed speech recognition front-end & what next," in *Proceedings IEEE Automatic Speech Recognition and Understanding Workshop*, 2001.
- [86] P. Aarabi and G. Shi, "Phase-based dual-microphone robust speech enhancement," *IEEE Transactions on Systems, Man and Cybernetics*, vol. 34, no. 4, pp. 1763–1773, 2004.
- [87] F. Asano, M. Goto, K. Itou, and H. Asoh, "Real-time sound source localization and separation system and its application to automatic speech recognition," in *Proceedings Eurospeech*, 2001, pp. 1013–1016.

- [88] K. Nakadai, H. G. Okuno, and H. Kitano, "Auditory fovea based speech separation and its application to dialog system," in *Proceedings IEEE/RSJ International Conference on Intelligent Robots and Systems*, 2002, pp. 1314–1319.
- [89] P. Renevey, R. Vetter, and J. Kraus, "Robust speech recognition using missing feature theory and vector quantization," in *Proceedings Eurospeech*, 2001, pp. 1107–1110.
- [90] J. Barker, L. Josifovski, M. Cooke, and P. Green, "Soft decisions in missing data techniques for robust automatic speech recognition," in *Proceedings IEEE International Conference on Spoken Language Processing*, vol. I, 2000, pp. 373–376.
- [91] S. Yamamoto, J.-M. Valin, K. Nakadai, J. Rouat, F. Michand, T. Ogata, and H. G. Okuno, "Enhanced robot speech recognition based on microphone array source separation and missing feature theory," in *Proceedings IEEE International Conference on Robotics and Automation*, 2005, pp. 1489–1494.
- [92] R. P. Lippmann, E. A. Martin, and D. B. Paul, "Multi-style training for robust isolated-word speech recognition," in *Proceedings IEEE International Conference on Acoustics, Speech, and Signal Processing*, 1987, pp. 705–708.
- [93] M. Blanchet, J. Boudy, and P. Lockwood, "Environment adaptation for speech recognition in noise," in *Proceedings European Signal Processing Conference*, vol. VI, 1992, pp. 391–394.
- [94] D. O'Shaughnessy, "Interacting with computers by voice: automatic speech recognition and synthesis," *Proceedings of the IEEE*, vol. 91, no. 9, pp. 1272–1305, Sept. 2003.
- [95] M. L. Seltzer and R. M. Stern, "Subband parameter optimization of microphone arrays for speech recognition in reverberant environments," in *Proceedings IEEE International Conference on Acoustics, Speech, and Signal Processing*, 2003, pp. 408–411.
- [96] M. Cooke, P. Green, and M. Crawford, "Handling missing data in speech recognition," in *Proceedings IEEE International Conference on Spoken Language Processing*, 1994, Paper 26.20.
- [97] M. Cooke, P. Green, L. Josifovski, and A. Vizinho, "Robust automatic speech recognition with missing and unreliable acoustic data," *Speech Communication*, vol. 34, pp. 267–285, 2001.
- [98] J. Barker, M. Cooke, and P. Green, "Robust ASR based on clean speech models: An evaluation of missing data techniques for connected digit recognition in noise," in *Proceedings Eurospeech*, 2001, pp. 213–216.
- [99] J. Picone, "Signal modeling techniques in speech recognition," *IEEE Proceedings*, vol. 81, no. 9, pp. 1215–1247, 1993.
- [100] H. V. hamme, "Robust speech recognition using missing feature theory in the cepstral or LDA domain," in *Proceedings Eurospeech*, 2003, pp. 1973–1976.

- [101] —, “Robust speech recognition using cepstral domain missing data techniques and noisy masks,” in *Proceedings IEEE International Conference on Acoustics, Speech, and Signal Processing*, 2004, pp. 213–216.
- [102] B. Raj, M. L. Seltzer, and R. M. Stern, “Reconstruction of missing features for robust speech recognition,” *Speech Communication*, vol. 43, no. 4, pp. 275–296, 2004.
- [103] M. L. Seltzer, B. Raj, and R. M. Stern, “A bayesian framework for spectrographic mask estimation for missing feature speech recognition,” *Speech Communication*, vol. 43, no. 4, pp. 379–393, Sept 2004.
- [104] J. Ming, P. Jancovic, and F. J. Smith, “Robust speech recognition using probabilistic union models,” *IEEE Transactions on Speech and Audio Processing*, vol. 10, no. 6, pp. 403–414, 2002.
- [105] J. Ming and F. J. Smith, “Speech recognition with unknown partial feature corruption – a review of the union model,” *Computer Speech and Language*, vol. 17, pp. 287–305, 2003.
- [106] H.-Y. Cho and Y.-H. Oh, “On the use of channel-attentive MFCC for robust recognition of partially corrupted speech,” *IEEE Signal Processing Letters*, vol. 11, no. 6, pp. 581–584, 2004.
- [107] I. McCowan, A. Morris, and H. Bourlard, “Improved speech recognition performance of small microphone arrays using missing data techniques,” in *Proceedings IEEE International Conference on Spoken Language Processing*, 2002, pp. 2181–2184.
- [108] S. D. Peters, P. Stubble, and J.-M. Valin, “One the limits of speech recognition in noise,” in *Proceedings IEEE International Conference on Acoustics, Speech, and Signal Processing*, 1999, pp. 365–368.
- [109] A. Lee, T. Kawahara, and K. Shikano, “Julius – An open-source real-time large vocabulary recognition engine,” in *Proceedings Eurospeech*, 2001, pp. 1691–1694.
- [110] I. Zeljkovic and S. Narayanan, “Improved hmm phone and triphone models for real-time asr telephony applications,” in *Proceedings IEEE International Conference on Spoken Language Processing*, vol. 2, 1996, pp. 1105–1108.
- [111] L. Deng, J. Droppo, and A. Acero, “Exploiting variances in robust feature extraction based on a parametric model of speech distortion,” in *Proceedings IEEE International Conference on Spoken Language Processing*, 2002, pp. 2449–2452.
- [112] J. Droppo, A. Acero, and L. Deng, “Uncertainty decoding with SPLICE for noise robust speech recognition,” in *Proceedings IEEE International Conference on Acoustics, Speech, and Signal Processing*, 2002, pp. 57–60.
- [113] R. Pichevar, J. Rouat, C. Feldbauer, and G. Kubin, “A bio-inspired sound source separation technique based on a spiking neural network in combination with an enhanced analysis/synthesis filterbank,” in *Proceedings European Signal Processing Conference*, 2004.

- [114] S. Pfeiffer, C. Parker, and C. Schremmer, “Annodex: a simple architecture to enable hyperlinking, search & retrieval of time–continuous data on the web,” in *Proceedings ACM SIGMM International Workshop on Multimedia Information Retrieval*, 2003, pp. 87–93.